Fall 2021

Investigating the Chemistry of Harmful Algal Blooms And Microbial Communities in the Natural Environment

Samuel Patrick Putnam

Investigating the Chemistry of Harmful Algal Blooms and Microbial Communities In The Natural Environment

by

Samuel Patrick Putnam

Bachelor of Science
Baylor University, 2016

Submitted in Partial Fulfillment of the Requirements

For the Degree of Doctor of Philosophy in

Chemistry

College of Arts and Sciences

University of South Carolina

2021

Accepted by:

John Ferry, Major Professor

S. Michael Angel, Committee Member

Ken Shimizu, Committee Member

Alan Decho, Committee Member

Tracey L. Weldon, Interim Vice Provost and Dean of the Graduate School

ACKNOWLEDGEMENTS

Although this dissertation is the culmination of my graduate research, science is not performed in a vacuum and this work would not have been possible without the help and support of a number of people.

First I would like to thank my parents for all of the love and support they have given me throughout grad school and my life. I would like to thank my advisor, Dr. John Ferry, for his guidance and, and for teaching me to not just do science but to think like a scientist. I also would like to acknowledge my group members who helped with this work, especially Dr. Meagan Smith who collaborated with me on much of my research and who is a great scientist and friend. I also thank Dr. Susan Richardson for her help with mass spectrometry and instilling a love of instrumentation, and Dr. Timothy Shaw and his group for their help with sediment nutrient data. Thank you also to Dr. Geoff Scott for his constant support and encouragement both scientifically and personally. I'd like to thank my long-time best friend Dr. Sydney Niles for encouraging me to choose this path and supporting me through it.

Finally I would like to thank the WaterWatch group of Lake Wateree Association, specifically Randy Kelley and Dick Foote. Citizen science is key to monitoring the communities we all share, and without them this work would not have been possible.

ABSTRACT

Cyanobacteria has existed on the planet for over 3 billion years, and as technology, science, and industry have allowed us to shape our world, these changes have caused a proliferation of biomass. Higher carbon dioxide levels in the atmosphere, warmer temperatures, and rapid increases in the nutrient cycle have created excellent growing conditions for cyanobacteria, making them endemic in fresh waters throughout the world. The work in this dissertation was directed towards the secondary metabolites produced by cyanobacteria and other surrounding microbes and understanding their concentrations and release in natural systems. Analytical methods were developed for the extraction and quantification of the Lyngbya wollei toxins produced by *Microseira wollei* and found in a bloom occurring in Lake Wateree, SC. In collaboration with a local citizen science group, the bloom in this lake was monitored over the course of nearly two years, including toxin measurements as well as other water quality parameters. A model was adapted and used as a diagnostic to identify the main driver of the bloom, legacy sedimentary phosphorus. An extension of this model was also developed to estimate the potential toxin burden in biomass given a sediment phosphorus concentration. Although toxin was readily detected within the cells, the release mechanism was unclear. A lake being treated with pesticide to control a bloom of *Microseira wollei* was used as a natural laboratory to examine the change in toxin withing the biomass during that treatment. A

significant decrease in intracellular toxin was observed in the field, but when experiments with a manifold of pesticides were performed in the laboratory, there was no increase in water column toxin concentration. Further experiments demonstrated that toxin is sequestered within the cells even under conditions that cause death and can be released with the addition of protons through acidification.

N-acyl-homoserine lactones are a group of quorum sensing molecules that control a variety of community behaviors, and can be difficult to detect in natural samples due to their transient nature. Liquid chromatography mass spectrometry methods were developed for the individual molecular detection of these signals and tested with lab grown and natural cultures.

TABLE OF CONTENTS

LIST OF TABLES

LIST OF FIGURES

LIST OF ABBREVIATIONS

ESI ..... Electrospray Ionization

HAB ..... Harmful Algal Bloom

HCB ..... Harmful Cyanobacterial Bloom

LWT ..... Lyngbya wollei toxin

LWT1 ..... Lyngbya wollei Toxin 1

LWT2/3 ..... Lyngbya wollei Toxin 2/3

LWT4 ..... Lyngbya wollei Toxin 4

LWT5 ..... Lyngbya wollei Toxin 5

LWT6 ..... Lyngbya wollei Toxin 6

PST ..... Paralytic Shellfish Toxin

Q-TOF ..... Quadrupole Time-of-Flight

STX ..... Saxitoxin

SCP ..... Sodium Carbonate Peroxyhydrate

TQ ..... Triple Quadrupole

UPLC ..... Ultra-Performance Liquid Chromatograph

CHAPTER 1

HARMFUL CYANOBACTERIAL BLOOMS, RESERVOIRS, AND CITIZEN SCIENCE IN THE SOUTHEAST

1.1 HARMFUL CYANOBACTERIAL BLOOMS

Cyanobacteria have enjoyed a long and prosperous life on Earth, with fossil evidence showing remains dating back 3.5 billion years.[1] These organisms have particularly proliferated in freshwater systems as anthropogenic inputs of nutrients including nitrogen and phosphorus have increased dramatically in the past centuries due to large scale agriculture and urbanization. Increased nutrient availability and higher global temperatures have increased the growth capability of these microbes and led to harmful cyanobacterial bloom becoming more of a regular blight than a transient nuisance.[2] Effects that cause these blooms to become harmful include blockage of infrastructure, taste and odor issues with drinking water, and loss of tourism revenue due to unsightly recreational conditions. Blooms can also have secondary effects on the surrounding microbial community; upon the mass death of a bloom oxygen levels can be rapidly depleted by bacterial decomposition of the dead mat material.[3] However, the area of greatest concern for human health is the toxic secondary metabolites produced by many HCBs. These toxins range widely in chemical structure and methods of action, and it is often unclear which species are responsible for which specific toxins. HCBs producing toxic secondary metabolites have an effect on their environment by causing fish kills as well as choking out competitive plants and microbes.[4] Since surface water and reservoirs are often used as drinking water sources, HCBs are also a public health concern. Despite the risk posed by these toxins, they are not often regulated and analytical methods are not standardized. This poses a scientific and regulatory challenge to develop

methods and sensible guidelines to understand and control the risk of toxin exposure.

1.2 RESERVOIRS AND MAN-MADE IMPOUNDMENTS

Nutrient control schemes are often implemented to control the growth of cyanobacteria in lakes and watersheds and improve overall water quality. There is considerable dogma within the community that phosphorus is most frequently the limiting nutrient, and phosphorus levels in the water determine the extent to which an HCB may grow. This can depend greatly on the body of water; frequently these generalizations do not include reservoir and man-made systems where water flow is significant through the environment. Iron-rich soils in the southeast United States have large potential to act as a phosphorus sink, precipitating phosphorus from a soluble phase to insoluble inorganic forms. Despite nutrient control measures such as total maximum daily loads (TMDLs) being implemented in recent decades, many reservoirs were built in the early 19th century and have had decades longer to accumulate phosphorus. In this way phosphorus is more like a legacy sediment contaminant than a water column nutrient as it is typically used.

Another feature of reservoirs and man-made impoundments that leads to HCB growth is the shallow overall depth and dendritic nature. Many shallow and isolated coves in a water body present a large area for photic growth, especially for non-planktonic benthic blooms. This large growth area also extends to structures such as stormwater and residential ponds, which are very common in the US and southeast region.[5] These ponds are often privately owned, and high

in nutrients due to their proximity to residential and agricultural areas. The proliferation of man-made impoundments requires a different set of regulation and thinking as they are environments that frequently exceed the bounds of what is traditionally considered “normal” conditions.

1.3 LAKE WATEREE AND CITIZEN SCIENCE

Lake Wateree is a reservoir formed by the impoundment of the Catawba River and Wateree Creek. The outflow of the lake from the southern dam is the Wateree River, which eventually joins with the Congaree River to form the Santee River and drain to the coast. Built in 1919 for hydroelectric power generation and managed by Duke Energy, the lake also provides drinking water and recreational area to the surrounding communities. With a shoreline of 291 km and an average depth less than 7 m, there are many shallow coves that can and have been colonized by benthic cyanobacteria.[6] WaterWatch, a citizen science group that is part of the Lake Wateree Association, has been monitoring water quality on the lake since the 1990s.[7] Citizen science groups perform an essential role in monitoring watersheds and lakes; neither state organizations nor academic researchers are capable of monitoring every body of water continuously. By involving the local residents in the science of their water, not only is data collection improved but water quality changes can be caught much earlier. This also provides citizens with a connection to the type of science and environmental work their tax dollars are supporting, and encourages them to support further funding.

Although this work focuses on a multi-year study in Lake Wateree, the conclusions and findings are not specific only to that water body. Models, regulations, and textbooks are oftentimes based on the limnology of natural lakes and rivers and do not account for the unique differences presented by a man-made system. By building datasets and models in reservoirs, greater understanding and predictive ability can be achieved in these environments found throughout the southeast and the entire world.

1.4 REFERENCES

(1) Paerl, H. W.; Paul, V. J. Climate change: Links to global expansion of harmful cyanobacteria. *Water Research* **2012**, *46* (5), 1349-1363, Article. DOI: 10.1016/j.watres.2011.08.002.

(2) Visser, P. M.; Verspagen, J. M. H.; Sandrini, G.; Stal, L. J.; Matthijs, H. C. P.; Davis, T. W.; Paerl, H. W.; Huisman, J. How rising CO2 and global warming may stimulate harmful cyanobacterial blooms. *Harmful Algae* **2016**, *54*, 145-159, Review. DOI: 10.1016/j.hal.2015.12.006.

(3) Paerl, H. W.; Otten, T. G. Harmful Cyanobacterial Blooms: Causes, Consequences, and Controls. *Microbial Ecology* **2013**, *65* (4), 995-1010. DOI: 10.1007/s00248-012-0159-y (acccessed 2021-10-12T15:37:22).

(4) Paerl, H. W.; Fulton, R. S.; Moisander, P. H.; Dyble, J. Harmful Freshwater Algal Blooms, With an Emphasis on Cyanobacteria. *The Scientific World Journal* **2001**, *1*, 76-113. DOI: 10.1100/tsw.2001.16 (acccessed 2021-10-12T15:37:00).

(5) Beckingham, B.; Callahan, T.; Vulava, V. Stormwater Ponds in the Southeastern U.S. Coastal Plain: Hydrogeology, Contaminant Fate, and the Need for a Social-Ecological Framework. *Frontiers in Environmental Science* **2019**, *7*. DOI: 10.3389/fenvs.2019.00117.

(6) EPA, U. *Report on Wateree Lake, Fairfield, Kershaw, and Lancaster Counties South Carolina*; 440; https://nepis.epa.gov/, 1975.

(7) Clyburn, K.; Willis, R.; King, J. *Lake Wateree Water Watch 2019 Annual Report*; Lake Wateree Water Watch, https://sites.google.com/site/watereewaterwatch, 2021.

CHAPTER 2

GROWTH OF THE HARMFUL BENTHIC CYANOBACTERIA *LYNGBYA WOLLEI* IS DRIVEN BY SEDIMENTARY PHOSPHOROUS[1]

[1] Putnam, S.P., Smith, M.L., Metz, T.T., Womer, A.M., Sellers, E.J., McClain, S.J., Crandell, C.A., Scott, G.I., Shaw, T.J., and Ferry, J.L. Submitted to *Water Research* 10/29/2021

2.1 ABSTRACT

Models for harmful cyanobacterial blooms (HCBs) in fresh waters are usually predicated on the relationship between cyanobacterial ecology and dissolved nutrients, particularly phosphorous. Here we show legacy sedimentary phosphorous as the primary driver of a benthic HCB. Biogeographical surveys by teams of citizen science volunteers working with the University of South Carolina identified over 200 blooms of *Lyngbya wollei* in Lake Wateree, SC. The observed *Lyngbya wollei* biomass in the lake was 5.2 x 10^6 kg, affecting 60% of the lake's shoreline. This growth occurred under water quality conditions that were near or below the regulatory total maximum daily load (TMDL) for phosphorous and nitrogen. A series of established predictive models for cyanobacterial biomass growth were applied as diagnostics to determine the cause; the only variable that tested as statistically significant was sedimentary phosphorous. Concentrations of the *Lyngbya wollei* toxins (LWTs) 1, 4, 5, and 6 were determined at multiple sites over an 18-month period and a toxin inventory was calculated. Toxin profiles between sites differed at the 95% level of confidence, establishing each site as a unique bloom. This data was used to adapt an existing biomass model to enable prediction of LWT burden and health risk.

2.2 INTRODUCTION

The anthropogenic phosphorous cycle has increased the input of phosphorous to watersheds by a factor of three relative to the historical rate.[1] Inorganic phosphorous often reacts with transition metals to produce poorly soluble complexes therefore its transport through watersheds is dominated by

the movement of particles in the water column rather than as a free ion.[2] Built reservoirs are particularly vulnerable to persistent sediment contamination by phosphorous when fast-moving rivers and streams slow abruptly before dams and suspended phosphorous-rich particles settle. These constructed lakes can be highly supportive of the rapid growth of benthic microbial colonies, particularly species such as *Lyngbya wollei* capable of nitrogen fixation.[3] Biomass is a notable feature of benthic cyanobacterial blooms, often reaching cell densities significantly higher than planktonic harmful algal blooms (HABs).[4, 5] Large biomass combined with their tendency to produce toxic secondary metabolites can cause these blooms to become harmful cyanobacterial blooms (HCBs).[6] Built lakes are often used heavily for recreation and as drinking water sources and the resulting intersection between human use needs, nutrient-laden sediment, and HCBs can lead to high health risk in the affected population.

Lyngbya wollei (aka *Microseira wollei*) is a genetically diverse filamentous benthic cyanobacteria that is becoming increasingly widespread across the eastern United States and southern Canada.[7, 8] It is particularly responsive to climate change and its growth rate correlates strongly and positively with higher temperatures, increased stratification, and increased anoxia.[9] *Lyngbya wollei* is capable of producing biomass in excess of 5-15 kilograms wet weight per square meter of sediment surface.[4, 10] It produces several congeners of saxitoxin including decarbamoyl saxitoxins, gonyautoxins, and the *Lyngbya wollei* toxins 1 through 6 (LWTs 1-6) (Figure A.1).[11, 12] Historically the LWTs have been difficult to analyze by immunoassays, and mass spectrometric analyses are subject to

issues like interference from co-extracted ion suppressing agents or entrained inorganic materials.[13] This has further complicated the development of risk and toxin exposure models for this HCB.

Lyngbya wollei colonies are stable toward overwintering and may persist for years; therefore their occurrence is difficult to predict using seasonal algal growth models based on dissolved nutrients.[14] This work addresses a bloom of distinct and persistent colonies in Lake Wateree SC, focusing on the role of sedimentary phosphorous instead of dissolved. The lake is a man-made reservoir at the confluence of the Catawba River and Wateree Creek that is bounded by the Cedar Creek Reservoir Dam at the northern end and Lake Wateree Dam at the southern end. Lake Wateree is a source of drinking water, electricity, and a recreational resource for surrounding communities. The Catawba River basin is heavily populated with more than two million residents but phosphorous controls on wastewater were installed for the largest treatment plants in the region less than twenty years ago, implying the presence of significant legacy phosphorous in this watershed. On average 46% of all incoming phosphorous is retained in the lake every year, adding to the sedimentary burden (Figure 2.1).

Recurrent blooms of *Lyngbya wollei* have been observed in Lake Wateree at least since 2010. Its distribution in the lake was mapped independently by U of SC researchers working with WaterWatch citizen scientist volunteers as well as Duke Energy employees. The most recent mapping efforts reported several hundred colonies of *Lyngbya wollei* around the lake that affected as much as

60% of the shoreline and comprised more than 50% of species occurrence in the entire lake in a 2019 survey.[15, 16] Nutrient data was also collected from the water column and sediments around the lake. This work focused on resolving between the contributions of phosphorous in the water column and sediments as a driver for *Lyngbya wollei* growth in the lake as well as developing a predictive model of LWT burdens in the algal biomass.

2.3 MATERIALS AND METHODS

2.3.1 SITE SELECTION

Three locations in Lake Wateree were chosen for routine algal grab samples: Site 1 [34.416054, -80.863473], Site 2 [34.334926, -80.708297], and Site 3 [34.364058, -80.699524] (Figure 2.2). Site 1 was in the northern part of the lake and experienced regular exceedances of the phosphorous total maximum daily load (TMDL) within the last 18 years (Figure 2.1). Sites 2 and 3 were on the southern end of the lake, each within 1000 m of drinking water intake sites for the towns of Lugoff / Elgin, and Camden SC, respectively. Grab sample sites were monitored biweekly from July 2018 through October 2019. All three sites were at a minimum nautical distance of 3.5 km apart, which allowed each bloom area to be considered independent and was confirmed by toxin analysis. Additional sites depicted on the map were used for algal and LWT qualification (Figure 2.1, Table A.1). Sampling and algal surveys were conducted in collaboration with groups of citizen scientist volunteers during the sampling period.

2.3.2 SAMPLING PROCEDURE

Algal grab samples were collected from mats with a skimmer net and rinsed in lake water. Macroscopic debris (sticks, leaves, etc.) were also removed at the time of collection. Samples were placed in 50 mL centrifuge vials and stored at 0 ^{o}C during transport (< 6 hours). Upon arrival in the laboratory samples were immediately frozen in liquid nitrogen and then lyophilized in a Labconco FreeZone 6 lyophilizer. Unless otherwise indicated, all subsequent analytical work was done on freeze dried samples. Freeze dried samples were stored sealed at -20°C until additional workup as required per analyte.

2.3.4 *LYNGBYA WOLLEI* TOXIN EXTRACTION AND ANALYSIS

All extractions were performed on 100 mg subsamples of lyophilized algae from the different sites (n=3 samples collected at each field site for each sampling event). The LWTs were isolated from the algae matrix by extraction into 10.0 mL of 0.100 M acetic acid. Extraction was accomplished by first shaking the sample to ensure thorough wetting followed by 15 min of sonication. Samples were then centrifuged for five min. After centrifugation an aliquot of acid extract was removed, filtered through a 0.45-micron nylon filter, diluted by a factor of 50 in 0.100 M acetic acid to minimize signal suppression, and analyzed by liquid chromatography mass spectrometry (Figure A.2).[13]

Saxitoxin standards (100 µg/g in HCl) were supplied by the US Food and Drug Administration (USFDA) and used as surrogate standards for quantification of the LWTs due to the lack of commercially available standards. High resolution

qualification was done on an Agilent (Santa Clara, CA) 6545 quadrupole time-of-flight mass spectrometer to confirm toxin (LWTs 1-6) presence with accurate mass data using a published method.[13] Samples were analyzed using a Waters (Milford, MA, USA) Acquity ultra performance liquid chromatography (UPLC) coupled with a Xevo triple quadrupole mass spectrometer (MS/MS) equipped with an electrospray ionization source (ESI). For both qualification and quantification, separations were performed on a BEH Amide (2.1x150 mm) 1.7 µm particle size column (Waters). The mobile phases were aqueous 5.6 mM formate buffered at pH 3.5 (A) and 95/5, acetonitrile/water 5.6 mM formate buffer at pH 3.5 (B). The chromatographic method began with 80% B held for one minute, ramped to 60% B over the next 3 minutes and held for 2 minutes, at 7 minutes returned to the original conditions over one minute (80% B) and held for re-equilibration for 8 minutes (16 minutes total). Flow rate was 0.35 mL/min throughout.

All saxitoxin calibration solutions were made up in 3 mM HCl and source conditions were optimized manually in the positive ion mode. All algal extracts were analyzed using the same operational parameters. Analytes of interest were optimized manually through chromatography from solutions of extracted algae. Selected ion monitoring (SIM) was used for analysis of LWT1 (m/z = 379), LWT4 (m/z = 241), LWT5 (m/z = 299) and LWT6 (m/z = 283).

2.3.5 TOTAL CARBON ANALYSIS

Total carbon and inorganic (non-combustible) content analysis was performed using a Shimadzu TOC-L instrument with a solid sample module

(SSM) calibrated weekly against a glucose standard. Approximately 40 mg of lyophilized algae was placed in a tared ceramic boat and combusted at 900°C with excess oxygen to measure total carbon. This sample was weighed again post-combustion to determine the mass of the remaining inorganic material.

2.3.6 16S rRNA ANALYSIS

Amplification and sequencing of the 16S rRNA was performed at Molecular Research (Shallowater, TX). The BLASTn search was used to taxonomically classify the final operational taxonomical units using databases derived from RDPII and NCBI.[17]

2.3.7 PHOSPHOROUS DETERMINATION

Multiple sediment cores were collected at sites 2 and 3 in Lake Wateree. Cores were sliced into horizontal sections and stored at -20°C in polypropylene bottles until analysis. Subsamples were taken of the individual sections, weighed, and heated at 55°C until a constant mass was achieved. Dried sediments were then ground into a powder, sieved at 125 microns, divided into 500 mg subsamples, then exposed to a sequential extraction process for total phosphorous.[18] A 100 mg phosphorous/L stock solution (KH_2PO_4) was prepared as the working calibration standard and calibration curves were made in the range of 0.01 to 0.30 mg P/L. Optical absorbance of the processed samples was measured in glass cells at 880 nm. Samples with absorbance greater than one were diluted to maintain analyses in the linear portion of the response curve.

2.3.8 STATISTICAL TREATMENT OF DATA AND MODELS

All samples were analyzed in replicate (n=3) to determine standard deviation and confidence intervals. All error bars shown represent the 95% confidence interval. Error was propagated for laboratory operations where appropriate. Individual samples were averaged, and the 95% confidence interval calculated based on Student's t-test. Historical water quality parameters were obtained through data reported by South Carolina Department of Health and Environmental Control (SC DHEC) on the STORET (USEPA) database. Error estimates for the citizen science mapping efforts were based on an estimated 10% interval regarding shoreline coverage.[16] Statistical overlap of models with field observations was calculated using Gaussian distributions in R (R Core Team 2021).

2.4 RESULTS AND DISCUSSION

2.4.1 ALGAE IDENTIFICATION AND BIOMASS MAPPING

The geographical extent of the blooms on Lake Wateree was established in 2015 by WaterWatch, a local volunteer citizen science water monitoring program. WaterWatch estimated that by 2019, 60% of the 291 km of shoreline was affected, with mats typically extending 5 m from the shoreline.[16] Grab samples of the mats were collected and micrographs submitted to the Phytoplankton Monitoring Network (NOAA), who determined the samples were dominated by *Lyngbya wollei*.[19] Identification was further qualified by genetic characterization (16S) of freeze-dried mat material collected in the field. 16S

rRNA analysis showed that *Lyngbya wollei* comprised 53% of the genetic content of the mat. Conservatively based on a mean mat biomass density of 6 kg/m^2 and historical mapping, the current study estimated that Lake Wateree was supporting approximately an upper limit 5.2 x 10^6 kg of *Lyngbya wollei* growth.[16]

2.4.2 CONTACT WITH SEDIMENTS

The presence of planktonic HCBs often correlates with high levels of bioavailable phosphorous in the water column.[20] However, benthic HCBs are also in contact with sediments, raising the potential for sedimentary contributions to the bioavailable phosphorous. This hypothesis was tested by measuring the inorganic content of *Lyngbya wollei*-dominated microbial mats over an extended period. *Lyngbya wollei* undergoes a period of senescence during the winter months when biomass stays essentially constant, but mat growth falls to near zero.[21] The percentages of carbon and inorganic material were monitored in *Lyngbya wollei* mat grab samples obtained from three sites around Lake Wateree over an eighteen-month period (Figure 2.3). Total carbon analysis over the 347 samples yielded a mean elemental carbon content of 28.1 ± 0.7% and a mean inorganic content of 27.6 ± 0.6% in dry samples. Assuming particle entrainment in the mat from the water column was constant over the year, an assumption supported by the brief 50 day hydraulic retention time of the lake, the inactive winter period should have shown a significant increase in inorganic content in the mat samples relative to high-growth periods.[22] Instead, the correlation between inorganic content and time was essentially flat, with an $r^2 < 0.05$, indicating that entrained particulates in the mat came from the more constant sedimentary

source. A probable mechanism for this is bubble-driven lift or sloughing of microbial mats, where bubbles of photosynthetically generated O_2 or microbially generated CO_2 and CH_4 create enough buoyancy for the mat to lift off the sediment surface.[23] Substantial quantities of surface sediment are lifted in this process, which was observed frequently (> 20 times) in Lake Wateree during monitoring. These major lift events are also supplemented by other factors including the lowering and raising of the lake level by hydroelectric operations and wave action from wind or passing watercraft. These observations supported the hypothesis that mat-driven turnover of sediments allowed benthic microbial communities ready access to sequestered sediment bound nutrients.

2.4.3 SEDIMENTARY PHOSPHOROUS AND BIOMASS

Sediments in Lake Wateree accumulated phosphorous at an average annual rate of $1.67 \pm 0.58 \times 10^5$ kg/yr based on analysis of historical water column phosphorous measurements from 2001 - 2019 (Figure 2.1). Surface sediment samples up to 10 cm in depth were collected over 15 months (n = 10) and analyzed for total phosphorous for this project. Mean sedimentary phosphorous in the zone where mat-driven turnover was active was 0.146 ± 0.009 mg P per g of wet sediment.

An exhaustive series of predictive models for total cyanobacterial biomass, including benthic cyanobacteria (CBB) were developed by Beaulieu et al. from the National Lake Assessment dataset (n=1147 lakes).[14] CBB was calculated based on observables that alternately included surface water temperature (SWT), a combined model for total nitrogen and surface water

temperature (TN+SWT), total nitrogen (TN), chlorophyll a (Chl a), and total phosphorous (TP) (Table 2.1).[14] These models were also used as diagnostics to test the hypothesis that sedimentary phosphorous was the dominant variable for predicting *Lyngbya wollei* by comparing field observed biomass to modelled biomass based both on the 2001-2019 year water column averages (Table A.2) and total sedimentary phosphorous obtained from sediment cores.

Equations 1-5 were used to estimate Lyngbya wollei biomass and compared to field biomass estimates to validate the choice of variables. The percentage overlap of the Gaussian distributions for each model and the field data were calculated. SWT, TN + SWT, TN, Chl a, and TP all estimated a range of biomass that overlapped field measurements by less than 0.001% (Figure 2.4). Sedimentary phosphorous loading was also used as an input parameter for equation 5 (Table 2.1) under the assumption it was bioavailable to benthic algae. Given that the model input value was solution phase phosphorous, the sedimentary phosphorous was converted to a pseudo-aqueous concentration from calculating the dilution of total sediment phosphorous to the volume of the lake. This calculation was based on a total lake surface area of 5.61×10^7 m^2 and a wet sediment density of 1.45 g/cm^3 and returned the equivalent aqueous concentration of 3.12 mg/L. This value was input to equation 5 (Table 2.1) and the output corrected for inorganic content, resulting in a predicted biomass of 1.97×10^6 kg. This was in close agreement with the field observed number of 5.24×10^6 kg and Gaussian overlap obtained in this manner was 5.3% (Figure A.3). The large increase in percent overlap for this sediment phosphorous model

compared to the other water quality parameters supported the hypothesis that sediment phosphorous was the main driver of biomass. Notably in this case the degree of overlap was used as a diagnostic to indicate the importance of sedimentary phosphorous and was not presented as a quantitative predictor of model accuracy. This hypothesis was further supported by analysis of the historical record of the ratio of phosphorous over chlorophyll in the waters of the lake (Figure A.4). The relationship was essentially flat over a timespan that included the introduction and expansion phase of *Lyngbya wollei* colonies in the lake ($r^2 < 0.25$). Given that the lake added over 5×10^6 kg of biomass in this same period, it is unlikely the water column could have been the sole source of the phosphorous needed to support this massive growth.

2.4.4 TOXIN MEASUREMENTS

LWTs 1 through 6 were confirmed by high resolution mass spectrometry using a series of structurally verified mass fragments identified in a previous study.[13] Analytes matched theoretical masses to within 5 ppm, verifying their identity. Data was averaged for each quantified toxin (LWTs 1, 4, 5, & 6) over the entire study period and presented as a per site toxin profile (Figure 2.5). Toxin concentrations ranged over several orders of magnitude, dropping as low as 1.3 µg/g C for LWT1 and as high as 339 µg/g C for LWT5 at Site 2 (Table A.3). Although all the measured toxins were saxitoxin congeners they do not exhibit the same degree of neurotoxicity as saxitoxin or each other or saxitoxin itself. LWT 5 is nominally the most impactful of the LWTs with 14% the equivalent toxicity to SXT while the other LWTs trail to less than 1%.[24]

Analysis of variance (ANOVA) was performed on the summed total of toxin for each of the three monitored sites (n = 29) to determine if the sites had statistically different total concentrations of toxin. The summed toxin at the three sites was found to be distinct at greater than the 99% confidence level ($p = 0.004$), further supporting the treatment of the blooms in the lake as distinct infestations.

Not all LWTs are thought to be generated through the same biosynthetic pathway; for example LWTs 1, 4, and 6 are hypothesized to be generated through a different pathway than LWT5.[12] Of the four LWTs quantified in this study only LWT5 is known to be neurotoxic to mammals. The ratio of the concentrations between LWT5 and the nontoxic LWTs (sum of LWT1, 4, 6) over time was calculated to give insight regarding the potential environmental health risk of a *Lyngbya wollei* bloom in a more focused manner than raw concentration. ANOVA of the relationship between the ratio and time (over the period samples were collected) showed that this “toxic to nontoxic” ratio was also distinct between the locations ($p < 3 \times 10^{-6}$). The ratio was also plotted over time to interrogate temporal variations in the lake at large (Figure A.5). Using measured field data this relationship showed variability, but no correlation with any linear trend ($r^2 < 0.01$).

2.4.5 MODELING TOXIN

An empirical modification of the CBB model (Table 2.1, Eq. 5) was developed to estimate LWTs 1, 4, 5, and 6 from sedimentary phosphorous concentration. Corrections were developed for LWT mass, inorganic content in

the algae, and the habitable volume of the lake. Since the original model was developed using a large proportion of planktonic algae a correction was needed to adapt for the smaller volume of the lake that was habitable by benthic algae. This volume was estimated to be 1.5×10^9 L for Lake Wateree based on field-observed algae coverage, or about 0.4% of the total lake volume (175 km shoreline, 5 m wide mat, lakebed slope of 22 degrees). Inorganic material measurements yielded a correction factor applied to wet algae of 1.05 ± 0.06. Toxin as a ratio of biomass (α_x) is presented for each of the quantified LWTs in Table 2.2.

2.4.6 TOXIN MODEL VALIDATION

The primary field data set was used to develop an exhaustive mean of toxin to biomass ratio. An independent bloom location in the lake (Site 4) was used as a validation set for the model. The average sedimentary phosphorous value from this site was 0.043 mg P per g of sediment, which converted to a water column concentration of 1.49 mg/L (see above). This was input to the model using the LWT specific coefficients to generate an estimated toxin content in *Lyngbya wollei* biomass. Microbial mat samples were collected over a seven-month period and analyzed for LWT content to test the model predictions. Concentrations are presented as µg toxin per m^2 of the mat. The Gaussian overlap of the adjusted model at Site 4 was 41%, 8.1×10^{-12} %, 53%, and 28% for LWT1, LWT4, LWT5, and LWT6 respectively (Figure 2.6, inset). The means for field observations and the model agreed at the 95% confidence interval for all the toxins except LWT4. Agreement between means with low percentage overlap

was a result of the large standard deviation of the field measurements; a prolonged dataset could have yielded a lower standard deviation and brought the model more into agreement with the field. The non-toxic metabolite LWT4 was significantly underpredicted by the model and showed no statistically significant overlap with field observations. The biosynthetic pathway for LWT4 has not been experimentally verified, but was proposed to be an intermediate between LWT1 and LWT6.[12] If the biosynthetic pathways of either of the other products are reversible then LWT4 may not have been at equilibrium at this site. If abiotic reactions, particularly hydrolyses or esterification, occurred in this system in parallel with biosynthetic production of LWT4 then it was possible this empirical model did not include the necessary variables to predict its fate.

2.4.7 LAKE INVENTORY

Harmful cyanobacterial blooms can vary in intensity and binary occurrence within a water body, but during active periods they may generate significant quantities of toxin than can persist in sediments for up to a hundred years.[25] Predicting the environmental impact of harmful cyanobacterial blooms through quantifying their growth and toxin input to lakes is a critical goal for ensuring access to safe drinking and recreational water resources in the future. A useful metric for evaluating the risk that HCBs pose to a water body is to estimate a total mass-based burden of toxin to understand the potential hazard to human health. Based on field observations of algal mass and extensive toxin quantification Lake Wateree was determined to have a total inventory of 8.1 kg of saxitoxin equivalents, calculated from mouse assay toxicity.[24] If this mass of toxin

was released from the mat, the concentration in the area of the lake where the algae is present could experience saxitoxin equivalent concentrations as high as 5.6 µg/L, a level high enough to exceed the safe contact threshold according to Ohio EPA values.[26]

2.4.8 ENVIRONMENTAL RELEVANCE

The majority of the lakes in the Southeastern US are manmade, many created for hydroelectric power in the early 20th century and now used additionally for recreation and drinking water. These lakes are typified by river input followed by large settling basins at dams.[27] This structure is particularly effective at removing particulate phosphorous sources from incoming waters. A common consequence of this is high sedimentary phosphorous burdens in these lakes, leaving them vulnerable to blooms of benthic cyanobacteria capable of sedimentary disturbances through mat-lifting mechanisms. Setting TMDLs is an accepted strategy for controlling planktonic HCBs in the water column. The current work shows that a similar strategy for controlling benthic HCBs may require inclusion of sedimentary phosphorous in nutrient control plans as well.

Lyngbya wollei accumulates in these systems in persistent microbial mats and can be spread over a wide area within a water body. These mats are known to generate neurotoxic secondary metabolites that are sodium channel blockers. LWT 5 is the functionally strongest sodium channel blocker, scaled against saxitoxin at 14% as toxic. The proposed toxin-specific modifications to the cyanobacterial biomass model enabled prediction of the effective toxicity of a

Lyngbya wollei mat by allowing the most accurate prediction of the most toxic of the LWTs (LWT 5).

Practical assessment of the human and environmental health risks posed by benthic HCBs is difficult given the diversity of toxin production they exhibit. For example, there are known *Lyngbya wollei* blooms that have not exhibited any toxicity to local fauna or detectable LWTs when extracted.[8] Therefore the best risk assessment for HCBs and HCB toxin inventories is based on detailed field observations and samples, but these are often prohibitively expensive and time consuming.[28] The current work, set in a lake that was essentially saturated with a stable, persistent HCB, generated a series of empirical models for estimating biomass and toxin inventories in a benthic HCB driven by sedimentary phosphorous.

2.5 REFERENCES

(1) Rittmann, B. E.; Mayer, B.; Westerhoff, P.; Edwards, M. Capturing the lost phosphorus. *Chemosphere* **2011**, *84* (6), 846-853. DOI: 10.1016/j.chemosphere.2011.02.001 (acccessed 2021-07-06T15:15:56).

(2) Stoddard, J. L.; Van Sickle, J.; Herlihy, A. T.; Brahney, J.; Paulsen, S.; Peck, D. V.; Mitchell, R.; Pollard, A. I. Continental-scale increase in lake and stream phosphorus: are oligotrophic systems disappearing in the United States? *Environmental Science & Technology* **2016**, *50* (7), 3409-3415. DOI: 10.1021/acs.est.5b05950 (acccessed 2021-07-06T15:15:00).

(3) Tian, J.; Ge, F.; Zhang, D.; Deng, S.; Liu, X. Roles of phosphate solubilizing microorganisms from managing soil phosphorus deficiency to mediating biogeochemical P cycle. *Biology* **2021**, *10* (2), 158. DOI: 10.3390/biology10020158 (acccessed 2021-07-06T15:22:01).

(4) Phlips, E. J.; Ihnat, J.; Conroy, M. Nitrogen-fixation by the benthic fresh-water cyanobacterium Lyngbya-wollei. *Hydrobiologia* **1992**, *234* (1), 59-64. DOI: 10.1007/bf00010779.

(5) Pham, T.-L.; Dao, T.-S.; Tran, N.-D.; Nimptsch, J.; Wiegand, C.; Motoo, U. Influence of environmental factors on cyanobacterial biomass and microcystin concentration in the Dau Tieng Reservoir, a tropical eutrophic water body in Vietnam. *Annales de Limnologie - International Journal of Limnology* **2017**, *53*, 89-100. DOI: 10.1051/limn/2016038 (acccessed 2021-08-13T23:05:49).

(6) Hudon, C.; De Seve, M.; Cattaneo, A. Increasing occurrence of the benthic filamentous cyanobacterium Lyngbya wollei: a symptom of freshwater ecosystem degradation. *Freshwater Science* **2014**, *33* (2), 606-618. DOI: 10.1086/675932.

(7) Hudon, C.; Gagnon, P.; Larabie, S. P.; Gagnon, C.; Lajeunesse, A.; Lachapelle, M.; Quilliam, M. A. Spatial and temporal variations of a saxitoxin analogue (LWTX-1) in Lyngbya wollei (Cyanobacteria) mats in the St. Lawrence River (Quebec, Canada). *Harmful Algae* **2016**, *57*, 69-77. DOI: 10.1016/j.hal.2016.06.001.

(8) Joyner, J. J.; Litaker, R. W.; Paerl, H. W. Morphological and genetic evidence that the cyanobacterium Lyngbya wollei (Farlow ex Gomont) speziale and Dyck encompasses at least two species. *Applied and Environmental Microbiology* **2008**, *74* (12), 3710-3717. DOI: 10.1128/Aem.02645-07.

(9) Paerl, H. W.; Huisman, J. Climate - Blooms like it hot. *Science* **2008**, *320* (5872), 57-58, Editorial Material. DOI: 10.1126/science.1155398. Paerl, H. W.; Huisman, J. Climate change: a catalyst for global expansion of harmful cyanobacterial blooms. *Environmental Microbiology Reports* **2009**, *1* (1), 27-37. DOI: 10.1111/j.1758-2229.2008.00004.x. O'Neil, J. M.; Davis, T. W.; Burford, M. A.; Gobler, C. J. The rise of harmful cyanobacteria blooms: The potential roles of eutrophication and climate change. *Harmful Algae* **2012**, *14*, 313-334. DOI: 10.1016/j.hal.2011.10.027.

(10) Duke, B. Laboratory and field responses of target and non-target species to algaecide exposures. **2007**.

(11) Foss, A. J.; Phlips, E. J.; Aubel, M. T.; Szabo, N. J. Investigation of extraction and analysis techniques for Lyngbya wollei derived Paralytic Shellfish Toxins. *Toxicon* **2012**, *60* (6), 1148-1158. DOI: 10.1016/j.toxicon.2012.07.009. Foss, A. J.; Phlips, E. J.; Yilmaz, M.; Chapman, A. Characterization of paralytic shellfish toxins from Lyngbya wollei dominated mats collected from two Florida springs. *Harmful Algae* **2012**, *16*, 98-107. DOI: 10.1016/j.hal.2012.02.004.

(12) Mihali, T. K.; Carmichael, W. W.; Neilan, B. A. A putative gene cluster from a Lyngbya wollei bloom that encodes paralytic shellfish toxin biosynthesis. *PLOS One* **2011**, *6* (2). DOI: 10.1371/journal.pone.0014657.

(13) Smith, M. L.; Westerman, D. C.; Putnam, S. P.; Richardson, S. D.; Ferry, J. L. Emerging Lyngbya wollei toxins: A new high resolution mass spectrometry method to elucidate a potential environmental threat. *Harmful Algae* **2019**, *90*, 101700.

(14) Beaulieu, M.; Pick, F.; Gregory-Eaves, I. Nutrients and water temperature are significant predictors of cyanobacterial biomass in a 1147 lakes data set. *Limnology and Oceanography* **2013**, *58* (5), 1736-1746.

(15) Hartis, B. M.; Molloy, E. *An update on aquatic plants in the Catawba-Wateree river reservoirs*; Duke Energy Aquatic Plant Management Program, https://www.duke-energy.com, 2020. https://desitecoreprod-cd.azureedge.net/_/media/pdfs/community/lakes-and-rec/aquatic-plants-catawba-wateree.pdf?la=en&rev=09288a6138ee4d0791b437eab458c449.

(16) Clyburn, K.; Willis, R.; King, J. *Lake Wateree Water Watch 2019 Annual Report*; Lake Wateree Water Watch, https://sites.google.com/site/watereewaterwatch, 2021.

(17) Sayers, E. W.; Beck, J.; Bolton, E. E.; Bourexis, D.; Brister, J. R.; Canese, K.; Comeau, D. C.; Funk, K.; Kim, S.; Klimke, W.; et al. Database resources of the National Center for Biotechnology Information. *Nucleic Acids Research* **2021**, *49* (D1), D10-D17. DOI: 10.1093/nar/gkaa892 (acccessed 2021-07-23T18:01:07).

(18) Ruttenberg, K. C. Development of a sequential extraction method for different forms of phosphorus in marine sediments. *Limnology and oceanography* **1992**, *37* (7), 1460-1482. Wang, C.; Zhang, Y.; Li, H.; Morrison, R. J. Sequential extraction procedures for the determination of phosphorus forms in sediment. *Limnology* **2013**, *14* (2), 147-157. Ma, H.; Zhao, B.; Li, L.; Xie, F.; Zhou, H.; Zheng, Q.; Wang, X.; He, J.; Changwei, L. Fractionation trends of phosphorus associating with iron fractions: An explanation by the simultaneous extraction procedure. *Soil and Tillage Research* **2019**, *190*, 41-49. Ruban, V.; López-Sánchez, J.; Pardo, P.; Rauret, G.; Muntau, H.; Quevauviller, P. Harmonized protocol and certified reference material for the determination of extractable contents of phosphorus in freshwater sediments–a synthesis of recent works. *Fresenius' journal of analytical chemistry* **2001**, *370* (2), 224-228. EPA, U. Method 365.3: Phosphorous, All Forms (Colorimetric, Ascorbic Acid, Two Reagent). https://www.epa.gov/sites/default/files/2015-08/documents/method_365-3_1978.pdf, 1978.

(19) Science, N. C. f. C. O. *Phytoplankton Monitoring Network*. 2017. https://coastalscience.noaa.gov/research/stressor-impacts-mitigation/pmn/ (accessed 2021.

(20) Hamilton, D. P.; Salmaso, N.; Paerl, H. W. Mitigating harmful cyanobacterial blooms: strategies for control of nitrogen and phosphorus loads. *Aquatic Ecology* **2016**, *50* (3), 351-366, Article. DOI: 10.1007/s10452-016-9594-z.

(21) Bridgeman, T. B.; Penamon, W. A. Lyngbya wollei in western Lake Erie. *Journal of Great Lakes Research* **2010**, *36* (1), 167-171. DOI: 10.1016/j.jglr.2009.12.003.

(22) National Water Information System data. U.S. Geological Survey: 2017.

(23) Delwiche, K.; Gu, J.; Hemond, H.; Preheim, S. P. Vertical transport of sediment-associated metals and cyanobacteria by ebullition in a stratified lake. *Biogeosciences* **2020**, *17* (12), 3135-3147. DOI: 10.5194/bg-17-3135-2020 (acccessed 2021-07-23T14:23:36). Mendoza-Lera, C.; Federlein, L. L.; Knie, M.; Mutz, M. The algal lift: Buoyancy-mediated sediment transport. *Water Resources*

Research **2016**, *52* (1), 108-118. DOI: 10.1002/2015wr017315 (acccessed 2021-07-23T14:22:59).

(24) Onodera, H.; Satake, M.; Oshima, Y.; Yasumoto, T.; Carmichael, W. W. New saxitoxin analogues from the freshwater filamentous cyanobacterium Lyngbya wollei. *Natural Toxins* **1997**, *5* (4), 146-151. DOI: 10.1002/19970504NT4.

(25) Zastepa, A.; Taranu, Z. E.; Kimpe, L. E.; Blais, J. M.; Gregory-Eaves, I.; Zurawell, R. W.; Pick, F. R. Reconstructing a long-term record of microcystins from the analysis of lake sediments. *Science of the Total Environment* **2017**, *579*, 893-901, Article. DOI: 10.1016/j.scitotenv.2016.10.211.

(26) EPA, O. *Harmful algal blooms: public water system and other Ohio EPA surface water monitoring*. (accessed 2021 August 8th).

(27) Renwick, W. H.; Sleezer, R. O.; Buddemeier, R. W.; Smith, S. V. Small artificial ponds in the United States: impacts on sedimentation and carbon budget. In *Proceedings of the Eighth Federal Interagency Sedimentation Conference*, 2006; pp 738-744.

(28) Chaffin, J. D.; Bratton, J. F.; Verhamme, E. M.; Bair, H. B.; Beecher, A. A.; Binding, C. E.; Birbeck, J. A.; Bridgeman, T. B.; Chang, X.; Crossman, J.; et al. The Lake Erie HABs Grab: A binational collaboration to characterize the western basin cyanobacterial harmful algal blooms at an unprecedented high-resolution spatial scale. *Harmful Algae* **2021**, *108*, 102080. DOI: 10.1016/j.hal.2021.102080 (acccessed 2021-08-13T22:45:59).

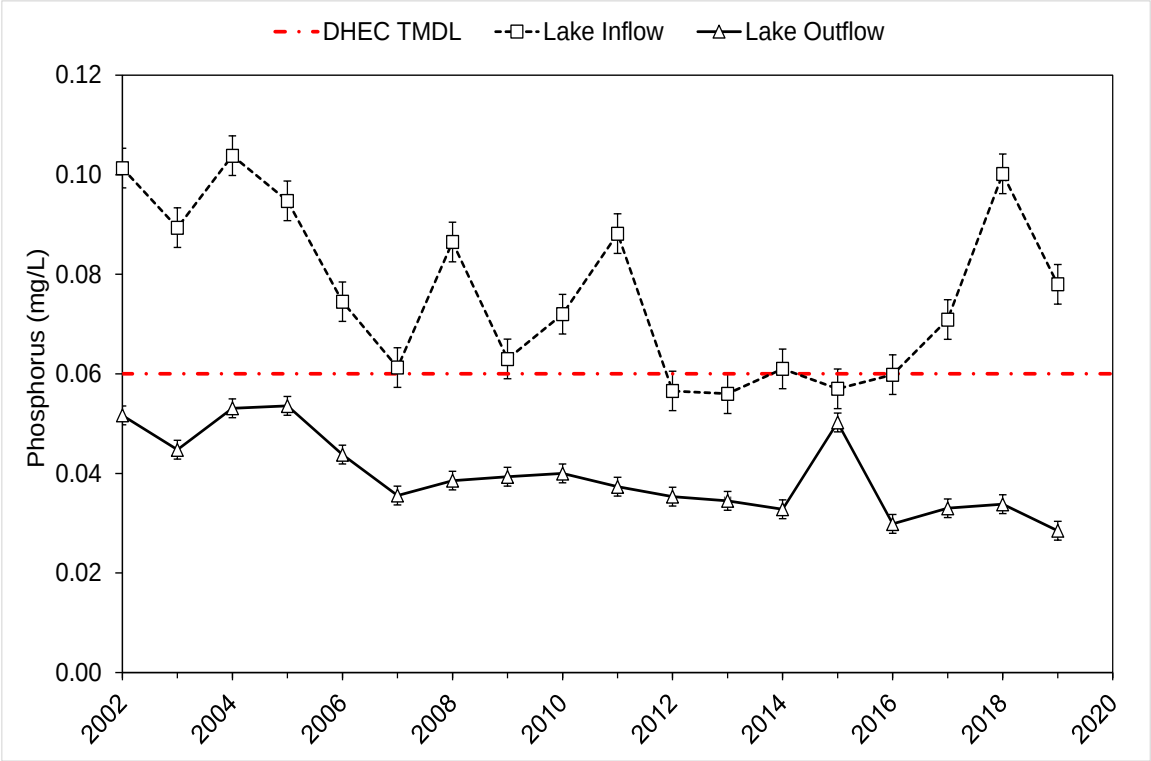

Figure 2.1 Historical annual average phosphorous concentrations were obtained at the Cedar Creek Dam (inflow, ■) and Lake Wateree Dam (outflow, ▲). Lower concentrations at the outflow indicated the lake was a sink for incoming phosphorous (average retention 46% over the period shown); data obtained through STORET and collected by South Carolina Department of Health and Environmental Control (SC DHEC). The dashed red line represents the current total maximum daily load for phosphorous (TMDL) set by SC DHEC.

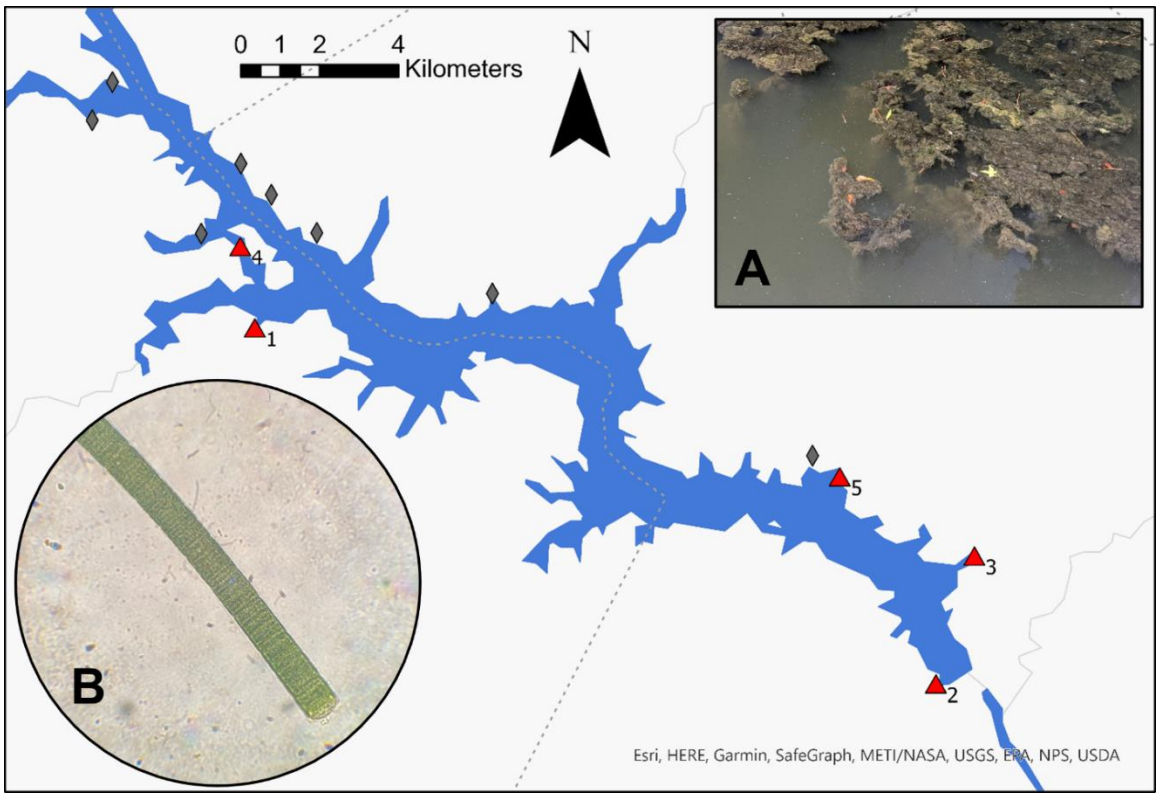

Figure 2.2 Microbial mats (A) were analyzed microscopically (B) and genetically and showed a preponderance of Lyngbya wollei in the biomass. Mats were sampled at multiple locations in Lake Wateree. Toxins were quantified (▲) and qualified (◊) at thirteen locations around the lake (sample coordinates provided in Table A.1).

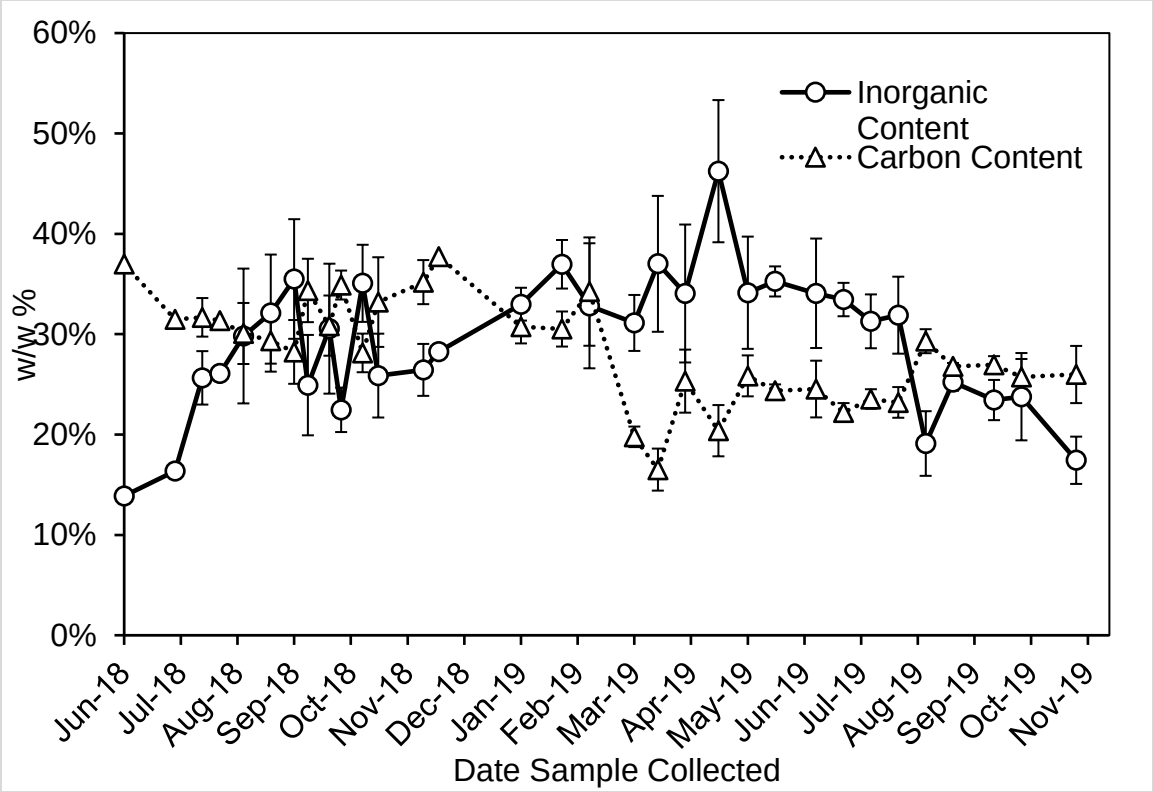

Figure 2.3 Lyngbya wollei-dominated microbial mats often incorporated more inorganic material (○) than carbon (Δ) at the monitored sites. The poor correlation between inorganic content of the mats and turbidity of the water column ($r^2 < 0.1$, not shown) indicated it was unlikely to be the source of the inorganic content, consistent with the hypothesis that sediments were the source of inorganic particulates in the mat.

Table 2.1 Models for cyanobacterial biomass (CBB) were developed by Beaulieu et. al. The characteristic name of the parameter used by STORET is reported for each equation. Units are µg/L for all concentration parameters, °C for temperature.

Model Equation	STORET Characteristic	Eq. #
$\log_{10}(CBB) = -0.48 + 0.11 \cdot (SWT)$	Temperature, water	(1)
$\log_{10}(CBB) = -3.18 + 1.11 \cdot \log_{10}(TN) + 0.10 \cdot SWT$	Kjeldahl nitrogen + Temperature, water	(2)
$\log_{10}(CBB) = -1.14 + 1.22 \cdot \log_{10}(TN)$	Kjeldahl nitrogen	(3)
$\log_{10}(CBB) = 1.24 + 1.11 \cdot \log_{10}(Chl\ a)$	Chlorophyll a	(4)
$\log_{10}(CBB) = 1.28 + 0.69 \cdot \log_{10}(TP)$	Phosphorous	(5)

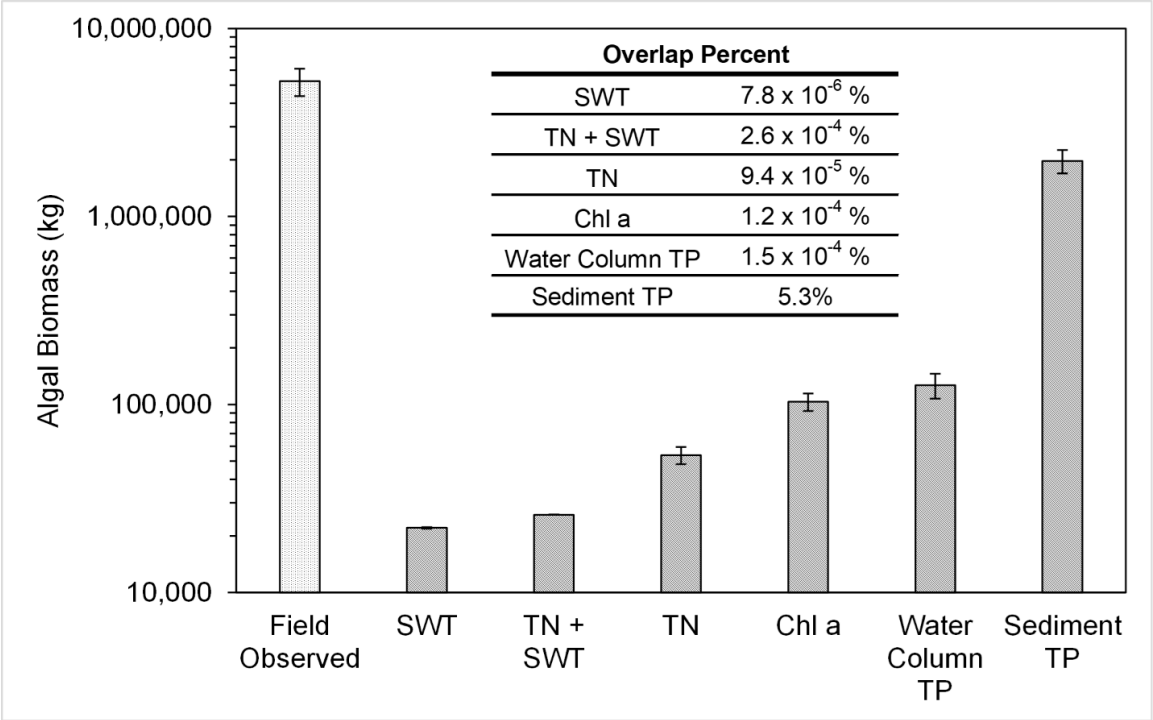

Figure 2.4 Cyanobacterial biomass (CBB) in Lake Wateree obtained from field observations and calculated from models developed by Beaulieu et al. Water quality parameters used to calculate CBB include surface water temperature (SWT), a combined model for total nitrogen and surface water temperature (TN+SWT), total nitrogen (TN), chlorophyll a (Chl a), and total phosphorous (TP). The TP model was used with both water column phosphorous as well as phosphorous from sediment measurements to calculate two different predictions of CBB. Inset shows overlap percent of Gaussian distributions of field observed and model calculated CBB.

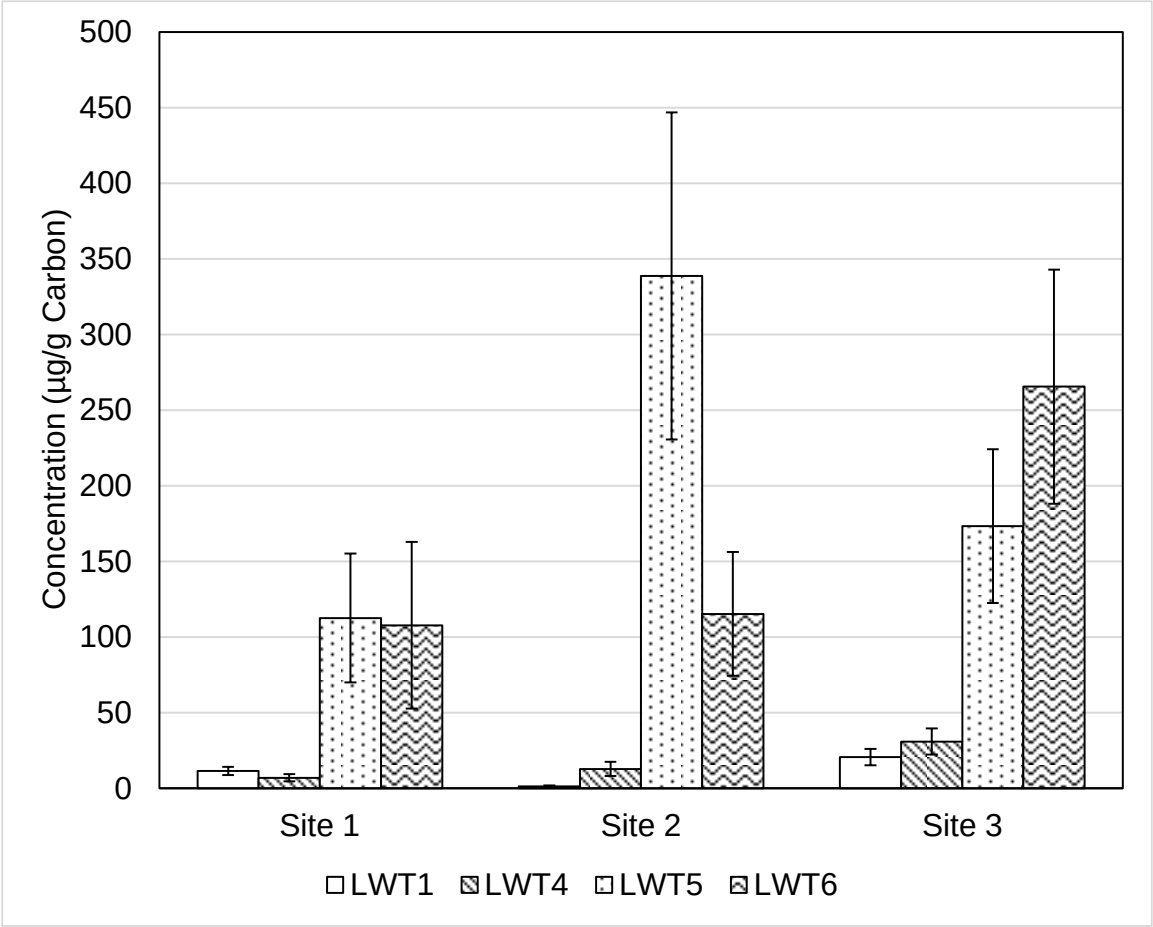

Figure 2.5 Concentration of each observed LWT in µg/g of carbon, separated by regularly monitored site. The summed total of the measured toxins was found by ANOVA to be statistically distinct at each location, supporting the treatment of each bloom site as a distinct colony.

Table 2.2 Table of coefficients for converting Lyngbya wollei biomass to the various LWTs. Uncertainty is presented as 95% confidence interval.

Toxin	α_x	Uncertainty
LWT1	5.83×10^{-7}	1.34×10^{-7}
LWT4	9.19×10^{-7}	2.10×10^{-7}
LWT5	1.10×10^{-5}	2.37×10^{-6}
LWT6	9.45×10^{-6}	2.03×10^{-6}

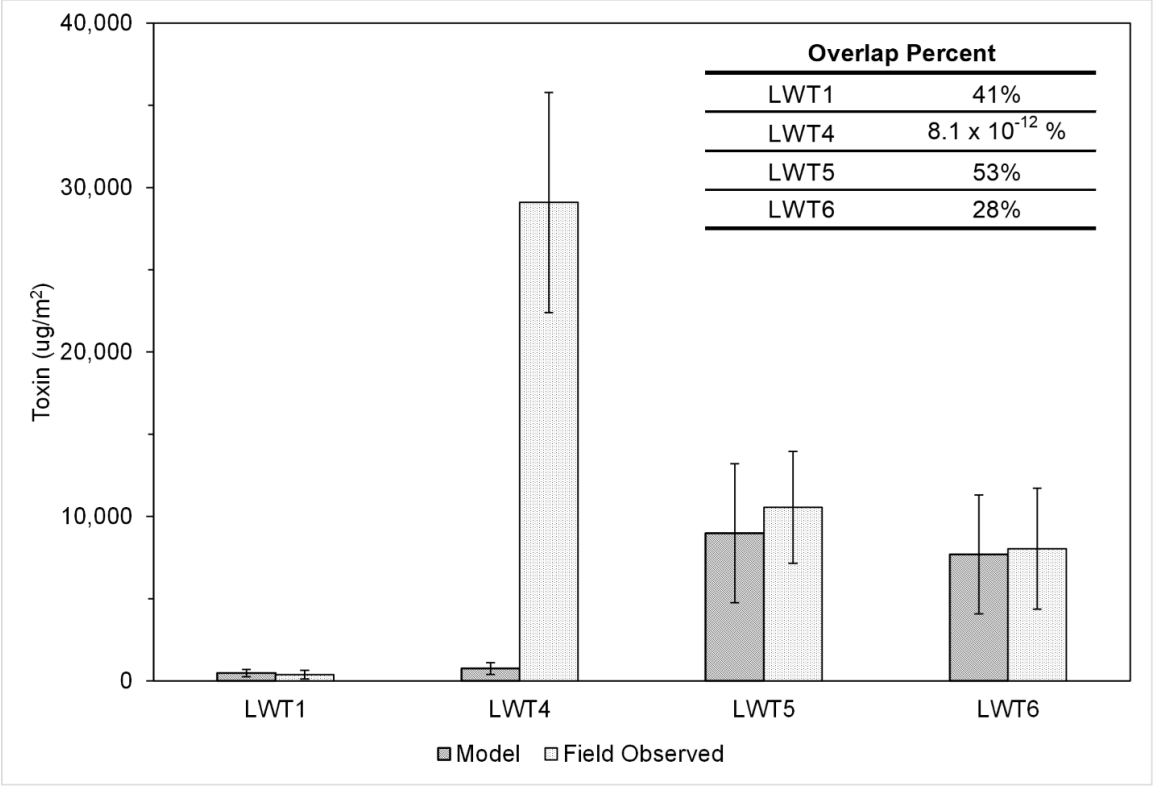

Figure 2.6 Modeled toxin per m^2 vs field observed toxin. Modeled toxin was corrected for inorganic content, habitable volume of the lake, and multiplied by the toxin:biomass ratio (Table 2.2). Measured toxin amounts were based on field samples; sediment phosphorous concentrations for the model were obtained from sediment core samples over the same period as the algal grab samples. The inset table shows the Gaussian overlap of the model for each LWT.

CHAPTER 3

PESTICIDE INDUCED RELEASE OF ALGAL TOXINS FROM A NATURAL SYSTEM[1]

[1] Putnam, S.P., Metz, T.T., and Ferry, J.L. To be submitted to *Harmful Algae*

3.1 ABSTRACT

The increasing prevalence of harmful algal blooms and their associated toxic products has led to many algal control strategies, including the application of pesticides to kill a target bloom. However, death of an algal bloom can have unintended consequences if harmful secondary metabolites such as toxins are released into the water column. Here we hypothesize that the toxin is stored within the cells and released through directed metabolic activity, not through cell death only. Natural samples of Microseira wollei were collected during a pesticide application in a local lake; toxin analysis showed a decrease in Lyngbya wollei toxins (LWTs) after pesticide application. Live samples were transported to the laboratory and dosed with realistic amounts of various pesticides used for algal control, monitoring the presence of toxin in the water column throughout the experiment. No pesticide caused any measurable amount of toxin release from the biomass. LWTs were measured after pesticide dosing by an acetic acid spike, showing 66 to 81% of initial toxin remaining. This experiment provides evidence that LWTs within Microseira wollei are isolated from the surrounding environment and are not released upon cell death by pesticide.

3.2 INTRODUCTION

As harmful algal blooms (HABs) increase in frequency and severity, they are becoming more of a threat to human health.[1, 2] Particularly in freshwater systems where surface water is processed for drinking, it is important to have safe and effective control methods for blooms. HABs pose several issues with drinking water, from taste and odor compounds to toxic secondary metabolites.

As a result, many agencies are starting HAB treatment programs to proactively control the growth and spread of algae.

There are many ways to eliminate or control HABs, including physical dredging and removal, nutrient management, reservoir drawdowns, and chemical pesticides. Frequently the cheapest and simplest solution for HAB control is through application of a chemical that kills the cells. There are several common modes of action for algal herbicides which are usually selected based on the specific species being treated. Copper or other metallic based pesticides are toxic to the cells and cause death directly once a threshold level is reached.[3] Other pesticides inhibit systems critical to reproduction and survival, like photosynthesis or lipid synthesis.[4] Oxidative pesticides are more commonly used with tougher filamentous algae like *Phormidium, Lyngbya,* and *Anabaena.* Strong oxidizers like percarbonate and potassium permanganate are typical; while these are very strong oxidizers, they are not specific and can lead to a variety of abiotic side reactions.

Typically only the biological results of a pesticide application are considered, and pesticide effectiveness is based only on reducing live cell counts in a given environment. However, HABs produce secondary metabolites that pose a human health risk and the release and fate of these metabolites must be considered as part of the effectiveness of the pesticide. Toxin release mechanisms vary depending on the specific algae. Physical release is possible from the lysing of cells and destruction of organelles that contain toxin. This is observed within the common harmful cyanobacterium *Microcystis aeruginosa*,

both with passive externally-caused death and programmed apoptosis.[5] There are also transport proteins that actively export toxin from the cells such as multidrug and toxin extrusion (MATE) proteins.[6] To fully assess the impacts of pesticides and ensure their application is a net benefit to human health, the release and subsequent fate of toxins must be examined.

Dean Swamp is an impounded area that is a part of Lake Marion in South Carolina (Figure 3.1). A bloom of *Lyngbya wollei* was persistent in the area, and as a result Santee Cooper Biological Services (who are responsible for the lake) decided to apply pesticide to the bloom. *Lyngbya wollei* produces the Lyngbya wollei toxins (LWTs) which are part of the saxitoxin family. Dean Swamp presented a unique opportunity to study a natural system during pesticide application that was relatively small and isolated from the larger lake. Benthic, filamentous blooms like *Lyngbya wollei* are common in the shallow reservoirs of the southeast and so this area is representative of a typical system in the region.

3.3 MATERIALS AND METHODS

3.3.1 SOLVENTS AND STANDARDS

Saxitoxin standards (100 µg/g in HCl) were supplied by the US Food and Drug Administration (USFDA) and used as surrogate standards for quantification. LC/MS grade acetonitrile was purchased from VWR, and formic acid and ammonium formate were purchased from Fisher Scientific. Nanopure water (18 MΩ cm) was prepared using an E-Pure water system (Barnstead, Dubuque, IA, USA).

3.3.2 FIELD SAMPLING AND DATA COLLECTION

Algal samples were collected from 4 different locations within Dean Swamp where *Lyngbya wollei* was present. Samples were collected starting May 26th 2020 through June 4th 2020, with the pesticide treatment on May 26th. The chosen pesticide for application was Captain XTR (SePRO), a copper ethanolamine complex, dosed to a final concentration of 1 ppm in the treated area. Field measurements were also collected using a ProPlus sonde (YSI); dissolved oxygen and pH were recorded at multiple points throughout the lake.

3.3.3 ALGAE EXTRACTION AND LIQUID CHROMATOGRAPHY MASS SPECTROMETRY QUANTIFICATION

All extractions were performed on 100 mg subsamples of lyophilized algae from the different sites. The LWTs were isolated from the algae matrix by extraction into 10.0 mL of 0.100 M acetic acid.[7] Extraction was accomplished by first shaking the sample to ensure thorough wetting followed by 15 min of sonication. Samples were then centrifuged for five min. After centrifugation an aliquot of acid extract was removed, filtered through a 0.45-micron nylon filter, diluted by a factor of 50 in 0.100 M acetic acid to minimize signal suppression, and analyzed by liquid chromatography mass spectrometry.

All LWTs were quantified against an external saxitoxin standard due to the lack of commercially available standards. Samples were analyzed using a Waters (Milford, MA, USA) Acquity ultra performance liquid chromatography (UPLC) coupled with a Xevo triple quadrupole mass spectrometer (MS/MS) equipped with an electrospray ionization source (ESI).[8] All separations were performed

using a BEH Amide (2.1x150 mm) 1.7 µm particle size column (Waters). The mobile phases were aqueous 5.6 mM formate buffered at pH 3.5 (A) and 95/5, acetonitrile/water 5.6 mM formate buffer at pH 3.5 (B). The chromatographic method began with 80% B held for one minute, ramped to 60% B over the next 3 minutes and held for 2 minutes, at 7 minutes returned to the original conditions over one minute (80% B) and held for re-equilibration for 8 minutes (16 minutes total). Flow rate was 0.35 mL/min throughout.

3.3.4 TOTAL CARBON ANALYSIS

Total carbon and inorganic (non-combustible) content analysis was performed using a Shimadzu TOC-L instrument with a solid sample module (SSM) calibrated weekly against a glucose standard. Approximately 40 mg of lyophilized algae was placed in a tared ceramic boat and combusted at 900°C with excess oxygen to measure total carbon. This sample was weighed again post-combustion to determine the mass of the remaining inorganic material.

3.3.5 TOXIN STABILITY AND REACTION QUENCHING

To preserve each timepoint sampling until toxin analysis could be performed, several quenching agents were tested to determine the stability of toxin in the presence of the pesticides used. Ascorbic acid, citric acid, cysteine, and methanol were all tested with a toxin extract and sampled to determine the amount of toxin degraded over time.

3.3.6 PESTICIDE DOSING

Live *Lyngbya wollei* samples from Dean Swamp were brought back to the lab for dosing with pesticide. 100 mL of coarse filtered lake water was combined

in a flask with 5 g of wet algae, and 1 mL of pesticide solution. Pesticides were all chosen based on their recommended use for algae control and were dosed at the maximum recommended level from the label (Table 3.1). Each pesticide experiment was repeated in triplicate along with a lake water control. Flasks were stirred on an orbital incubator for 72 hrs open to atmosphere and lit with normal room lights. A 100 uL aliquot was removed at each time point for toxin monitoring and diluted with 900 uL of methanol to quench any pesticide reactions. Reactions were monitored every 1 hour for the first six hours, then every 3 hours for the next 30 hours, then every 6 hours for the next 36 hours.

A second experiment was performed in the same way as above but with increasing dosages of Captain XTR. Dosages were 1, 5, 10, 50, and 100 ppm metallic copper and were run alongside a lake water and 0.1 M acetic acid control experiments. These reactions were similarly monitored for 72 hours, after which acetic acid was spiked into each flask to a final concentration of 0.1 M.

3.4 RESULTS AND DISCUSSION

3.4.1 FIELD OBSERVATIONS AND TOXIN

Dissolved oxygen (DO) and pH were measured at five different sites in the Dean Swamp area immediately before and after pesticide treatment, as well as six days after treatment. DO was low at some of the sites before treatment, ranging from 6.75 mg/L down to 2.36 mg/L (Figure 3.2). The day after pesticide treatment DO dropped for all the measured sites, ranging from 5.33 to as low as 0.39 mg/L. When DO was measured again six days after treatment, levels had returned to a more normal concentration, ranging from 6.89 to 4.78 mg/L. pH did

not have the same pattern of change, with only one of the sites showing a significant drop after treatment from 6.33 to 5.14 (Figure 3.3). Six days after treatment pH stabilized for all sites in a range of 6.4 - 6.8.

A small fish kill was observed the day after treatment, consisting of around 20 observed dead fish. Species composition was primarily Threadfin and Gizzard Shad, with some Bluegill and Brown Bullhead Catfish also observed. Low dissolved oxygen levels and toxicity from the copper-based algaecide are both stress factors that can lead to fish kills. However, the dead fish were primarily smaller species, which usually are less affected by low dissolved oxygen. This suggests that the primary driver of the kill was toxicity, from either the copper algaecide or toxin that was released from algal mats following the application.

Toxin samples collected from four sites were analyzed for total LWT content, normalized against the carbon in the sample to account for the variable inorganic material of mat grab samples (Figure 3.4). Three of the four sites showed higher toxin levels before the pesticide treatment, with concentrations falling in the days after treatment. Toxin concentration stabilized with all sampled locations showing less than 350 ug toxin per gram of carbon. This drop in toxin levels within the biomass was hypothesized to be due to release of toxin out of the cells during the pesticide application, whether by physical destruction of cell structures or by a stress induced biotic response. In order to further characterize this response, a series of lab experiments were developed to examine the release mechanism in a more controlled environment.

3.4.2 TOXIN STABILITY IN THE PRESENCE OF PESTICIDES

Since the analysis of each set of timepoint samples took longer than the spacing between timepoints, a preservation method was needed to ensure sample stability until analysis could be performed. To determine the degradation of toxin in the absence of quenching, the percentage of remaining toxin after one hour as compared to a blank was plotted (Figure 3.5). The copper-based pesticides did not cause much degradation, but the oxidative pesticides removed 30 to 70% of toxin. The four selected quenching agents were tested with Diquat as it caused the greatest degradation and the reaction was allowed to progress for 72 hours, the maximum hold time of the samples (Figure 3.6). 50% methanol was chosen as the most effective, showing no statistically significant degradation after 72 hours.

3.4.3 PESTICIDE RELEASE

Throughout the initial experiment, none of the experimental conditions showed any detectable release of toxin into the aqueous phase. Although dosings were chosen at the highest recommended level, micrographs of the algae taken before and after the pesticide experiment showed no significant visual differences in the algae. *Lyngbya wollei* is anecdotally known to be a difficult species to kill, and so it was hypothesized that the pesticide dosage was not sufficient to cause cell death and release of toxins under the artificial laboratory conditions.

3.4.4 EFFECT OF COPPER DOSING AND ACETIC ACID

After observing no toxin release, a second experiment was designed and performed to increase the dosing of one selected pesticide (Captain XTR) over a range extending to two orders of magnitude higher than the initial dosage. Despite this increase in pesticide concentration, only minimal toxin was released, less than 2% of the amount observed by a standard acetic acid extraction (Figure 3.7). Once acetic acid was added at the end of this 72 hour experiment, toxin was released into the water at 66 to 81% of that present from the standard acetic acid extraction.

3.4.5 CELL DEATH AND TOXIN RELEASE

Experimental conditions were chosen to ensure the death of cells, yet only minimal toxin release was observed. This indicates that the biomass does not release toxin under cell death conditions caused by pesticide modes of death. The presence of significant amount of toxin remaining in the cells after 72 hours of pesticide exposure demonstrates that this toxin reservoir within the cells is relatively isolated from the outside environment surrounding the cell.

Given that acetic acid causes consistent release of toxin from cells, the process of toxin export may be influenced by the concentration of protons in solution. Since cell death is not enough to cause release, there may be an active process by which the cell releases its toxin; this process could be promoted by the presence of acid. One possible method of export is the multidrug and toxin extrusion (MATE) protein. MATE transports organic cations across membranes by exchanging them with protons.[6] The LWT's dual positive charges make it an

ideal candidate for transport by a MATE protein, and this transport process explains the lack of toxin release with cell death.

A limited set of conditions where toxin release is possible has a large impact on potential treatment strategies. If cell death is achieved without activating the toxin export process, a significant health risk of algal control can be reduced. The toxins would remain within their structures in the cell instead of being released all at once, allowing the toxin to degrade slowly over time. However, further studies of toxin fate in the environment are need to determine the lifetime within dead cells and assess the risk of dead algal biomass.

3.5 REFERENCES

1. Visser, P. M.; Verspagen, J. M. H.; Sandrini, G.; Stal, L. J.; Matthijs, H. C. P.; Davis, T. W.; Paerl, H. W.; Huisman, J., How rising CO2 and global warming may stimulate harmful cyanobacterial blooms. *Harmful Algae* **2016,** *54*, 145-159.

2. Paerl, H. W.; Huisman, J., Climate change: a catalyst for global expansion of harmful cyanobacterial blooms. *Environmental Microbiology Reports* **2009,** *1*, (1), 27-37.

3. Bishop, W. M.; Rodgers, J. H., Responses of Lyngbya wollei to Exposures of Copper-Based Algaecides: The Critical Burden Concept. *Archives of Environmental Contamination and Toxicology* **2012,** *62*, (3), 403-410.

4. Nagai, T.; Taya, K., Estimation of herbicide species sensitivity distribution using single-species algal toxicity data and information on the mode of action. *Environmental Toxicology and Chemistry* **2015,** *34*, (3), 677-684.

5. Hu, C.; Rzymski, P., Programmed Cell Death-Like and Accompanying Release of Microcystin in Freshwater Bloom-Forming Cyanobacterium Microcystis: From Identification to Ecological Relevance. *Toxins* **2019,** *11*, (12), 706.

6. Nies, A. T.; Damme, K.; Kruck, S.; Schaeffeler, E.; Schwab, M., Structure and function of multidrug and toxin extrusion proteins (MATEs) and their relevance to drug therapy and personalized medicine. *Archives of Toxicology* **2016,** *90*, (7), 1555-1584.

7. Foss, A. J.; Phlips, E. J.; Aubel, M. T.; Szabo, N. J., Investigation of extraction and analysis techniques for Lyngbya wollei derived Paralytic Shellfish Toxins. *Toxicon* **2012,** *60*, (6), 1148-1158.

8. Smith, M. L.; Westerman, D. C.; Putnam, S. P.; Richardson, S. D.; Ferry, J. L., Emerging Lyngbya wollei toxins: A new high resolution mass spectrometry method to elucidate a potential environmental threat. *Harmful Algae* **2019,** *90*, 101700.

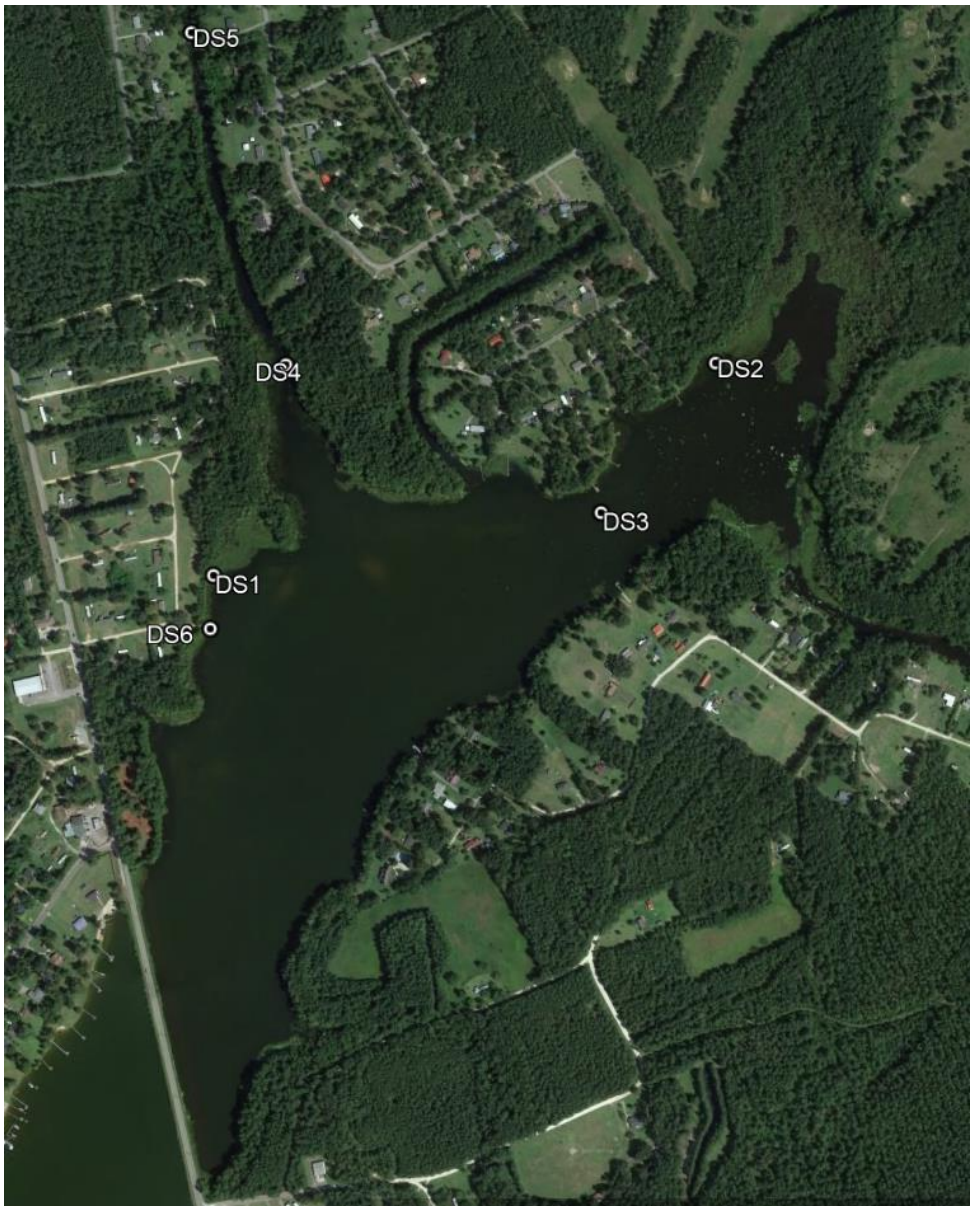

Figure 3.1 Aerial image of Dean Swamp showing the six sampling locations used for grab samples and water parameter measurements. The causeway that impounds the area and separates it from Lake Marion is seen in the lower left of the image.

Table 3.1 Trade name, active ingredient, and dosage concentration for each of the pesticides used in this study. All dosages were selected from the maximum allowable dose from the label or EPA documentation, and converted to mg/L.

Pesticide	Active Ingredient	Dosage (mg/L)
Captain XTR	Copper Ethanolamine	**11.0**
Diquat	Diquat dibromide	**0.7**
Copper Sulfate	Copper sulfate	**2.0**
Phycomycin	Sodium percarbonate	**16.7**
Oxone	Potassium monopersulfate	**5.2**
Cairox	Potassium permanganate	**10**

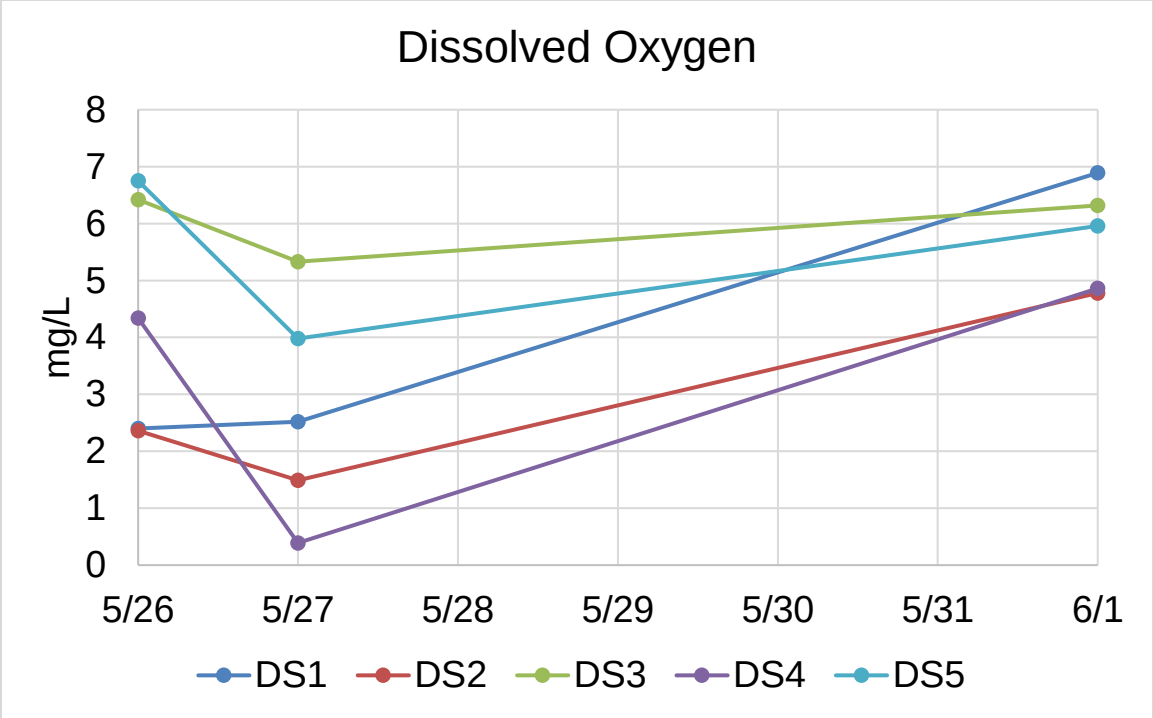

Figure 3.2 Dissolved oxygen measurements for five locations within Dean Swamp. Pesticide application was performed after the first measurement was collected. After an initial drop in oxygen concentration, all sites recovered to levels near the concentration before treatment.

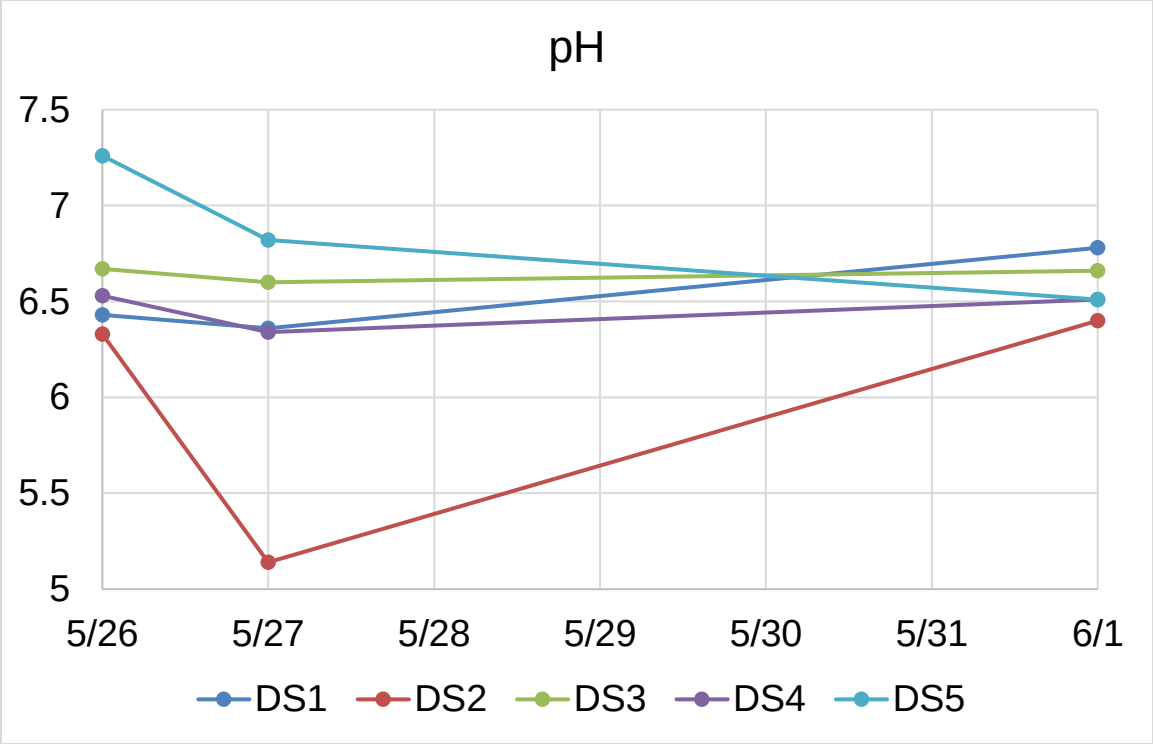

Figure 3.3 pH measurements for five locations within Dean Swamp. Pesticide application was performed after the first measurement was collected. Only minor variation in pH was seen over time and between sites, with the exception of DS2 which experienced a more pronounced drop before returning to normal levels.

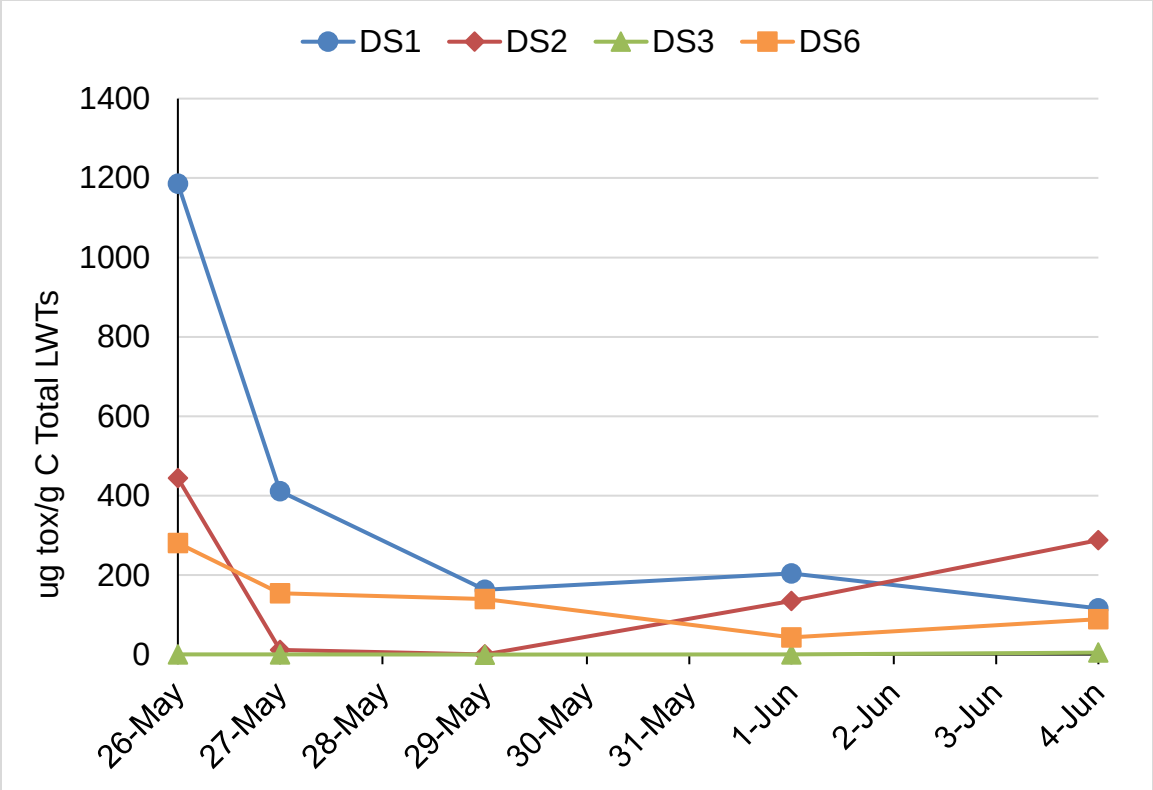

Figure 3.4 Lyngbya wollei toxin (LWT) measurements made on algal grab samples before and after pesticide application. The pesticide was applied following the first data point. Toxin concentration is normalized against carbon content to account for differences in inorganic material entrained within samples. DS1, DS2, and DS6 all showed significant drops in intracellular toxin after treatment, with DS3 showing minimal toxin throughout.

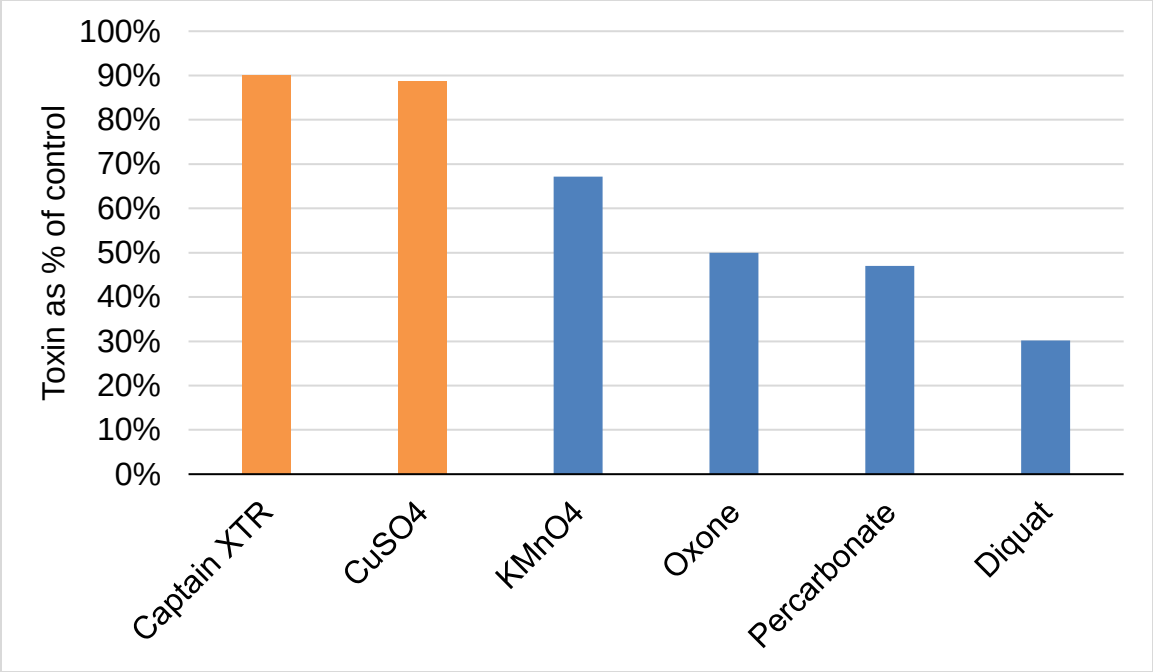

Figure 3.5 Stability of LWTs in the presence of pesticides. All pesticides were added to a toxin extract at the level in Table 3.1 and allowed to react for one hour. Concentration is presented as a percent of the control sample with no pesticide added. The copper-based pesticides are shown in green, and oxidative pesticides are in blue.

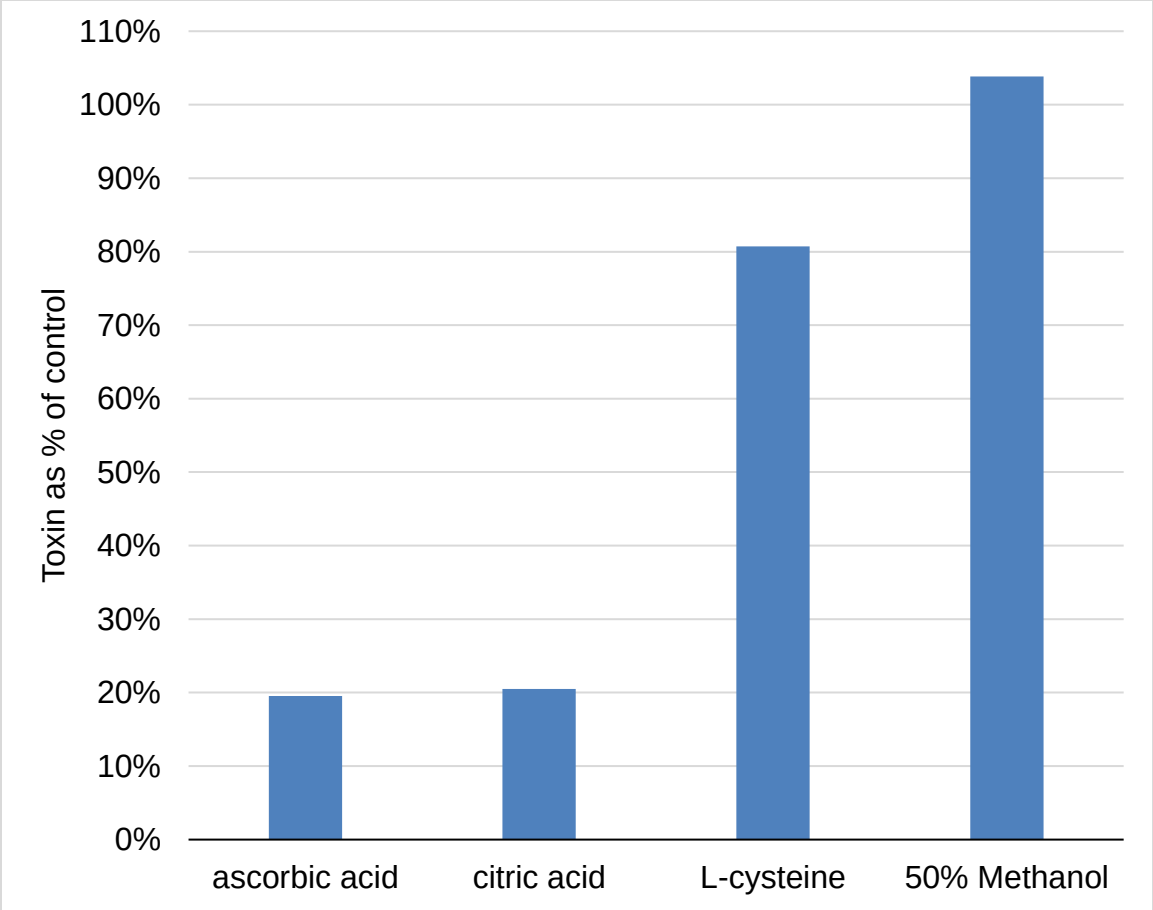

Figure 3.6 Relative toxin degradation of four selected quenching agents. All quenching agents were tested with Diquat and allowed to react for 72 hours. No statistically significant degradation was observed with 50% methanol as the quenching solution.

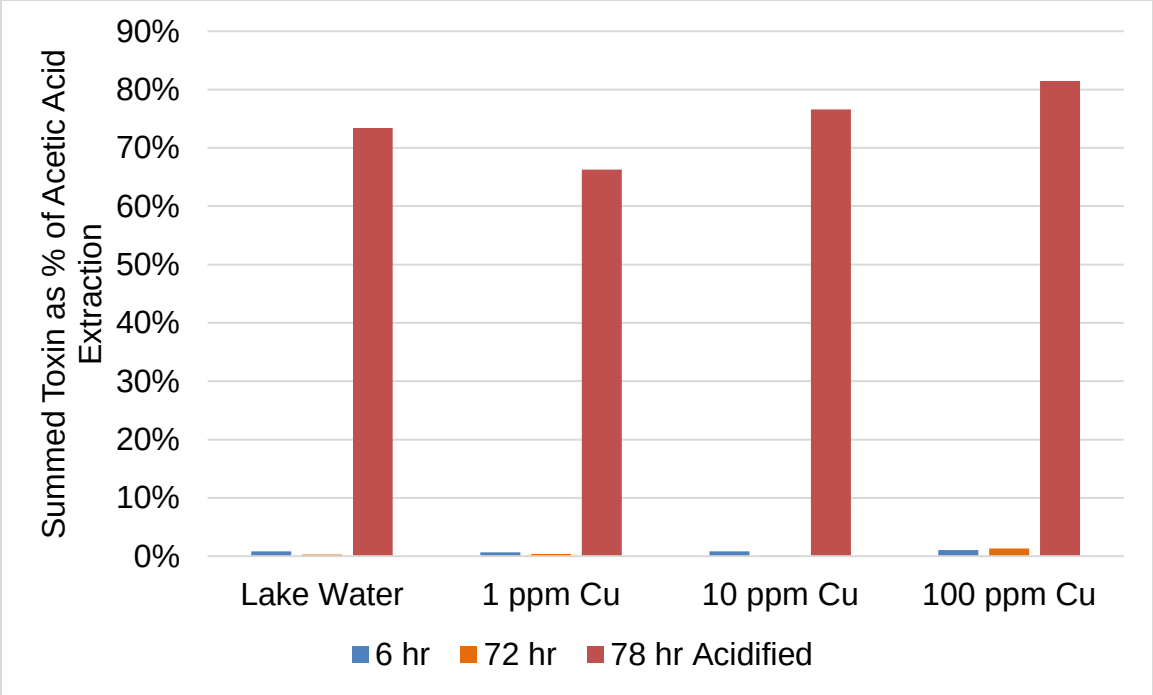

Figure 3.7 Summed toxin of reactions performed on algae in the presence of lake water and increasing dosages of Captain XTR, labeled here by the ppm metallic copper present in solution. Very minimal toxin release was observed in the 72 hours of the experiment, less than 1.5% of the amount present in the cells when extracted with acetic acid. After acetic acid was added to the reactors, toxin was released.

CHAPTER 4

ACYL-HOMOSERINE LACTONE QUANTIFICATION THROUGH DIRECT INJECTION LIQUID CHROMATOGRAPHY MASS SPECTROMETRY[1]

[1] Putnam, S.P., Leighton, R.E., Decho, A.W., and Ferry, J.L. To be submitted to *Journal of Chromatography A*

4.1 ABSTRACT

Molecular techniques such as liquid chromatography mass spectrometry (LCMS) can provide powerful and rapid analysis for biological samples that are frequently investigated through biosensors and assays. Here we show that LCMS can be used to provide sensitive, fast, and molecule specific analysis of acyl-homoserine lactones (AHLs) in lab cultured and naturally collected samples. AHLs are quorum sensing molecules used in chemical communication of microbes. As they are transient signals, they are found in nature at low concentrations and are easily degraded. Instrumental limits of quantification were found in aqueous solution for 10 AHLs to be 0.50 nM or lower with a signal-to-noise ratio of at least 10. Injection solvent affects were tested and a 50% acetonitrile solvent was found to increase the sensitivity of the instrument. Natural samples of *Lyngbya* and *Phormidium* were analyzed for AHLs alongside a lab-grown culture of *Pseudomonas* that was confirmed to produce AHLs. Biologically produced AHLs from the *Pseudomonas* culture were qualified and quantified. *N*-heptanoyl-DL-homoserine lactone (C7) was spiked into all samples as an internal standard to determine the matrix effects on and biological consumption of an AHL signal.

4.2 INTRODUCTION

Quorum sensing is a method of communication within microbial communities that relies on the production of molecular signals that are released into the environment.[1] These signals allow large microbial mats to communicate between cells and regulate group behavior such as biofilm formation, light

production, and creation of secondary metabolites. Once these molecules reach a certain “threshold” concentration a difference in gene expression is observed.[2]

The acyl-homoserine lactones (AHLs) are a group of molecules consisting of a five-membered lactone ring with a variable amide-linked side change, ranging in length from 4 – 18 carbons. Many different genera of bacteria use AHLs to communicate, with community responses depending on the specific AHL structure.[3] These signals are an important connection between environmental conditions and microbe behavior; the link between conditions and response can allow for prediction of microbial communities. Many bacteria can be pathogenic in some way, posing a significant human health risk. The pathogenic response of the community can be dependent on environmental conditions; only under the right conditions is a threshold of quorum sensing compounds reached and a specific response caused. In addition to predictive capability, the quorum sensing link provides a means by which to control microbe behavior, either promoting certain beneficial behavior or limiting harmful ones.

Detection of AHLs is frequently accomplished through bioassays that directly react to the presence of the molecules and produce a colorimetric response.[4] Although this method gives a true biological response to these molecular signals, it lacks the ability to definitively discern between different individual molecules and can be difficult to quantify.[5] Additionally, detection limits can often be high and the analysis requires a time consuming liquid-liquid extraction. Liquid chromatography mass spectrometry (LCMS) methods have several advantages over bioassays, including speed of analysis, specificity, and

detection limits.[6, 7] By directly injecting aqueous samples and avoiding an extraction and concentration step, sample throughput is greatly increased.

The ability to investigate AHL responses with knowledge of individual molecule concentrations gives insight into which particular signaling “switch” causes a specific behavior. This type of analysis allows the investigation of quorum sensing and signaling on the chemical level, examining the root causes and not just the biological outcomes. LCMS methods can also be combined with the use of a bioassay as a prescreen to effectively examine natural samples and identify quorum sensing in the environment. This combination of methods can enable observations outside of controlled lab cultures and allow for more understanding of signaling in nature.

4.3 MATERIALS AND METHODS

4.3.1 SOLVENTS AND STANDARDS

N-butyryl-DL-homoserine lactone (C4), *N*-hexanoyl-DL-homoserine lactone (C6), *N*-heptanoyl-DL-homoserine lactone (C7), *N*-octanoyl-DL-homoserine lactone (C8), *N*-decanoyl-DL-homoserine lactone (C10), *N*-dodecanoyl-DL-homoserine lactone (C12), *N*-(3-oxohexanoyl)-DL-homoserine lactone (3oC6), *N*-(3-oxooctanoyl)-DL-homoserine lactone (3oC8), *N*-(3-oxodecanoyl)-DL-homoserine lactone (3oC10), *N*-(3-oxododecanoyl)-DL-homoserine lactone (3oC12), and *N*-(3-oxotetradecanoyl)-DL-homoserine lactone (3oC14) were purchased from Sigma Aldrich. LC/MS grade acetonitrile was purchased from VWR, and formic acid was purchased from Fisher Scientific.

Nanopure water (18 MΩ cm) was prepared using an E-Pure water system (Barnstead, Dubuque, IA, USA).

4.3.2 CELL CULTURING AND FIELD SAMPLE COLLECTION

The bacterial strains were used as follows: *Pseudomonas aeruginosa* (PAO1 – ATCC BAA-47) for acyl homoserine lactone extraction; *Agrobacterium tumefaciens* (NTL4) as the biosensor for AHL detection and confirmation. Tryptic soy broth (TSB) was used for maintenance and growth of PAO1. 10 µL of cryogenic stock (maintained in 25% final volume glycerol at -80°C) of PAO1 was taken, pipetted on TSB agar plates, streaked to isolation, then incubated overnight (16 hours) at 30°C. The next day a single bacterial colony was taken and used to inoculate 5 mL TSB, incubated overnight (16 hours) with shaking (180 rpm) at 30°C. 50 µL of the overnight culture was used to inoculate three conical tubes each containing 49.05 mL of fresh TSB media, incubated with shaking (180 rpm) at 30°C and each culture grown until early stationary phase (36 hours). The stationary phase cultures were then centrifuged (4000 rpm, 10 minutes), and supernatant taken, and syringe filtered (0.22 µM, PES membrane) and acidified (~pH 2) for liquid-liquid extractions and/or LC/MS analysis.

Luria-Bertani (LB) broth supplemented with tetracycline (5 µg/mL) and streptomycin (50 µg/mL) was used for maintenance and growth of NTL4. 10 µL of cryogenic stock (maintained in 25% glycerol at -80°C) of NTL4 was taken, pipetted on LB agar plates, streaked to isolation, then incubated for 48 hours at 30°C. A single bacterial colony was taken and used to inoculate 5 mL LB, incubated overnight (16 hours) with shaking (180 rpm) at 30°C. 50 µL of the

overnight culture was used to inoculate 49.05 mL of fresh LB media, incubated with shaking (180 rpm) at 30°C and grown until late exponential phase (32 hours). Then the 50 mL of late exponential phase NTL4 was quickly mixed with melted 100 mL of LB with 1.12 grams of agar and 10 mg X-gal (500 µL of 20 mg/ml stock in DMF) to use for pouring onto a thin layer chromatography plate.

Grab samples containing *Lyngbya* and *Phormidium* were collected from naturally occurring colonies in Lake Wateree, SC. Algal samples were wrung out to remove excess water and transported back to the laboratory. Samples were confirmed to contain the target algae by microscopy. All analysis was performed within 6 hours of collection in the field.

4.3.3 AHL LIQUID-LIQUID EXTRACTION AND TLC BIOSENSOR OVERLAY CONFIRMATION ASSAY

45 mLs of filtered and acidified PAO1 supernatant was mixed with three equal volumes of acidified ethyl acetate (135 mL, 0.5% acetic acid) and incubated at room temperature (20°C) for 10 mins with shaking (180 rpm) The ethyl acetate supernatant mixture was allowed to settle in separatory funnel, and ethyl acetate fractions (top layer) taken and pooled. This process was repeated two more times, pooling all ethyl acetate fractions together. The pooled ethyl acetate fractions were then subjected to rotary evaporation in a round bottom flask until only residue remained. The residue was scraped from flask with a sterile spatula and resuspended in 2 mL acidified ethyl acetate (0.5% acetic acid) and stored at -80°C until used for spot plating TLC plate for biosensor overlay assay.

Stock solutions (1mM) of AHLs used for the TLC biosensor overlay confirmation assay were prepared by dissolving AHLs in ethyl acetate that had been acidified with glacial acetic acid (0.05% [vol/vol]), and stocks were stored at −20°C. The AHLs used in this biosensor confirmation study were as follows: *N*-3-oxododecanoyl-L-homoserine lactone (3OC12), *N*-3-oxooctanoyl-L-homoserine lactone (3OC8), N-butyryl-L-Homoserine lactone (C4). 10 µL of 5 µM of the AHLS were spotted onto a TLC plate, 2 cm from bottom of plate, 2 cm apart, allowed to dry, then plate was put into a glass chamber containing 200 mL 60% methanol and allowed for chromatogram to develop until solvent to front is approximately 15 cm from starting line (~ 3 hours). TLC plate was then removed from glass chamber, dried in fume hood, and then plate labeling tape was placed around edge of plate to form a wall to prevent spill from the biosensor bacteria-soft agar mixture. The plate was then prewarmed for 10 mins at 37°C, then the bacteria biosensor-soft agar mixture (150 mL) was then poured onto TLC plate, allowed to solidify, and then placed in sterile plastic tub and incubated for 18-24 hours at 30°C. Developed blue spots on plate indicate NTL4 detecting AHLs, with the large chained AHLS appearing near the origin (bottom of plate) and smaller chained AHL appearing farther along the plate.

4.3.4 BIOLOGICAL SAMPLE PROCESSING AND RECOVERY ANALYSIS

For the Pseudomonas culture, a 15 mL aliquot was removed from each inoculation and spiked with C7 AHL to a final concentration of 100 nM. C7 was chosen as an internal standard as it is infrequently found as a signal in naturally occurring microbial communities. This solution was then centrifuged at 3,600 rcf

for 5 minutes, then 10 mL of supernatant was removed and filtered with a 0.22 µm filter. The sample was then acidified with hydrochloric acid to a final concentration of 0.015 M to ensure closing of the lactone ring for analysis.[8] This process was repeated spiking an equivalent volume of deionized water instead of C7 as a control.

For the naturally collected samples, approximately 500 mg of algae was combined with 15 mL of lake water and briefly shaken. This suspension was then spiked, centrifuged, filtered, and acidified in the same way as above. Samples were quantified by LCMS to determine the recovery of C7 from each sample.

4.3.5 LIQUID CHROMATOGRAPHY MASS SPECTROMETRY

All qualification and quantification was performed on a Acquity ultra performance liquid chromatography (UPLC) system coupled with a Xevo TQ tandem quadrupole mass spectrometer (MS/MS) equipped with an electrospray ionization (ESI) source (Waters Corporation, Milford, MA, USA). Separations were performed on a BEH C18 (2.1 x 50 mm, 1.7 µm particle size, Waters) column heated to 30 °C. The mobile phases were water with 0.1% by volume formic acid (A) and acetonitrile with 0.1% by volume formic acid (B). A mobile phase gradient was run starting at 5% B held for 0.25 minutes, ramped to 95% B over 3.25 minutes and held for 0.5 minutes, then ramped to 5% B over 1 minute (5 minutes total).[6] Flow rate was 0.5 mL/min throughout.

All AHLs were analyzed in positive mode ESI with capillary voltage 1.50 kV, desolvation temperature 500 °C, desolvation gas flow 800 L/hr, cone gas flow

75 L/hr, and source temperature 150 °C.[9] All quantification was done based on the common lactone fragment present for all AHLs at m/z 102. Cone voltage and collision energy for each analyte are listed in Table 4.1.

4.3.6 CALIBRATION AND LIMIT OF DETECTION

Aqueous calibration solutions were prepared from stock standards in acetonitrile, with a final acetonitrile concentration no greater than 1% by volume. Calibration curves were run as a mixture of all AHLs, with the chromatographic method separating all peaks. Further dilutions of calibration solutions were made to find the instrumental limit of detection for AHLs in aqueous solution. Standards were run from 125 µM down to 0.1 µM. A calibration curve was also prepared in a 50% acetonitrile solution to test the solvent response of AHLs.

4.4 RESULTS AND DISCUSSION

4.4.1 CHARACTERISTICS OF AHLS

Instrument response of AHLs is relatively even across all tested AHL standards, with the 3-oxo AHLs exhibiting higher slopes and therefore greater sensitivity (Figure 4.1). All calibration curves were repeated in triplicate and showed good repeatability between trials. All AHLs exhibited a higher slope when injected in a 50% acetonitrile solution, with improvement ranging from 13% to 194% better than aqueous solution (Table 4.2). However, this effect does not scale with the length of the acyl side chain. Solubility of AHLs in aqueous solution decreases with increasing molecular weight and side chain length, but the concentrations used in this experiment are well below the solubility limit for the

AHLs used.[10] This indicates an increase in signal that came from the electrospray ionization efficiency, but without a trend in the data such an effect was difficult to elucidate.

The side chain length of AHLs increasing linearly with molecular weight leads certain characteristics of the materials to be highly predictable, namely chromatographic retention time. Increased side chain length leads to more non-polar molecules that interact more strongly with the non-polar stationary phase of the column and are retained longer. When a linear regression fit was applied separately to the alkyl and 3-oxo groups of AHLs a highly linear r^2 of 0.9934 and 0.9982 respectively was observed (Figure 4.2). This predictable relationship between mass and retention time allows for accurate estimation of AHL retention times without standards and can help identify unknown molecules that are part of the same family.

4.4.2 INSTRUMENTAL LIMIT OF DETECTION

Since AHLs are signals that by nature degrade quickly, it is necessary to be able to detect very low concentrations. Although there is no conclusive agreement on what concentration the threshold for communication is, it is likely well below 100 nM. This low concentration combined with degradation means a low detection limited is needed for investigation of AHLs in the environment. Calibration curves from 125 nM down to 0.1 nM were run for each AHL to determine the limit of quantification (Figure 4.3). Quantifiable signals were identified as an average signal-to-noise ratio of 10 or greater. A limit of quantification was found for each AHL and shown in Table 4.3. With the

exception of C8, all AHLs were quantifiable at 0.5 nM or less. C8 had a limit of 2.5 nM, which could be due to an interference with ionization efficiency from injecting all AHLs as a mix. Instrument quantification levels two to three orders of magnitude lower than the purported natural level allow for detection of natural signals even after significant degradation.

4.4.3 NATURAL SAMPLE AHL DETECTION

Extraction and detection were first tested with a verifiable and controlled lab culture known to produce AHLs. *Pseudomonas aeruginosa* was selected as it is known to produce several different AHL signals. After initial growth, the culture showed positive results for AHLs by the colorimetric screening assay using NTL4 (Figure 4.4). Although this method involved a significant concentration step to activate the bioassay, it gave a positive binary result to confirm the sample was suitable for further analysis by LCMS.

The naturally collected samples of *Phormidium* and *Lyngbya* were also analyzed by LCMS, but no detectable AHLs were found. This result emphasized the utility of biological screening before extraction and analysis. A bioassay positive result allows the development of methods with prior knowledge that the molecule is present; otherwise it is difficult to distinguish between failure of methods and lack of presence of the analyte. Field portable assays could further increase the reliability of testing as analysis closer to the time of collection decreases effects of signal degradation.

Pseudomonas aeruginosa had several detectable and quantifiable AHLs, including C4, C10, C12, 3oC10, 3oC12, and 3oC14 at concentrations of 0.8, 0.9, 1.0, 4.7, 96.3, and 5.4 nM respectively. This culture was known in the literature to produce C4 and 3oC12, but in our testing showed an additional four AHL species present. This demonstrated the value of a mass spectrometry based technique that can separate fully by molecule and give individually identifiable information.

4.4.4 C7 AHL INTERNAL STANDARD RECOVERY

While the samples collected from naturally occurring mats did not show any detectable AHLs, a spike of C7 as a internal quality control standard was performed in the presence of cells to evaluate the possible matrix or biological effects of the samples on the analysis process. Varying response was seen as compared to the nominal C7 dose, with relative response ranging from 10% to 75% (Figure 4.5). Lake water and *Phormidium* provided very similar responses around 70-75%, indicating that whatever effect the *Phormidium* sample had on C7 response was roughly equivalent to the effect of the surrounding lake water matrix. The *Lyngbya* sample had only 40% the nominal concentration, indicating a combination of matrix and biological effects. Although the sample was referred to as *Lyngbya* and it dominated the biomass, it was a grab sample that was not an axenic culture. Therefore the signal reducing effect of the sample is one attributed to the entire microbial community sampled and not necessarily a response directly from the *Lyngbya* in the sample.

The lab-grown *Pseudomonas* culture showed the largest decrease in signal intensity, dropping to 10% of the nominal spike. This culture was grown

under ideal conditions and was very active, exhibiting signaling behavior on both bioassay and LCMS techniques. Therefore its robust activity may have led it to degrade the signal. It is of interest that C7 was not found as a product of the culture; this signal may have been consumed despite not being an actively produced molecule. This indicates the effect multiple microbes living in the same physical area can have on one another.

4.4.5 ADVANTAGES OF DIRECT INJECTION MOLECULAR ANALYSIS

Although extraction and concentration techniques such as solid phase or liquid-liquid extraction have the advantage of increasing analyte concentration, they have several disadvantages that lead to a direct analysis technique being preferable. Firstly, any kind of extraction introduces additional time and sampling handling to the process. The AHLs are rapidly degraded in microbial environments and are semi-volatile which can mean extensive loss of sample during evaporation and concentration steps. Another significant advantage to direct analysis is the throughput of samples. A bioassay screen of a culture for AHL presence is a helpful tool for method development but takes significant time and resources and can be difficult to scale up. In contrast, LCMS techniques can effectively screen for all AHLs at once without using standards alongside each sample, all in an analysis time of 5 minutes. Especially when searching for examples of microbial signaling in the field, being able to cast a broad net and examine hundreds of samples quickly can assist in narrowing down the scope of locations to further study.

Any chemical analysis of easily degraded analytes is dependent on robust field sampling and preservation techniques. The low detection limits possible with LCMS analysis can be further improved by testing sample collection and preservation methods that are applied immediately after sampling in the field for maximum possible signal. With proper collection, LCMS detection of AHLs has the potential to surpass bioassays as the preferred technique for rapid screening of quorum sensing in the environment.

4.5 REFERENCES

1. Branda, S. S.; Vik, Å.; Friedman, L.; Kolter, R., Biofilms: the matrix revisited. *Trends in Microbiology* **2005,** *13*, (1), 20-26.

2. Gerwick, L.; Boudreau, P.; Choi, H.; Mascuch, S.; Villa, F. A.; Balunas, M. J.; Malloy, K. L.; Teasdale, M. E.; Rowley, D. C.; Gerwick, W. H., Interkingdom signaling by structurally related cyanobacterial and algal secondary metabolites. *Phytochemistry Reviews* **2013,** *12*, (3), 459-465.

3. Frey, R. L.; He, L.; Cui, Y.; Decho, A. W.; Kawaguchi, T.; Ferguson, P. L.; Ferry, J. L., Reaction of N-acylhomoserine lactones with hydroxyl radicals: rates, products, and effects on signaling activity. *Environmental Science & Technology* **2010,** *44*, (19), 7465-7469.

4. Sharif, D. I.; Gallon, J.; Smith, C. J.; Dudley, E., Quorum sensing in Cyanobacteria: N-octanoyl-homoserine lactone release and response, by the epilithic colonial cyanobacterium Gloeothece PCC6909. *The ISME Journal* **2008,** *2*, (12), 1171-1182.

5. Blosser, R. S.; Gray, K. M., Extraction of violacein from Chromobacterium violaceum provides a new quantitative bioassay for N-acyl homoserine lactone autoinducers. *Journal of Microbiological Methods* **2000,** *40*, (1), 47-55.

6. Ortori, C. A.; Dubern, J.-F.; Chhabra, S. R.; Cámara, M.; Hardie, K.; Williams, P.; Barrett, D. A., Simultaneous quantitative profiling of N-acyl-L-homoserine lactone and 2-alkyl-4 (1H)-quinolone families of quorum-sensing signaling molecules using LC-MS/MS. *Analytical and Bioanalytical Chemistry* **2011,** *399*, (2), 839-850.

7. Morin, D.; Grasland, B.; Vallee-Rehel, K.; Dufau, C.; Haras, D., On-line high-performance liquid chromatography-mass spectrometric detection and quantification of N-acylhomoserine lactones, quorum sensing signal molecules, in the presence of biological matrices. *Journal of Chromatography A* **2003,** *1002*, (1-2), 79-92.

8. Decho, A. W.; Visscher, P. T.; Ferry, J.; Kawaguchi, T.; He, L. J.; Przekop, K. M.; Norman, R. S.; Reid, R. P., Autoinducers extracted from microbial mats reveal a surprising diversity of N-acylhomoserine lactones (AHLs) and abundance changes that may relate to diel pH. *Environmental Microbiology* **2009,** *11*, (2), 409-420.

9. Ferguson, P. L.; Cui, Y. L.; Frey, R. L.; Ferry, J. L., Identification of hydroxyl radical oxidation products of N-hexanoyl-homoserine lactone by reversed-phase high-performance liquid chromatography coupled with electrospray ionization tandem mass spectrometry. *Rapid Communications in Mass Spectrometry* **2009,** *23*, (8), 1212-1220.

10. Decho, A. W.; Frey, R. L.; Ferry, J. L., Chemical challenges to bacterial AHL signaling in the environment. *Chemical Reviews* **2010,** *111*, (1), 86-99.

Table 4.1 Mass spectrometer conditions for all the measured AHLs. The mass spectrometer used was a Waters Xevo TQ tandem quadrupole instrument with electrospray ionization source run in the positive modes. Parameters for each AHL were optimized by a combination of software and manual tuning.

AHL	Parent ion (m/z)	Fragment ion (m/z)	Cone Voltage	Collision Energy (V)
C4	172	102	18	10
C6	200	102	18	10
C7	214	102	20	10
C8	228	102	22	10
C10	256	102	26	12
C12	284	102	26	12
3oC6	214	102	20	10
3oC8	244	102	24	10
3oC10	272	102	24	12
3oC12	300	102	26	12
3oC14	328	102	30	14

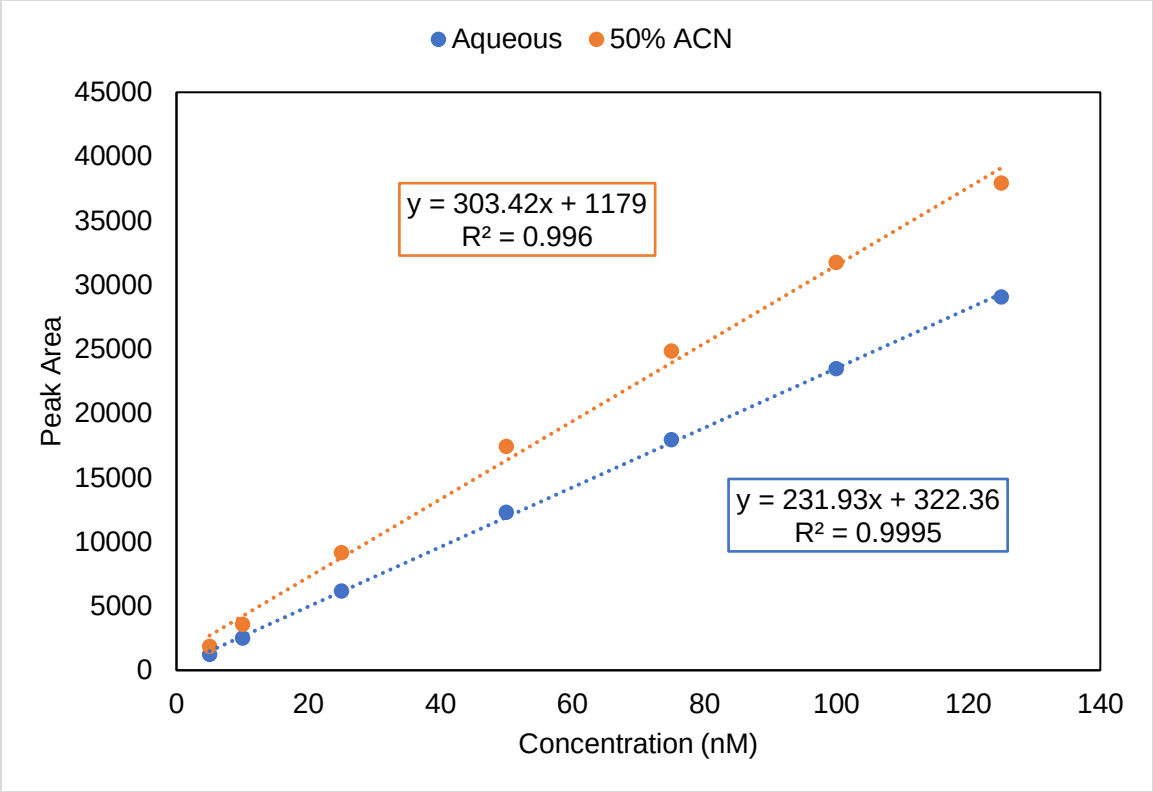

Figure 4.1 Calibration curves of C7 chosen as an example, in both aqueous solution as well as 50% acetonitrile (ACN) solution. The slope of the response curve for the 50% acetonitrile solution was higher than that of the aqueous solution; slopes and intercepts for each AHL are listed in Table 4.2.

Table 4.2 Calibration curve slopes and intercepts for all AHLs tested. Calibration curve was run from 5 to 125 nM. The 50% acetonitrile solution shows increased slope across all AHLs, ranging from an increase of 13% to 194% with an average increase of 66%.

	50% Acetonitrile		Aqueous	
	Slope	*Intercept*	*Slope*	*Intercept*
C4	206	522	163	410
C6	212	786	187	323
C7	303	1179	232	322
C8	317	744	213	254
C10	323	376	193	-841
C12	185	49	76	24
3oC6	438	1395	346	-778
3oC8	551	2617	410	1081
3oC10	598	1806	371	322
3oC12	544	970	294	-643
3oC14	387	786	132	-55

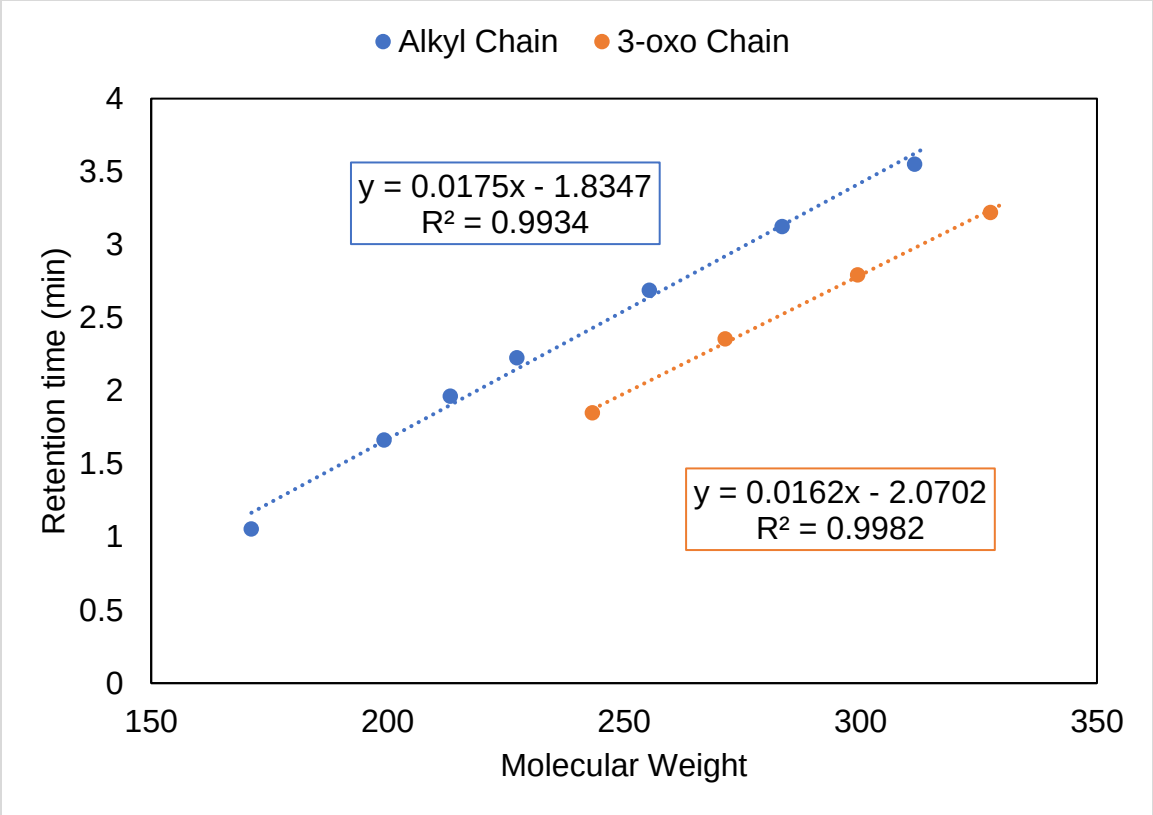

Figure 4.2 Linear correlation between chromatographic retention time and molecular weight. The changing length of the AHL side chain affects the polarity of the molecule and thus its retention time in a predictable way. The separate curves for alkyl chain and 3-oxo chain AHLs allow for the prediction of retention time of an AHL in the absence of standards.

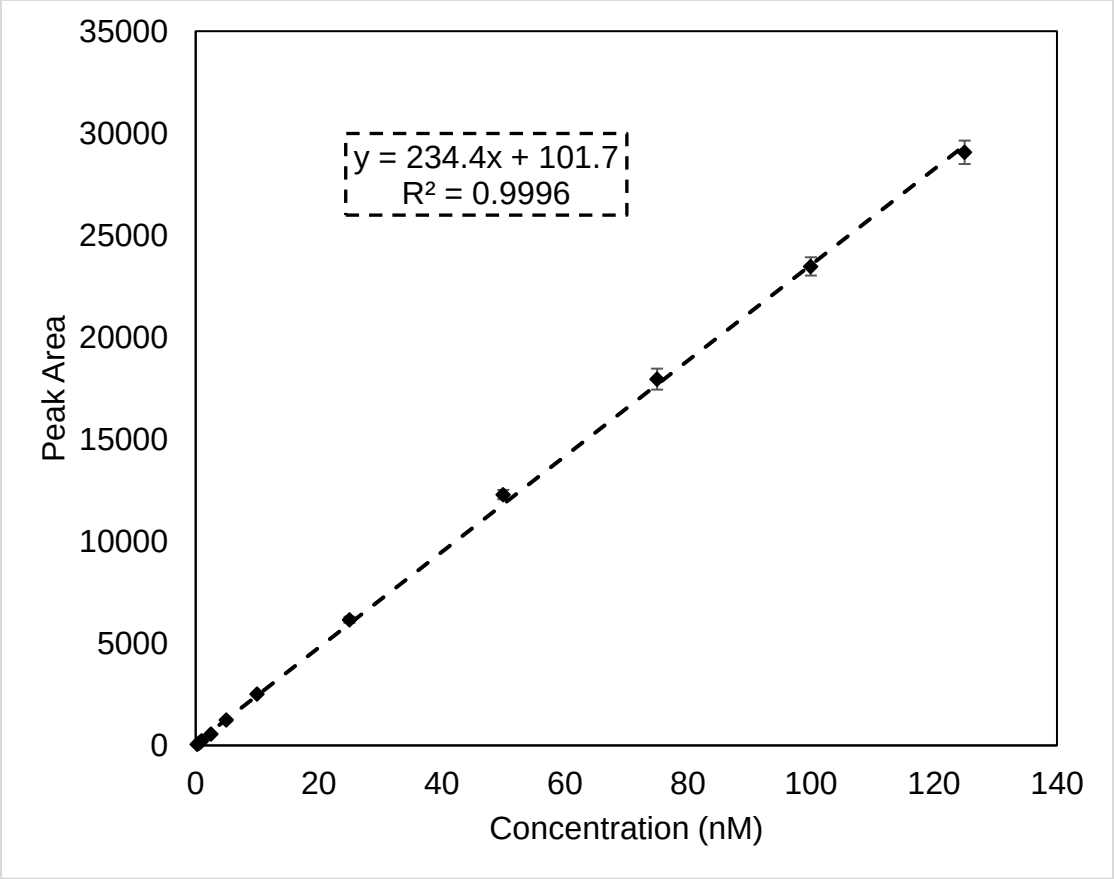

Figure 4.3 Calibration curve of C7 chosen as an example. Curve range is 0.25 to 125 nM, demonstrating the limit of detection and dynamic range of the instrumental response. The linear regression fit has a coefficient of determination of 0.9996, indicating excellent linearity.

Table 4.3 Observed experimental limit of quantification for all measured AHLs. Limit of quantification was determined based on a minimum average signal-to-noise ratio of 10 from triplicate calibration curves. All quantification limits are at or below 0.5 nM except for C8 which shows a limit of 2.50 nM.

AHL	C4	C6	C7	C8	C10	C12
nM	0.25	0.25	0.25	2.50	0.25	0.50

AHL	3oC6	3oC8	3oC10	3oC12	3oC14
nM	0.25	0.50	0.10	0.10	0.25

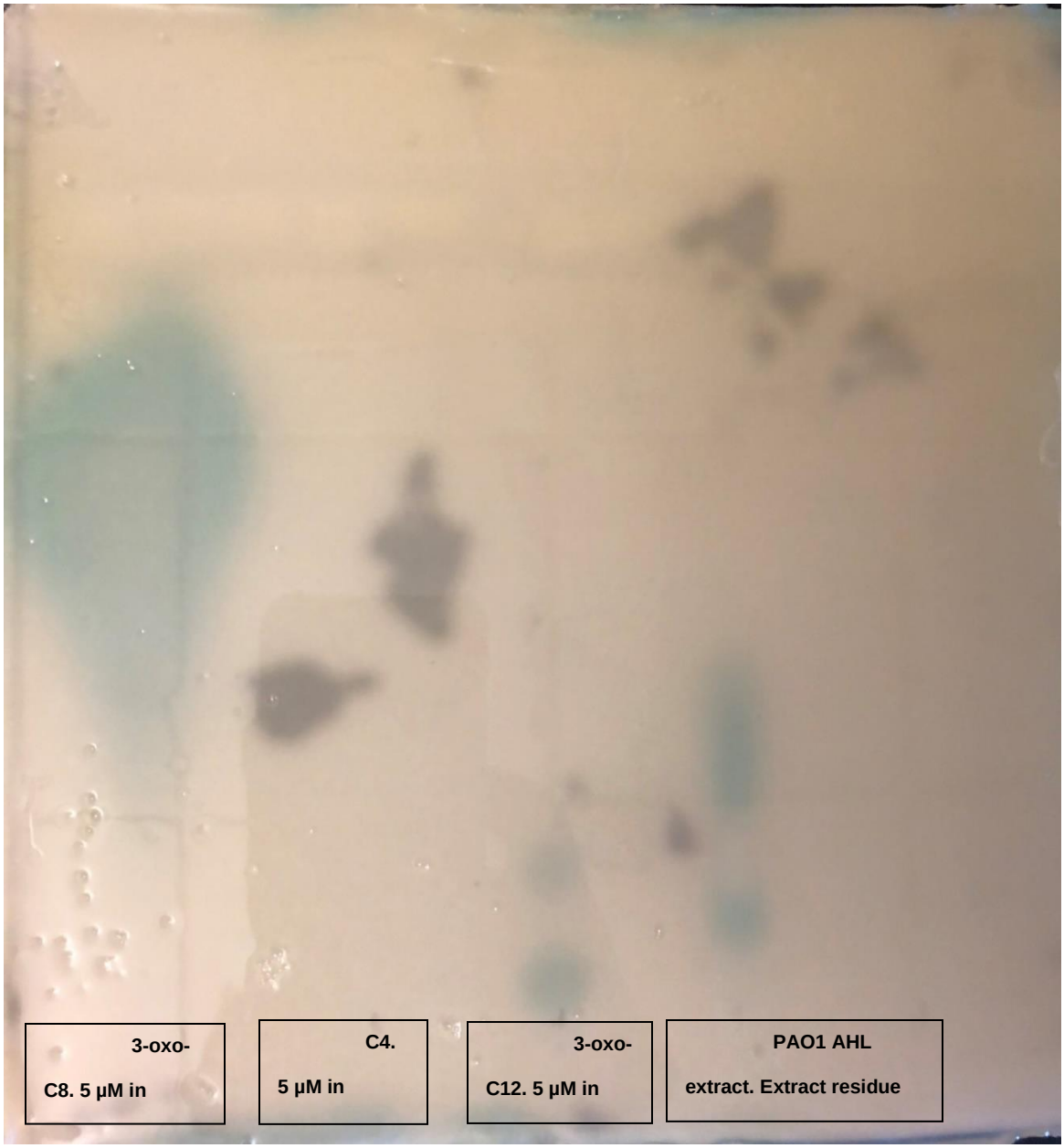

Figure 4.4 TLC biosensor plate for the detection of AHLs by NTL4. Standards of C4, 3oC8, and 3oC12 were used for comparison. The *Pseudomonas aeruginosa* (PAO1) extract showed signals for C4 and 3oC12 which was confirmed by mass spectrometry.

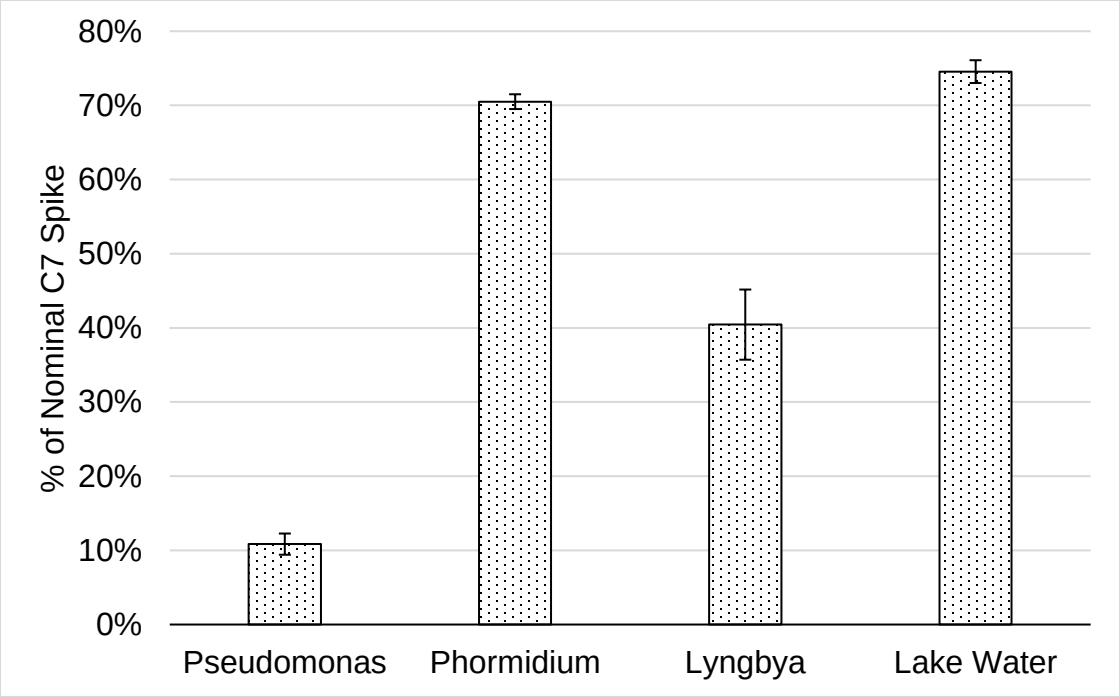

Figure 4.5 Detected C7 after spiking to a nominal 100 nM concentration in 4 samples. Lake water and Phormidium showed equivalent drops in signal, with larger decreases coming from the Lyngbya and Pseudomonas samples. Decreased signal may be due to the surrounding matrix differences, or from biological consumption of the signaling molecule.

APPENDIX A

SUPPLEMENTAL MATERIAL FOR CHAPTER 2

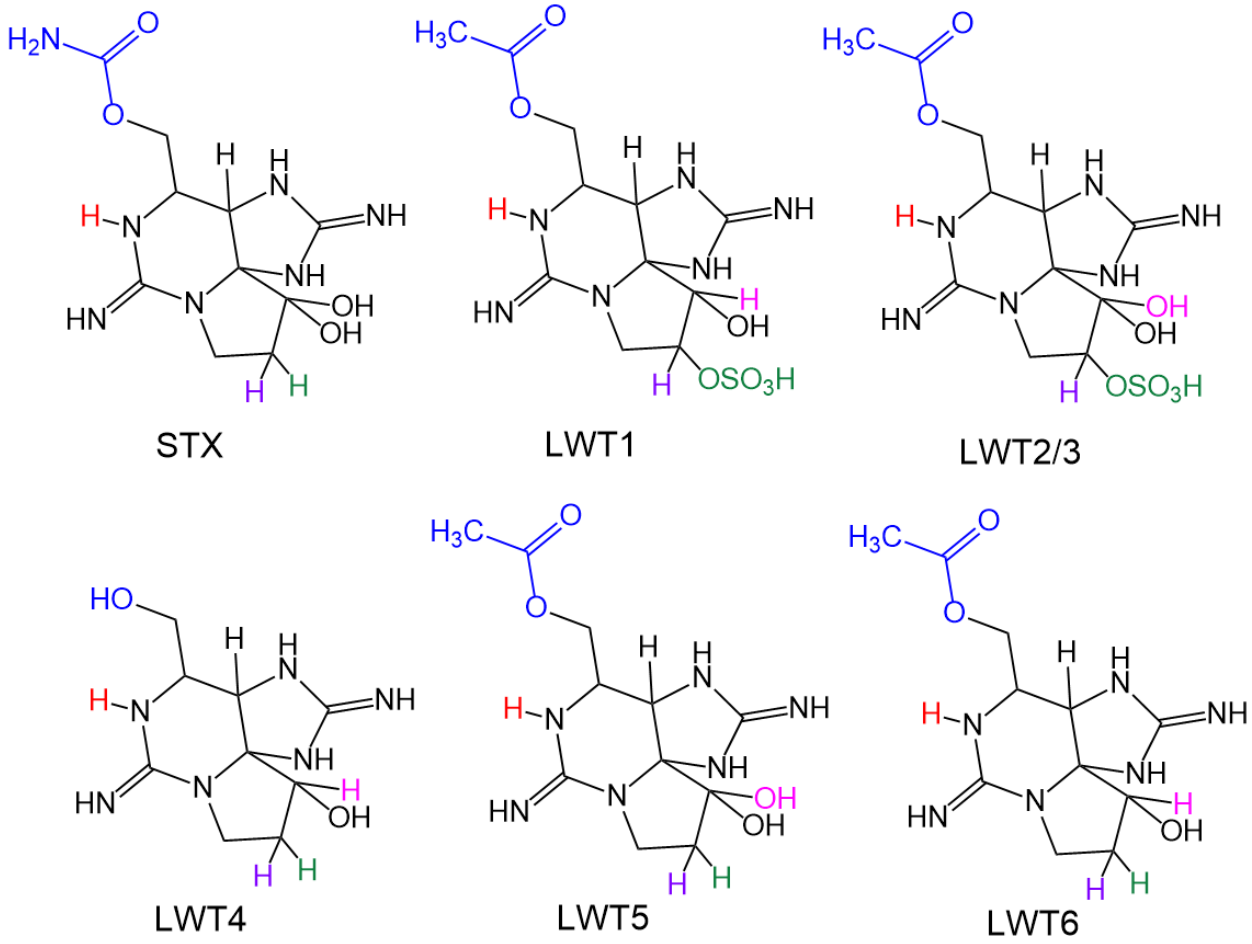

Figure A.1 Chemical structures of saxitoxin (STX), and the *Lyngbya wollei* toxins 1-6 (LWTs 1-6). Colored atoms and functional groups represent frequently encountered structural classes of saxitoxin congeners.

Sampling Locations	
Coordinates	*Name*
34.41605, -80.86347	Site 1
34.33492, -80.70829	Site 2
34.36405, -80.69952	Site 3
34.43457, -80.86677	Site 4
34.38210, -80.73021	Site 5
34.38662, -80.73639	Q1
34.42359, -80.80932	Q2
34.43723, -80.87565	Q3
34.43741, -80.84932	Q4
34.44610, -80.85968	Q5
34.45319, -80.86662	Q6
34.46306, -80.90049	Q7
34.47177, -80.89589	Q8

Table A.1 Coordinates of all sampling locations on Lake Wateree. Sites 1-5 were regularly monitored, with sites 1-3 monitored over an 18-month period and sites 4-5 monitored over a 7-month period. Sites Q1-Q8 were used for qualitative confirmation of algal and toxin presence.

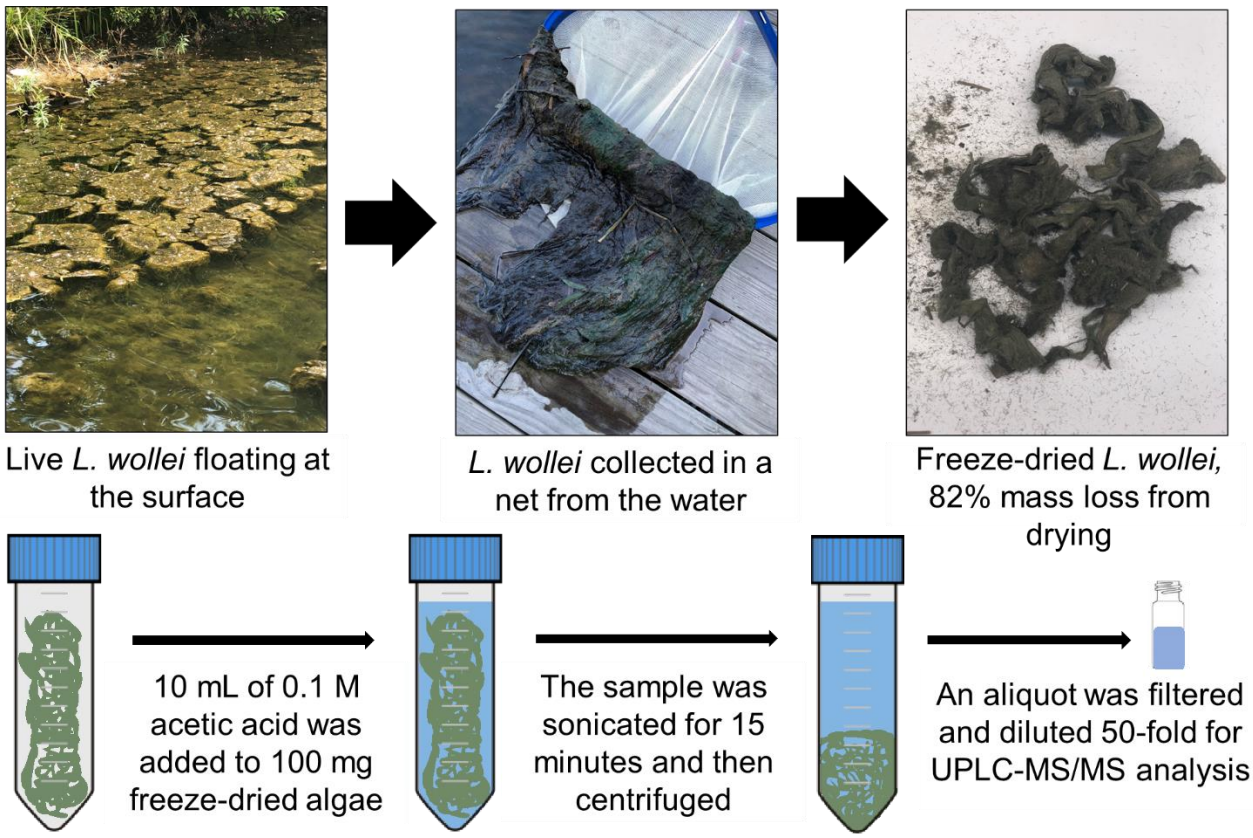

Figure A.2 Flowchart of sampling and analysis process for *Lyngbya wollei*-dominated microbial mat materials.

Lake Wateree Data 2001-2019

	Units	Average	Minimum	Maximum	Count
Chlorophyll a	µg/L	11.3	0.480	77.8	159
Kjeldahl Nitrogen	mg/L	0.475	0.110	12.0	318
Total Phosphorus	mg/L	0.058	0.020	0.320	319
Surface Water Temperature	°C	20.2	2.8	34.0	371

Table A.2 Water quality parameters obtained from the US EPA STORET database for Lake Wateree for the years 2001-2019. Data collected from two sites, one at the inflow to the lake and one at the outflow. Water quality portal call is below.

https://www.waterqualitydata.us/portal/#siteid=21SC60WQ_WQX-CL-089&siteid=21SC60WQ_WQX-CW-207&characteristicName=Chlorophyll%20a%2C%20corrected%20for%20pheophytin&characteristicName=Kjeldahl%20nitrogen&characteristicName=Phosphorus&characteristicName=Temperature%2C%20water&startDateLo=01-01-2001&startDateHi=01-01-2020&mimeType=csv

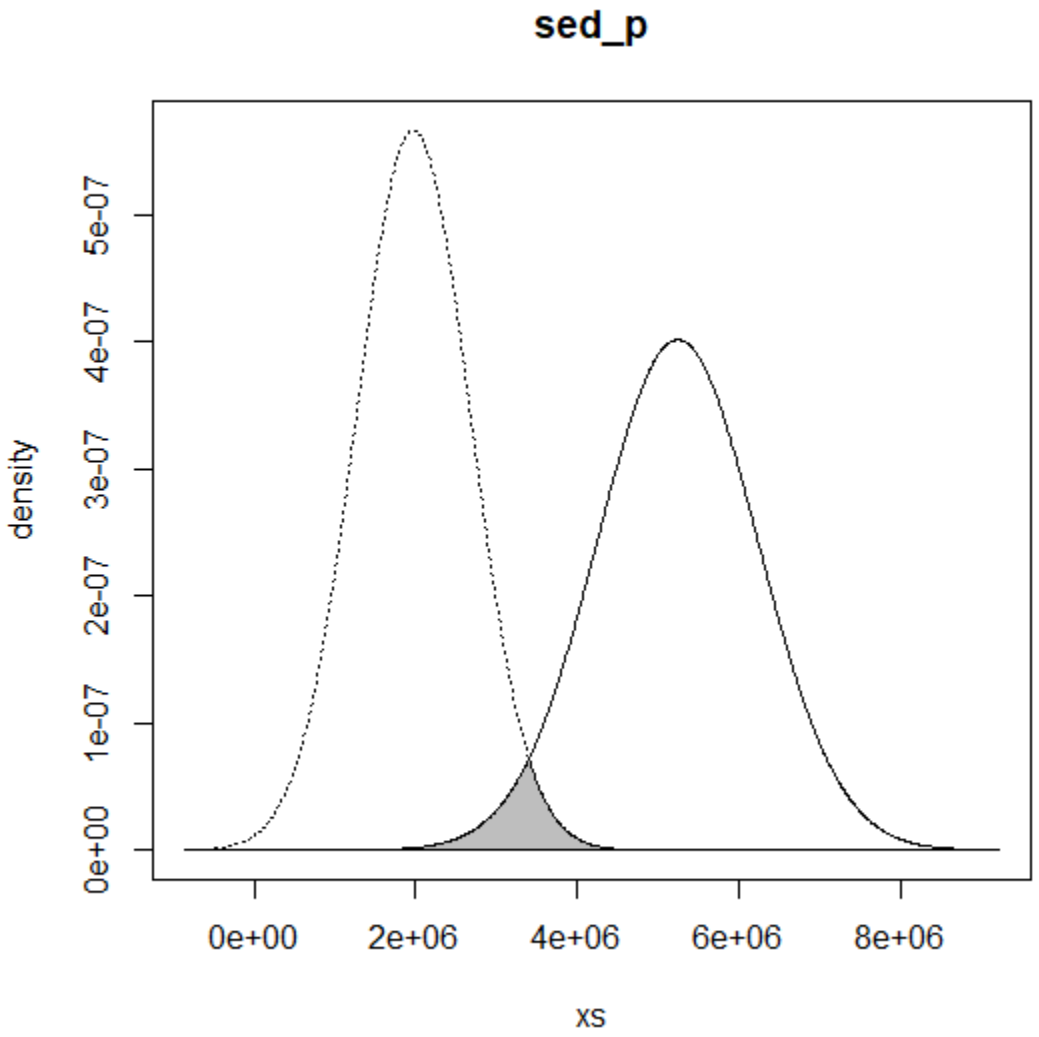

Figure A.3 Gaussian overlap of the distribution functions for modeled biomass based on sediment phosphorus calculations (dotted line) and field observed biomass (solid line).

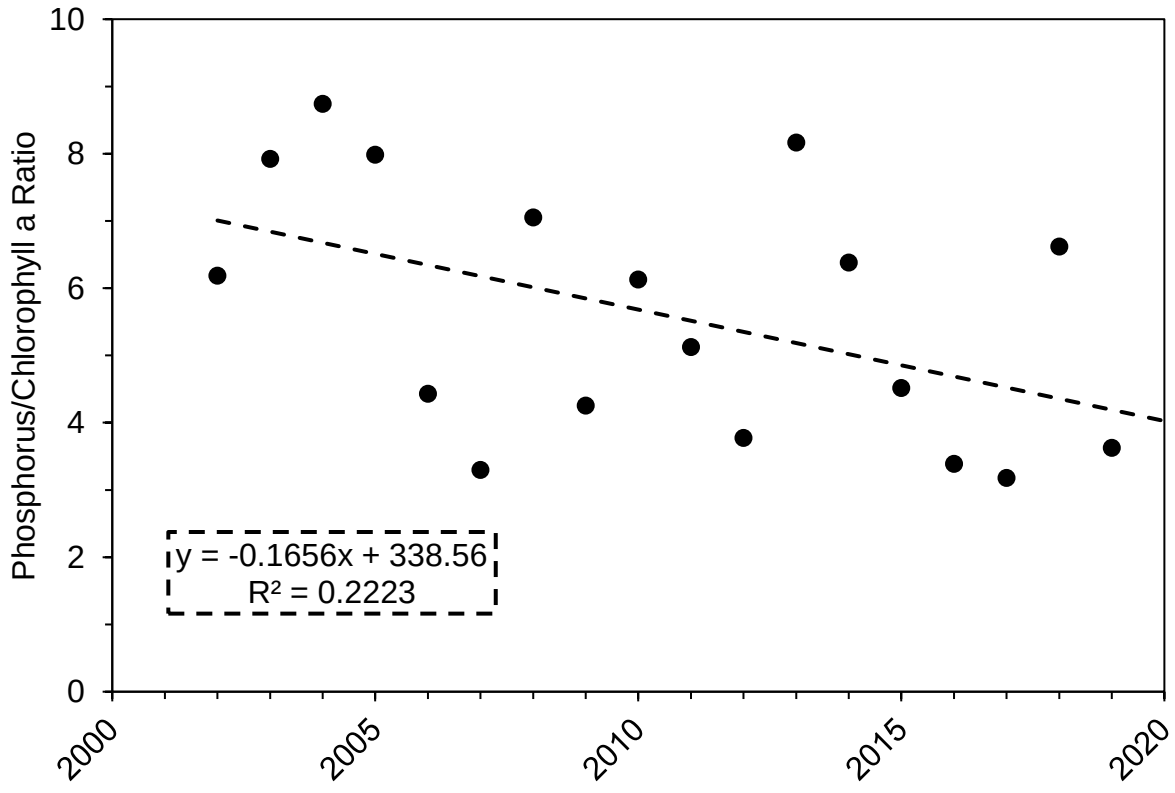

Figure A.4 Yearly average ratio of total phosphorus and chlorophyll (µg/L for both) plotted against time for Lake Wateree. Linear fit trendline shows a weak correlation with time; the phosphorus chlorophyll ratio is essentially flat.

Site Number	Date	Mass	Carbon %	Carbon Normalized Concentration (µg tox/g Carbon)			
				LWT 1	LWT 4	LWT 5	LWT 6
1	6/29/2018	103.0	37%	1.71E+01	2.13E+01	2.08E+02	2.16E+02
1	7/25/2018	111.0	28%	3.12E+01	1.01E+01	4.15E+02	5.81E+02
1	7/25/2018	104.0	23%	1.89E+01	3.30E+00	2.20E+02	2.96E+02
1	7/25/2018	99.0	29%	1.87E+01	9.77E+00	1.99E+02	2.82E+02
1	7/25/2018	113.0	31%	2.16E+01	1.34E+01	3.12E+02	7.56E+02
1	8/8/2018	110.0	32%	2.29E+01	1.50E+01	2.82E+02	5.57E+02
1	8/8/2018	105.0	28%	2.81E+01	1.89E+01	4.49E+02	6.75E+02
1	8/8/2018	113.0	32%	1.25E+01	2.98E+01	2.35E+02	4.46E+02
1	8/8/2018	92.0	39%	1.66E+01	2.51E+00	1.75E+02	1.05E+02
1	8/17/2018	95.0	32%	2.73E+01	1.75E+01	3.79E+02	6.57E+02
1	8/17/2018	104.0	31%	1.81E+01	7.57E+00	1.82E+02	2.42E+02
1	8/29/2018	108.0	36%	2.01E+01	1.51E+01	3.34E+02	5.16E+02
1	8/29/2018	94.0	35%	3.35E+00	6.21E-01	8.94E+01	4.22E+01
1	8/29/2018	116.0	36%	1.21E+01	8.50E+00	2.06E+02	2.22E+02
1	8/29/2018	108.0	35%	1.89E+01		2.41E+02	1.15E+02
1	9/12/2018	120.0	34%	1.34E+01	6.93E+00	1.26E+02	8.41E+01
1	9/12/2018	108.0	34%	1.76E+01	3.96E+00	1.55E+02	1.59E+02
1	9/12/2018	112.0	35%	1.30E+01	5.32E+00	2.84E+02	1.87E+02
1	9/12/2018	93.0	38%	1.80E+01	8.79E+00	2.50E+02	3.40E+02
1	9/24/2018	91.0	36%	2.71E+01	1.19E+01	6.41E+02	3.95E+02
1	9/24/2018	106.0	34%	1.15E+01	1.15E-01	1.14E+02	6.91E+01
1	9/24/2018	96.0	33%	2.00E+01		2.18E+02	1.27E+02
1	10/1/2018	93.0	38%	1.36E+01	7.80E+00	1.37E+02	7.57E+01
1	10/1/2018	110.0	34%	2.56E+01	1.67E+01	2.24E+02	2.21E+02
1	10/1/2018	96.0	46%	2.09E+01	8.46E+00	1.95E+02	3.79E+02
1	10/12/2018	105.0	33%	2.57E+01	2.80E+01	4.05E+02	2.38E+02
1	10/12/2018	97.0	37%	3.31E+01	2.67E+01	3.91E+02	5.84E+02
1	10/12/2018	116.0	37%	2.77E+01	1.48E+01	3.29E+02	4.02E+02
1	10/18/2018	115.0	32%	1.52E+01		1.56E+02	5.74E+01
1	10/18/2018	96.0	34%	1.04E+01	2.99E+00	1.03E+02	3.33E+01
1	10/29/2018	120.0	33%	1.49E+01	4.52E-01	8.14E+01	
1	10/29/2018	132.0	36%	9.97E+00	6.22E+00	1.14E+02	7.31E+00
1	10/29/2018	113.0	34%	1.34E+01	5.74E+00	1.21E+02	7.50E+00
1	11/6/2018	110.0	34%	2.98E+01	3.04E+01	3.59E+02	7.27E+01
1	11/6/2018	118.0	34%	1.15E+01	3.31E+00	1.55E+02	7.33E+00
1	11/6/2018	89.0	26%	2.14E+01		6.49E+01	
1	11/29/2018	120.0	26%	2.28E+01		1.69E+02	3.13E+00
1	11/29/2018	116.0	30%	1.02E+01		1.20E+02	

1	11/29/2018	112.0	31%	1.59E+01		5.40E+01	
1	12/7/2018	112.0	32%	1.88E+01		2.13E+02	5.05E+01
1	12/7/2018	99.0	33%	1.81E+01	4.35E+01	6.05E+02	3.14E+02
1	12/7/2018	114.0	28%	1.66E+01	8.08E-01	8.06E+01	
1	1/18/2019	102.0	17%	2.11E+01		1.55E+02	6.45E+00
1	1/18/2019	119.0	25%	1.45E+01		3.61E+01	
1	1/18/2019	118.0	22%	1.46E+01		3.98E+01	
1	2/8/2019	108.0	22%	1.50E+01		3.01E+01	
1	2/8/2019	90.0	19%	1.88E+01		2.46E+01	
1	2/8/2019	130.0	22%	1.07E+01		3.22E+01	
1	2/22/2019	117.0	19%	3.04E+00		7.44E+00	
1	2/22/2019	123.0	27%	5.99E+00		1.71E+01	
1	2/22/2019	118.0	48%	9.05E+00		1.03E+02	
1	3/17/2019	97.4	16%	5.92E+00			
1	3/17/2019	101.0	15%	8.05E+00	3.77E+00	3.02E+01	
1	3/17/2019	100.3	19%			5.13E+01	
1	3/29/2019	103.4	10%	1.81E+00			
1	3/29/2019	103.4	19%	1.80E+00			
1	3/29/2019	101.7	18%	2.31E+00	1.05E+00		
1	4/12/2019	97.9	31%	3.35E+00	7.54E+00	2.76E+01	
1	4/12/2019	103.4	32%	2.59E+00	9.24E+00	2.52E+01	
1	4/12/2019	97.7	17%	7.15E+00		5.56E+01	
1	4/29/2019	102.1	21%			1.46E+01	6.16E+00
1	4/29/2019	97.2	24%	5.20E+00	1.93E+01	6.48E+01	3.86E+01
1	4/29/2019	98.0	16%		5.70E-01	4.43E+00	
1	5/14/2019	97.0	27%	3.68E+00	2.05E+00	1.68E+00	1.34E+01
1	5/14/2019	97.1	22%	2.93E+00		1.03E+01	1.47E+01
1	5/14/2019	98.9	18%	2.38E+00			
1	5/28/2019	97.6	25%	5.84E+00	1.08E-01		
1	5/28/2019	98.7	23%	4.74E+00	5.89E+00	4.55E+00	3.15E+01
1	5/28/2019	97.5	24%	5.49E+00		6.00E+00	3.06E+01
1	6/18/2019	105.0	22%	3.32E+00			
1	6/18/2019	99.8	26%	8.50E-01			
1	6/18/2019	103.5	16%	3.56E+00			
1	7/2/2019	99.2	25%	4.74E+00	1.29E+01	2.39E+01	7.77E+01
1	7/2/2019	97.0	22%	8.53E+00	1.40E+01	3.53E+01	1.70E+02
1	7/16/2019	102.4	26%	6.45E+00	1.06E+01	2.42E+01	7.78E+01
1	7/16/2019	98.9	27%	4.97E+00	1.56E+01	2.22E+01	7.20E+01
1	7/16/2019	97.2	25%	4.78E+00	1.20E+01	3.55E+01	1.23E+02
1	7/30/2019	97.2	27%	5.49E+00	3.71E+00	3.47E+01	7.87E+01
1	7/30/2019	95.7	25%	8.98E+00	2.86E+01	5.56E+01	2.28E+02

1	7/30/2019	100.1	32%	6.38E+00		3.66E+01	2.90E+01
1	8/13/2019	102.4	34%	2.33E+00		6.45E+00	3.65E-02
1	8/13/2019	99.0	32%	3.24E+00		1.86E+01	2.91E+01
1	8/13/2019	105.8	36%	3.41E+00		1.19E+00	
1	8/27/2019	97.0	31%	3.69E+00	6.48E-01	1.47E-01	
1	8/27/2019	102.9	31%	7.11E+00	1.06E+01	3.94E+01	5.19E+01
1	8/27/2019	98.5	30%	6.41E+00	1.04E+01	2.19E+01	5.18E+01
1	9/17/2019	97.6	27%	5.13E+00		1.19E+01	3.07E+01
1	9/17/2019	100.5	30%	4.48E+00	5.70E+00	2.52E+01	2.58E+01
1	9/17/2019	101.0	28%	2.98E+00			
1	10/1/2019	99.1	32%	4.57E+00	5.10E+00	2.04E+01	3.39E+01
1	10/1/2019	98.4	26%	5.39E+00		2.32E+01	5.98E+00
1	10/1/2019	99.0	34%	2.80E+00	5.50E-01	1.15E+00	3.51E-01
1	10/29/2019	99.4	35%	3.16E+00	2.33E+00	8.86E+00	6.12E-01
1	10/29/2019	100.1	38%	2.87E+00			
1	10/29/2019	101.2	22%	7.40E+00		4.49E+01	1.20E+01
2	7/25/2018	106.0	34%	3.85E-01	2.65E+01	5.90E+02	4.27E+02
2	8/8/2018	103.0	33%		1.33E+00	3.32E+02	1.14E+02
2	8/8/2018	96.0	34%	5.61E-01	8.96E+00	3.11E+02	1.97E+02
2	8/8/2018	111.0	27%	3.81E-01	4.08E-01	3.76E+02	1.53E+02
2	8/8/2018	115.0	29%	2.04E-01	7.14E+00	4.90E+02	1.94E+02
2	8/29/2018	98.0	29%	7.07E-01	9.95E+00	3.52E+02	1.33E+02
2	8/29/2018	93.0	29%	7.67E-01	2.13E+01	4.82E+02	3.29E+02
2	8/29/2018	120.0	30%		1.86E+01	6.19E+02	3.90E+02
2	8/29/2018	118.0	27%	2.07E-01	1.81E+01	3.61E+02	2.05E+02
2	9/12/2018	134.0	28%	4.02E-01	2.20E+00	2.81E+02	1.05E+02
2	9/12/2018	104.0	31%	6.59E-01	1.02E+01	5.98E+02	3.33E+02
2	9/12/2018	134.0	23%	2.85E-01	2.04E+00	2.09E+02	7.44E+01
2	9/24/2018	117.0	22%	3.51E-01	2.63E+01	3.68E+02	9.79E+01
2	9/24/2018	123.0	26%	9.47E-01	1.09E+01	7.51E+02	1.67E+02
2	10/1/2018	97.0	29%	2.73E-01	4.65E+01	1.11E+03	3.41E+02
2	10/1/2018	110.0	34%	2.26E-01	4.48E+00	4.43E+02	1.19E+02
2	10/1/2018	90.0	33%	1.16E+00	2.21E+01	6.26E+02	2.55E+02
2	10/12/2018	108.0	41%		3.24E+01	8.68E+02	1.32E+02
2	10/12/2018	91.0	25%	5.28E-01	2.79E+00	5.82E+02	1.48E+02
2	10/12/2018	102.0	34%	2.39E-01	2.35E+01	8.45E+02	4.45E+02
2	10/18/2018	94.0	38%		1.39E+01	7.66E+02	1.24E+02
2	10/18/2018	111.0	38%	3.14E-01	1.33E+01	5.23E+02	4.34E+01
2	10/29/2018	127.0	25%	2.16E-01	1.35E+01	5.98E+02	5.15E+01
2	10/29/2018	100.0	30%	9.22E-01	4.58E+00	4.81E+02	3.09E+01
2	10/29/2018	110.0	24%	7.95E-01	3.23E+00	2.45E+02	1.56E+01

2	11/6/2018	119.0	30%	3.08E-01	7.68E+00	8.04E+02	1.57E+02
2	11/6/2018	104.0	34%	2.16E-01	1.82E+01	1.15E+03	3.00E+02
2	11/6/2018	120.0	30%	4.54E-01	5.57E+01	1.49E+03	4.65E+02
2	11/29/2018	109.0	31%	2.53E-01	4.00E+00	7.86E+02	1.11E+02
2	11/29/2018	127.0	30%	5.78E-01	5.75E+00	1.41E+03	8.92E+01
2	11/29/2018	94.0	33%	4.13E-01		4.99E+02	5.27E+01
2	1/18/2019	98.0	35%		1.19E+01	3.38E+02	1.06E+02
2	1/18/2019	85.0	38%	4.55E-01	1.48E+02	2.11E+02	1.47E+02
2	1/18/2019	88.0	33%	3.65E+00	1.40E+01	7.00E+02	1.50E+02
2	2/8/2019	94.0	26%	5.84E+00	7.01E+00	2.92E+02	3.27E+01
2	2/8/2019	103.0	28%	1.73E+00	5.18E+00	2.35E+02	4.53E+01
2	2/8/2019	123.0	30%	1.28E+01	9.32E+00	2.72E+02	7.44E+01
2	2/22/2019	95.0	32%		1.32E+01	3.37E+02	3.31E+01
2	2/22/2019	85.0	34%		2.22E+01	2.52E+02	3.41E+01
2	2/22/2019	81.0	34%		2.40E+01	2.89E+02	2.92E+01
2	3/17/2019	102.5	23%	1.68E+00	3.44E+00	3.55E+01	1.91E+01
2	3/17/2019	100.6	22%	1.35E+00	1.38E+00	8.85E+01	7.08E+01
2	3/17/2019	96.1	23%	1.32E+00		9.08E+01	
2	3/29/2019	98.0	21%	7.10E-01	3.50E+00	4.23E+01	
2	3/29/2019	101.0	16%	8.05E-01		5.67E+01	
2	3/29/2019	102.2	21%	2.81E+00	6.11E+00	7.29E+01	
2	4/12/2019	101.9	23%		1.02E+01	1.20E+02	4.02E+01
2	4/12/2019	104.0	28%	1.36E+00	3.77E+00	6.29E+01	1.23E+00
2	4/12/2019	107.0	28%		9.34E+00	1.33E+02	4.49E+01
2	4/29/2019	96.5	27%	1.20E+00	6.51E+00	1.37E+02	2.85E+01
2	4/29/2019	100.3	26%	1.64E+00		6.92E+01	
2	4/29/2019	101.2	27%	1.20E+00	8.78E+00	1.23E+02	5.03E+01
2	5/14/2019	102.6	36%	6.51E-01	1.44E-01	1.47E+02	7.51E+00
2	5/14/2019	97.9	35%	1.65E+00	1.37E+01	2.28E+02	8.54E+01
2	5/14/2019	97.6	36%	8.11E-01	6.19E+00	1.74E+02	5.93E+01
2	5/28/2019	98.7	30%	9.10E-01	2.02E+00	1.39E+02	4.33E+01
2	5/28/2019	101.5	29%	1.04E+00		1.12E+02	4.51E+01
2	5/28/2019	97.3	27%	1.44E+00	5.30E+00	5.69E+01	3.01E+01
2	6/18/2019	100.3	20%	1.64E+00		7.56E+00	
2	6/18/2019	102.6	29%	8.32E-01	1.24E+00	1.27E+02	2.04E+01
2	6/18/2019	105.0	33%	2.19E+00	2.90E+00	9.10E+01	2.87E+01
2	7/2/2019	101.1	20%	8.86E-01	4.40E+00	1.11E+02	8.34E+01
2	7/2/2019	98.1	21%			1.30E+02	9.74E+01
2	7/2/2019	102.1	20%	1.24E+00	5.65E+00	1.53E+02	1.69E+02
2	7/16/2019	98.2	24%	1.83E+00	1.63E+01	2.21E+02	1.83E+02
2	7/16/2019	98.8	24%	1.74E+00	1.68E+01	1.52E+02	1.64E+02

2	7/16/2019	103.9	22%	4.64E+00	8.99E+00	2.35E+02	2.01E+02
2	7/30/2019	98.9	21%	1.38E+00	3.09E+00	1.81E+02	7.47E+01
2	7/30/2019	101.5	15%	1.50E+00		1.87E+01	
2	7/30/2019	97.7	21%	9.09E-01		1.87E+02	7.82E+01
2	8/13/2019	102.3	28%	7.60E-01	8.78E+00	2.55E+02	1.97E+02
2	8/13/2019	99.3	29%		1.18E+01	2.28E+02	1.51E+02
2	8/13/2019	94.3	25%	1.87E+00	4.66E+00	1.21E+02	5.16E+01
2	8/27/2019	106.0	23%	1.52E+00	6.18E+00	8.37E+01	4.49E+01
2	8/27/2019	96.0	24%	1.40E+00		4.23E+01	1.26E+01
2	8/27/2019	96.0	22%	1.39E+00	1.79E+00	9.52E+01	4.08E+01
2	9/17/2019	97.3	27%	1.32E+00	3.05E+01	1.86E+02	1.62E+02
2	9/17/2019	98.8	25%	8.59E-01	3.29E+01	2.64E+02	3.62E+02
2	9/17/2019	97.3	23%	1.49E+00	2.41E+01	1.77E+02	2.02E+02
2	10/1/2019	96.6	27%	9.06E-01	1.23E+00	1.45E+02	1.54E+01
2	10/1/2019	95.4	22%	3.89E+00	3.57E+00	8.74E+01	7.00E+00
2	10/1/2019	98.2	23%	1.61E+00	1.27E+00	5.74E+01	
2	10/29/2019	95.2	21%		8.53E+00	1.52E+02	3.14E+01
2	10/29/2019	99.3	20%		2.25E+01	3.68E+01	2.37E+01
2	10/29/2019	95.0	20%	9.84E-01	2.31E+01	2.10E+02	1.15E+02
3	7/25/2018	101.0	35%	1.22E+01	2.94E+00	1.29E+02	4.82E+01
3	7/25/2018	99.0	31%	2.36E+01	7.35E+01	1.40E+02	1.27E+02
3	7/25/2018	96.0	33%	3.47E+01	5.59E+01	4.09E+02	1.12E+03
3	8/8/2018	104.0	32%	4.83E+01	7.38E+01	4.70E+02	1.29E+03
3	8/8/2018	96.0	30%	3.17E+01	6.16E+01	2.04E+02	2.30E+02
3	8/8/2018	97.0	34%	3.33E+01	4.41E+01	2.60E+02	3.12E+02
3	8/29/2018	106.0	33%	2.66E+01	1.47E+01	2.07E+02	4.89E+02
3	8/29/2018	119.0	34%	2.45E+01	1.15E+01	1.39E+02	2.01E+02
3	8/29/2018	111.0	15%	7.14E+01	2.73E+01	7.82E+02	9.53E+02
3	8/29/2018	94.0	23%	1.48E+01	1.88E+00	2.16E+02	1.77E+02
3	9/12/2018	99.0	21%	5.10E+01	1.20E+02	3.98E+02	4.39E+02
3	9/12/2018	92.0	31%	3.70E+01	2.18E+01	2.77E+02	3.99E+02
3	9/12/2018	105.0	25%	3.96E+01	5.78E+01	2.69E+02	3.76E+02
3	9/24/2018	116.0	16%	6.82E+01	1.14E+02	4.78E+02	4.55E+02
3	9/24/2018	96.0	28%	2.78E+01	4.78E+01	1.76E+02	1.90E+02
3	9/24/2018	118.0	34%	4.30E+01	7.23E+01	4.63E+02	8.67E+02
3	10/1/2018	96.0	30%	4.15E+01	2.01E+01	5.55E+02	6.77E+02
3	10/1/2018	106.0	26%	5.79E+01	1.26E+02	3.93E+02	1.01E+03
3	10/1/2018	114.0	39%	3.51E+01	1.80E+01	4.74E+02	6.12E+02
3	10/12/2018	97.0	22%	3.43E+01	4.56E+00	2.19E+02	3.15E+02
3	10/12/2018	99.0	22%	2.97E+01	1.00E+02	2.03E+02	1.27E+02
3	10/12/2018	107.0	28%	2.39E+01	3.13E+01	1.81E+02	1.65E+02

3	10/18/2018	105.0	31%	4.17E+01	9.07E+00	3.11E+02	1.34E+02
3	10/18/2018	115.0	37%	3.00E+01	2.00E+01	2.75E+02	2.66E+02
3	10/29/2018	102.0	23%	5.66E+01	2.00E+00	3.84E+02	2.05E+02
3	10/29/2018	100.0	19%	6.61E+01	1.73E+01	5.46E+02	5.31E+02
3	10/29/2018	130.0	29%	1.82E+01	2.24E+01	8.04E+01	4.31E+01
3	11/6/2018	105.0	30%	5.04E+01	2.02E+01	6.24E+02	4.36E+02
3	11/6/2018	87.0	30%	1.63E+01	1.52E+02	9.38E+01	4.02E+01
3	11/6/2018	103.0	51%	4.06E+01	2.10E+01	4.22E+02	3.57E+02
3	11/29/2018	110.0	51%	2.74E+01	5.92E+00	3.29E+02	2.18E+02
3	11/29/2018	121.0	45%	2.11E+01	4.14E+00	1.51E+02	8.74E+01
3	11/29/2018	104.0	39%	3.49E+01	1.63E+00	3.55E+02	1.21E+02
3	12/7/2018	109.0	32%	4.30E+01	3.58E+01	4.42E+02	2.17E+02
3	12/7/2018	105.0	52%	2.56E+01	3.76E+01	3.37E+02	1.75E+02
3	12/7/2018	121.0	50%	2.09E+01	3.22E+01	2.20E+02	1.03E+02
3	1/18/2019	84.0	35%	3.82E+00	2.89E+01	1.13E+01	
3	1/18/2019	104.0	36%	1.92E+01	4.33E+00	1.68E+02	4.42E+01
3	1/18/2019	125.0	36%	2.85E+01	8.45E+00	1.83E+02	8.67E+01
3	2/8/2019	97.0	39%	1.44E+01	8.05E+01	1.09E+02	3.22E+01
3	2/8/2019	109.0	41%	2.35E+01	4.99E+01	2.87E+02	1.69E+02
3	2/8/2019	95.0	47%	1.60E+01	1.06E+02	1.82E+02	1.19E+02
3	2/22/2019	104.0	30%	1.70E+01	1.43E+01	8.09E+01	2.93E+01
3	2/22/2019	84.0	41%	2.19E+01	5.77E+00	2.10E+02	8.09E+01
3	2/22/2019	148.0	43%	6.25E+00	8.84E-01	4.40E+01	
3	3/17/2019	104.0	19%	6.42E-01	4.14E+00	1.06E+02	
3	3/17/2019	99.7	18%	9.34E+00	4.55E+00	7.71E+01	1.22E+01
3	3/17/2019	98.2	22%	6.91E+00	1.09E+01	6.91E+01	2.28E+01
3	3/29/2019	101.2	17%	6.03E+00		2.12E+01	
3	3/29/2019	97.8	12%	9.49E-01			
3	3/29/2019	97.1	17%	9.26E-01	1.18E+00	5.27E-01	
3	4/12/2019	97.4	20%	1.19E+00	2.33E+00	3.08E-01	9.14E+00
3	4/12/2019	95.5	26%	5.07E+00	9.20E+00	6.09E+01	1.16E+02
3	4/12/2019	99.4	23%	5.85E+00	1.21E+01	5.92E+01	1.22E+02
3	4/29/2019	100.5	22%	6.17E+00	1.76E+01	8.17E-01	8.07E+01
3	4/29/2019	100.4	13%	6.71E+00	6.50E+00		
3	4/29/2019	104.0	9%	7.35E+00	7.67E-02		6.46E+00
3	5/14/2019	101.3	16%				
3	5/14/2019	96.6	24%	9.11E+00	3.99E+01	4.84E+01	1.81E+02
3	5/14/2019	95.8	19%	9.91E+00	3.72E+01	7.74E+00	1.47E+02
3	5/28/2019	100.8	20%	2.12E+01	3.54E+01	3.20E+01	2.88E+02
3	5/28/2019	104.0	19%	1.49E+01	5.43E+00	2.29E+01	1.08E+02
3	5/28/2019	98.4	21%	1.59E+01	2.06E+01	4.69E+01	3.07E+02

3	6/18/2019	98.4	25%	1.34E+01	3.88E+01	1.88E+02	5.60E+02
3	6/18/2019	95.8	26%	7.88E+00	1.13E+01	8.44E+01	1.36E+02
3	6/18/2019	96.9	23%	1.19E+01	3.81E+01	7.33E+01	2.58E+02
3	7/2/2019	100.2	23%	9.25E+00	4.00E+00	2.24E+01	7.39E+01
3	7/2/2019	95.8	22%	2.16E+01	8.92E+01	1.17E+02	7.66E+02
3	7/16/2019	95.1	19%	1.32E+01	3.10E+01	7.71E+01	4.50E+02
3	7/16/2019	98.4	24%	1.11E+01	3.09E+01	7.26E+01	4.31E+02
3	7/16/2019	96.3	22%	1.22E+01	3.72E+01	7.43E+01	3.64E+02
3	7/30/2019	98.6	24%	2.02E+01	6.49E+01	1.17E+02	9.56E+02
3	7/30/2019	99.8	21%	7.56E+00	2.20E+01	4.99E+01	8.06E+01
3	7/30/2019	98.2	23%	1.53E+01	5.85E+01	1.10E+02	6.43E+02
3	8/13/2019	97.1	28%	7.55E+00	1.19E+01	9.02E+01	1.36E+02
3	8/13/2019	97.6	24%	1.46E+01	5.17E+01	1.59E+02	1.07E+03
3	8/13/2019	95.4	28%	8.28E+00	3.37E+01	1.72E+02	5.73E+02
3	8/27/2019	98.5	27%	6.50E+00	1.63E+01	1.11E+02	3.08E+02
3	8/27/2019	97.8	26%	5.29E+00	9.66E+00	6.40E+01	9.15E+01
3	8/27/2019	97.2	27%	3.22E+00	1.11E+01	6.54E+01	7.33E+01
3	9/17/2019	95.2	28%	6.18E+00	4.05E-01	5.52E+01	
3	9/17/2019	97.2	28%	2.86E+00	2.86E+00	1.70E+01	4.68E+00
3	9/17/2019	97.2	27%	7.56E+00	8.30E+00	7.13E+01	1.44E+02
3	10/1/2019	100.7	25%	4.76E+00	1.18E+01	4.60E+01	1.21E+02
3	10/1/2019	96.8	23%	2.02E+00	1.37E+01	2.04E+01	1.63E+02
3	10/1/2019	95.7	21%	1.10E+01	2.75E+01	8.42E+01	4.07E+02
3	10/29/2019	96.7	25%	7.38E+00	2.27E+01	5.74E+01	9.37E+01
3	10/29/2019	96.0	25%	3.30E+00	1.63E+01	2.36E+01	6.42E+01
3	10/29/2019	96.0	27%	7.43E+00	3.54E+01	9.31E+01	2.12E+02
4	3/17/2019	99.5	23%	6.27E-01	1.69E+00	6.37E+01	
4	3/17/2019	94.9	23%	2.35E+00	3.23E+00	8.03E+01	
4	3/17/2019	95.4	23%	6.65E-01		1.29E+02	
4	3/29/2019	101.2	19%	1.00E+00	1.11E+01	6.00E+01	4.12E+00
4	3/29/2019	100.7	22%	1.47E+00		7.63E+01	
4	3/29/2019	99.8	21%	2.44E+00	2.57E+00	3.04E+01	
4	4/12/2019	106.0	32%	1.98E+00	1.06E+02	2.26E+01	1.04E+01
4	4/12/2019	102.9	34%	1.38E+00	1.09E+02	3.93E+01	
4	4/12/2019	98.8	33%	4.05E+00	1.23E+02	4.08E+01	1.83E+01
4	4/29/2019	98.4	27%		1.09E+02	1.68E+01	5.23E+00
4	4/29/2019	101.8	33%	1.37E-01	9.68E+01		3.33E+00
4	4/29/2019	101.9	25%		1.14E+02	1.86E+01	2.03E+01
4	5/14/2019	100.3	35%	1.02E+00	1.04E+02	5.21E+01	1.25E+01
4	5/14/2019	101.8	31%	3.80E-01	1.02E+02	5.66E+01	8.85E+01
4	5/14/2019	101.9	31%		1.02E+02	1.20E+01	6.64E-01

4	5/28/2019	99.8	27%		1.36E+02	2.80E+01	4.81E+01
4	5/28/2019	102.4	31%	7.24E-01	1.37E+02	2.18E+01	5.36E+01
4	5/28/2019	105.9	30%		9.46E+01	1.85E+01	4.26E+01
4	6/18/2019	102.2	22%	6.96E-01	1.55E+02	8.32E+01	3.82E+01
4	6/18/2019	99.5	34%	1.08E+01	1.15E+02	4.96E+01	8.76E+01
4	6/18/2019	102.7	32%		9.41E+01	3.70E+00	8.99E-01
4	7/2/2019	99.7	28%	6.92E-01	1.22E+02	1.49E+01	7.09E+01
4	7/2/2019	99.6	25%		1.52E+02	1.68E+01	
4	7/16/2019	101.8	33%		1.13E+02	3.26E+01	3.50E+01
4	7/16/2019	105.2	34%		1.12E+02	2.15E+01	2.88E+01
4	7/16/2019	100.2	33%	8.61E-01	1.08E+02	2.28E+01	3.42E+01
4	7/30/2019	98.2	34%	1.02E+00	1.21E+02	2.64E+01	3.53E+01
4	7/30/2019	96.9	36%	6.06E-01	1.12E+02	2.47E+01	4.50E+01
4	7/30/2019	98.0	35%	4.56E-01	1.10E+02	3.08E+01	1.33E+01
4	8/13/2019	101.7	35%		1.05E+02	1.50E+01	3.20E+01
4	8/13/2019	98.4	34%	1.40E+00	1.22E+02	2.15E+01	8.63E+00
4	8/13/2019	102.4	34%	4.50E-01	1.04E+02	2.17E+01	1.00E+01
4	8/27/2019	105.2	38%	6.67E-01	1.00E+02	3.19E+01	8.77E+00
4	8/27/2019	104.4	37%		8.95E+01	2.95E+01	9.91E+00
4	8/27/2019	106.6	34%	1.79E-01	4.33E+01		
4	9/17/2019	99.7	37%		9.27E+01	1.65E+01	
4	9/17/2019	102.3	36%		1.03E+02	3.50E+01	1.44E+01
4	9/17/2019	105.7	36%		8.66E+01	4.96E+00	
4	10/1/2019	103.0	39%		8.80E+01	1.67E+01	5.10E+00
4	10/1/2019	97.2	39%	3.66E-01	9.58E+01	5.19E+01	2.59E+01
4	10/1/2019	97.2	39%	3.20E-01	1.09E+02	5.22E+01	3.14E+01
4	10/29/2019	102.9	37%	1.42E+00	7.48E+01	2.81E+01	
4	10/29/2019	101.3	38%		6.92E+01	2.48E+01	
4	10/29/2019	96.9	28%	2.03E+00	1.46E+02	7.03E+01	2.91E+01
5	6/25/2019	98.0	26%	1.01E+01	7.05E+00	5.77E+01	1.05E+02
5	6/25/2019	95.3	25%	1.45E+01	1.40E+01	4.36E+01	1.58E+02
5	6/25/2019	103.7	27%	1.45E+01	1.94E+01	6.45E+01	1.67E+02
5	7/2/2019	96.2	15%	2.37E+01	1.92E+01	3.91E+01	5.53E+01
5	7/2/2019	99.1	26%	1.98E+01	5.25E+01	1.04E+02	4.09E+02
5	7/2/2019	95.0	22%	6.19E+00	1.90E+00	4.41E+00	4.03E+00
5	7/16/2019	98.3	27%	1.36E+01	3.02E+01	7.22E+01	2.26E+02
5	7/16/2019	101.5	29%	9.01E+00	1.39E+01	5.04E+01	1.25E+02
5	7/16/2019	97.5	28%	9.39E+00	1.02E+01	2.62E+01	2.67E+01
5	7/30/2019	96.9	26%	9.84E+00	2.41E+00	3.33E+01	9.29E+00
5	7/30/2019	98.9	28%	9.42E+00	1.03E+01	3.36E+01	5.04E+01
5	7/30/2019	96.3	24%	5.43E+00	8.43E-01	1.45E+00	

5	8/13/2019	101.1	28%	3.54E+00	2.69E-02	1.66E+01	
5	8/13/2019	96.4	26%	3.70E+00			
5	8/13/2019	99.0	23%	5.25E+00		2.40E+01	
5	8/27/2019	99.4	28%	8.09E+00	2.47E+00	9.76E+00	
5	8/27/2019	96.0	28%	9.68E+00	1.21E+01	7.65E+01	2.31E+01
5	8/27/2019	96.3	28%	8.03E+00	2.65E+00	4.05E+01	9.00E+00
5	9/17/2019	103.1	14%		5.78E+00		1.26E+01
5	9/17/2019	95.9	15%	6.94E+00	2.28E+01	1.52E+01	1.03E+02
5	9/17/2019	96.4	13%	7.09E-01	4.48E-01		
5	10/1/2019	96.6	23%	3.69E+00		1.74E+01	1.67E+01
5	10/1/2019	98.5	21%	2.63E+00	8.25E+00	6.32E+00	8.79E+01
5	10/1/2019	97.1	22%	6.01E+00		1.71E+01	6.10E+01
5	10/29/2019	95.6	17%	2.83E+00	1.02E+00		
5	10/29/2019	95.2	27%	4.14E+00	1.35E+00	1.41E+01	4.69E+01
5	10/29/2019	101.3	25%	3.98E+00		4.39E+01	1.79E+02

Table A.3 Data for all 5 listed sites presented as µg of toxin per gram of dry algae. Shaded cells represent non-detects.

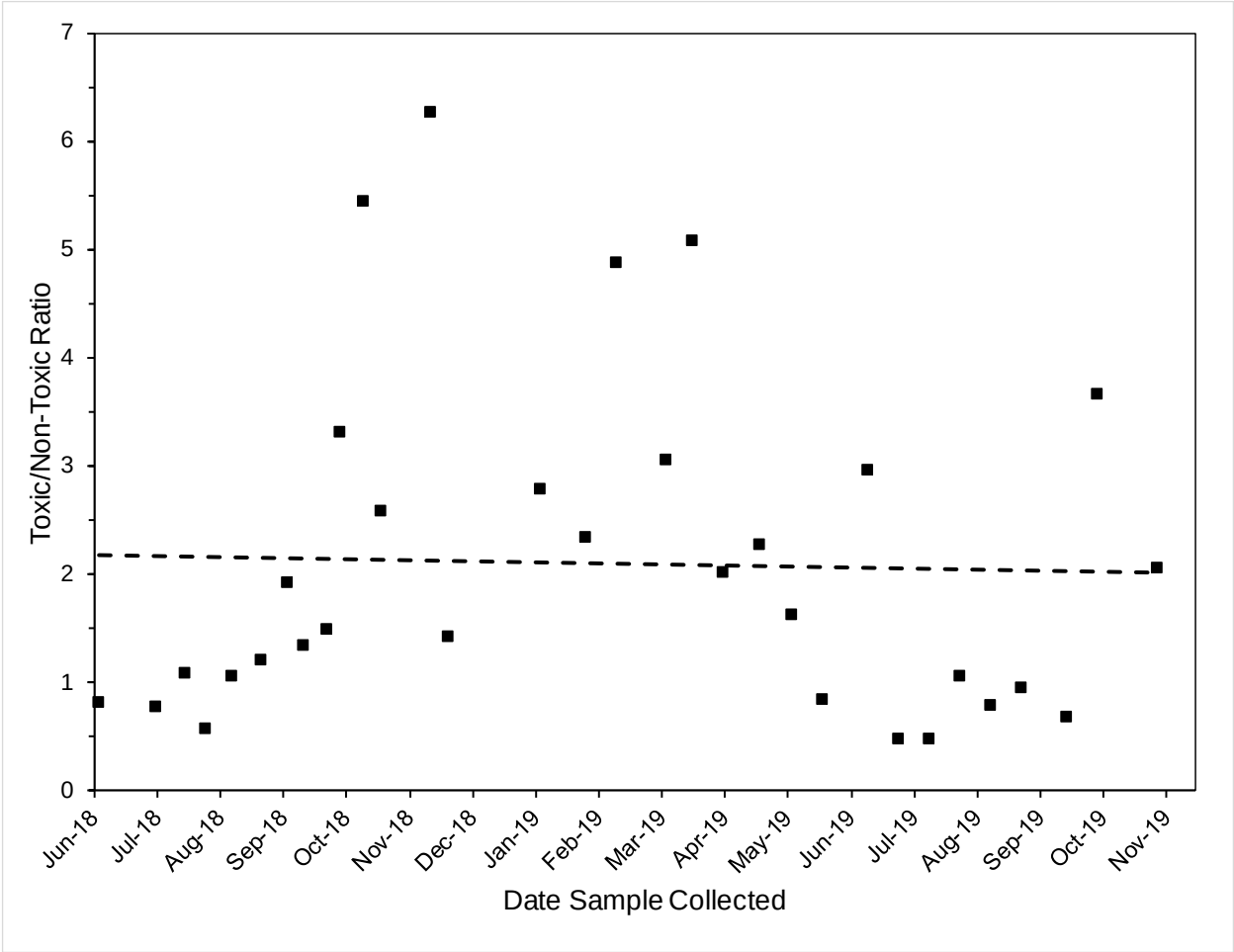

Figure A.5 The ratio of LWT5 over the sum of non-toxic LWTs (LWT1, 4, 6) showed essentially no time dependence over the study period ($r^2 < 0.01$). Each point is the average ratio from the three continuously monitored sites, dashed line is a linear fit.

APPENDIX B

R CODE FROM GAUSSIAN OVERLAP ANALYSIS, CHAPTER 2

```
#Script for phosphorus paper to calculate Gaussian overlap %


library(tidyverse)


# Functions ----------------------------------------------------
----------


#Function for determining overlap percentage. Generates x
sequence of values

#based on minimum and maximums of 4 sd's out from each mean, then
runs a density

#function out and finds distribution percentage of each tail.

get_overlap_coef <- function(mu1, mu2, sd1, sd2) {

  xs  <- seq(min(mu1 - 4 * sd1, mu2 - 4 * sd2),

             max(mu1 + 4 * sd1, mu2 + 4 * sd2),

             length.out = 1000)

  f1  <- dnorm(xs, mean = mu1, sd = sd1)

  f2  <- dnorm(xs, mean = mu2, sd = sd2)

  int <- xs[which.max(pmin(f1, f2))]

  l   <- pnorm(int, mu1, sd1, lower.tail = mu1 > mu2)

  r   <- pnorm(int, mu2, sd2, lower.tail = mu1 < mu2)

  l + r

}
```

```
# test numbers for function development
# mu1 <- 5
# mu2 <- 4.5
# sd1 <- 17
# sd2 <- 6


#When means are within a small range of each other
two_int_ovl <- function(mu1, mu2, sd1, sd2) {
  xs    <- seq(min(mu1 - 4 * sd1, mu2 - 4 * sd2),
               max(mu1 + 4 * sd1, mu2 + 4 * sd2),
               length.out = 1000)
  f     <-
    function(x)
      dnorm(x, mean = mu1, sd = sd1) - dnorm(x, mean = mu2, sd =
sd2)
  int.1 <- uniroot(f, lower = min(xs), upper = 0)
  int.1 <- int.1$root
  int.2 <- uniroot(f, lower = 0, upper = max(xs))
  int.2 <- int.2$root
  l_2   <- pnorm(int.1, mu2, sd2, lower.tail = TRUE)
  r_2   <- pnorm(int.2, mu2, sd2, lower.tail = FALSE)
  l_1   <- pnorm(int.1, mu1, sd1, lower.tail = TRUE)
  r_1   <- pnorm(int.2, mu1, sd1, lower.tail = FALSE)
  center <- 1 - l_1 - r_1
```

```
  sum(l_2, r_2, center)
}


#Plotting function based on same variables as overlap function
plot_overlap <- function(title, mu1, mu2, sd1, sd2) {
  xs  <- seq(min(mu1 - 4 * sd1, mu2 - 4 * sd2),
             max(mu1 + 4 * sd1, mu2 + 4 * sd2),
             length.out = 1000)
  f1  <- dnorm(xs, mean = mu1, sd = sd1)
  f2  <- dnorm(xs, mean = mu2, sd = sd2)

  plot(xs,
       f1,
       type = "l",
       ylim = c(0, max(f1, f2)),
       ylab = "density",
       main = title)
  lines(xs, f2, lty = "dotted")
  ys <- pmin(f1, f2)
  xs <- c(xs, xs[1])
  ys <- c(ys, ys[1])
```

```
  polygon(xs, ys, col = "gray")
}


# CBB Calculation ---------------------------------------------------
----------


#Data from mapping in the field
cbb_field_mu <- 5.24e6
cbb_field_sd <- 9.93e5


#From excel
cbb_mu <-
  c(
    chl = 1.03e5,
    tn = 5.38e4,
    tp = 1.27e5,
    swt = 2.21e4,
    tn_swt = 2.59e4,
    sed_p = 1.97e6
  )
cbb_sd <-
  c(
    chl = 8.54e4,
    tn = 8.30e4,
```

```
    tp = 8.86e4,
    swt = 9.24e2,
    tn_swt = 2.15e3,
    sed_p = 7.04e5
  )

#iterate function
cbb_output <-
  mapply(get_overlap_coef,
         mu1 = cbb_field_mu,
         cbb_mu,
         sd1 = cbb_field_sd,
         cbb_sd)
#Parameter Labels
param_list <- c("chl", "tn", "tp", "swt", "tn_swt", "sed_p")
#Output Matrix
cbb_ovl <- cbind(param_list, cbb_output)
write.table(cbb_ovl, file = "cbb_ovl.csv", sep = ",")

# LWT Calculation ----------------------------------------------
----------

#import LWT1, 5, 6 data from Phosphorus Data spreadsheet and make
lists
```

```
lwt_data <- read_csv("lwt_ovl_r_input.csv")


lwt_field_mu <- lwt_data$lwt_field_mu

lwt_field_sd <- lwt_data$lwt_field_sd

lwt_model_mu <- lwt_data$lwt_model_mu

lwt_model_sd <- lwt_data$lwt_model_sd


#Iterate 2 intercept function for 1, 5, 6

lwt_output <-

  mapply(two_int_ovl,

         lwt_field_mu,

         lwt_model_mu,

         lwt_field_sd,

         lwt_model_sd)


#Add in LWT4 which is different using original function and
hardcode data

lwt_output <- append(lwt_output, get_overlap_coef(29089, 747,
2208, 1588))


#labels for LWTs

lwt_name_list <- c("lwt1", "lwt5", "lwt6", "lwt4")

#Output matrix

lwt_ovl <- cbind(lwt_name_list, lwt_output)
```

```
write.table(lwt_ovl, file = "lwt_ovl.csv", sep = ",")


# CBB Plots ----------------------------------------------------
----------


mapply(plot_overlap,

       param_list,

       mu1 = cbb_field_mu,

       cbb_mu,

       sd1 = cbb_field_sd,

       cbb_sd)


# LWT Plots ----------------------------------------------------
----------


lwt_name_list <- c("lwt1", "lwt5", "lwt6")

mapply(plot_overlap,

       lwt_name_list,

       lwt_field_mu,

       lwt_model_mu,

       lwt_field_sd,

       lwt_model_sd)


plot_overlap("lwt4",29089, 747, 2208, 1588)
```

APPENDIX C

PUBLISHED PAPERS[1]

[1] Smith, M. L., Westerman, D. C., Putnam, S. P., Richardson, S. D., & Ferry, J. L. (2019). Emerging Lyngbya wollei toxins: A new high resolution mass spectrometry method to elucidate a potential environmental threat. *Harmful Algae*, *90*, 101700. https://doi.org/10.1016/j.hal.2019.101700

Published in final edited form as:

Harmful Algae. 2019 December ; 90: 101700. doi:10.1016/j.hal.2019.101700.

Emerging *Lyngbya wollei* toxins: A new high resolution mass spectrometry method to elucidate a potential environmental threat

Meagan L. Smith[1,2], **Danielle C. Westerman**[1,2], **Samuel P. Putnam**[1,2], **Susan D. Richardson**[1,2], **John L. Ferry**[1,2]

[1]University of South Carolina, Department of Chemistry and Biochemistry, 631 Sumter Street Columbia, SC 29208

[2]University of South Carolina, Center for Interactions of Climate Change on Oceans and Human Health, 921 Assembly St Suit 401, Columbia, SC 29208

Abstract

Mass spectrometric methods for the quantitative and qualitative analyses of algal biotoxins are often complicated by co-eluting compounds that present analytically as interferences. This issue is particularly critical for organic polyamines, where co-eluting materials can suppress the formation of cations during electrospray ionization. Here we present an extraction procedure designed specifically to overcome matrix-derived ion suppression of algal toxins in samples of Lyngbya

wollei, a filamentous benthic algae known to produce several saxitoxin analogues. Lyngbya wollei samples were collected from a large, persistent harmful algal bloom in Lake Wateree, SC. Six known Lyngbya wollei-specific toxins (LWT1–6) were successfully resolved and quantified against saxitoxin using hydrophilic interaction liquid chromatography coupled with triple quadrupole and quadrupole time-of-flight mass spectrometry. The parent ions $[M^{2+} – H^{+}]^{+}$ were observed for LWTs 1–6 and the $[M]^{2+}$ ion was observed for LWT5. High resolution mass spectra and unique fragmentation ions were obtained for LWTs 1–6. A dilution factor of 50 resulted in a linear calibration of saxitoxin in the algae matrix. Ion suppression was resolved by sample dilution, which led to linear, positive correlations between peak area and mass of the extracted sample ($R^2 > 0.96$). Optimized sample extraction method and instrument parameters are presented.

Keywords

cyanobacteria; saxitoxin; benthic; filamentous; quantification; liquid chromatography

Conflicts of interest
There are no conflicts to declare

Declaration of interests
The authors declare that they have no known competing financial interests or personal relationships that could have appeared to influence the work reported in this paper.

1. Introduction

Analogues of the neurotoxic alkaloid saxitoxin, also known as paralytic shellfish toxins are members of a class of naturally occurring secondary metabolites produced by freshwater cyanobacteria and marine dinoflagellates (Harada et al., 1982; Oshima et al., 1987). Saxitoxin is a selective sodium channel blocker that has been documented to be extremely toxic to a wide range of species, including humans (Carmichael, 1994; Jochimsen et al., 1998; Kao, 1993; Landsberg, 2002; Negri et al., 1995). To date, there are at least 57 known analogues of saxitoxin (Wiese et al., 2010) with varying levels of toxicity (by mouse bioassay), produced by a variety of genera including Anabaena (Al-Tebrineh et al., 2010; Humpage et al., 1994; Onodera et al., 1996), Cylindospermopsis (Lagos et al., 1999),
Aphanizomenon (Jackim and Gentile, 1968; Mahmood and Carmichael, 1986; Sawyer et al., 1968), Planktothrix (Pomati et al., 2003), and Lyngbya (Dell'Aversano, 2011). Lyngbya wollei (Farlow ex Gomont) Speziale & Dyck, a filamentous, benthic cyanobacteria, is a source of saxitoxin analogues known as Lyngbya wollei toxins (Carmichael et al., 1997; Cowell and Botts, 1994; Foss et al., 2012b; Onodera et al., 1997; Yin et al., 1997) (LWTs, Figure 1 and Figure S1).

The qualification and quantification of saxitoxin analogues can be challenging. Effect based assays, including the mouse bioassay (Cusick and Sayler, 2013; Schantz et al., 1958; Turner et al., 2012), in-vitro cell viability assays (Gallacher and Birkbeck, 1992; Jellett et al., 1992;
Kogure et al., 1988; Manger et al., 1993), enzyme-linked immune sorbent assay (Chu et al., 1992; Humpage et al., 2010), and receptor binding assay (Davio and Fontelo, 1984; Doucette et al., 1997; Usup et al., 2004; Van Dolan et al., 2012) can provide qualitative and quantitative toxicity information (Cusick and Sayler, 2013). However, these techniques report concentrations as summed saxitoxin equivalents and do not report the relative concentrations of different structural analogues. The latter is key for developing a detailed understanding of the relevant toxin biosynthetic pathways and understanding the synergistic toxic effects possible from complex toxin sources like Lyngbya wollei.

Mass spectrometric techniques are alternatives that typically have a wider linear dynamic range than most immunoassays and offer a higher level of structural information than effectbased assays (D'Agostino et al., 2019; Dell'Aversano, 2011; Dell'Aversano et al., 2005; Dell'Aversano et al., 2019; Foss et al., 2012b; Lajeunesse et al., 2012). However, the use of electrospray ionization mass spectrometry for the identification and quantification of polyamines like the saxitoxin analogues can be complicated by the presence of co-extracted materials that affect ionization efficiency in the source (Dell'Aversano, 2011; Foss et al., 2012b). The most commonly observed effect is suppression, resulting in non-linear calibration curves for the saxitoxin analogues

(Onodera et al., 1997; Annesley, 2003). Here we report the development of a new mass spectrometry method for accurate and precise measurement of Lyngbya wollei toxins at ng/L detection limits that overcomes ion suppression.

2. Materials and Methods

2.1. Materials

All chemicals were used as received. All aqueous solutions used 18 MΩ cm^{-1} (Barnstead Epure) water. All glassware was acid washed in 2 M HCl/0.1 M oxalic acid prior to oxidation in a muffle furnace to ensure it was trace metal and organic free. Acetonitrile (HPLC grade) was obtained from VWR BDH chemicals. Ammonium formate (98+%) was purchased from Alfa Aesar. Formic acid (certified ACS), glacial acetic acid (certified ACS PLUS), and hydrochloric acid (certified ACS Plus) were purchased from Fisher. Saxitoxin dihydrochloride in dilute hydrochloride standard solutions were obtained from NIST and Abraxis Inc.

2.2. Sampling

Lyngbya wollei grab samples were collected on November 6, 2018 from a surface floating mat on Lake Wateree, SC. Samples were collected in sterile 500-mL collection bottles and stored at 0°C during transport (less than three hours). Samples were processed immediately when received. Samples were rinsed lightly under deionized water to remove entangled detritus, drained of excess water, frozen in liquid nitrogen, and lyophilized. After lyophilization, algae samples were homogenized using a tissue grinder and stored at −20 °C until extraction.

2.3. Extraction method

Freeze dried algae samples were returned to room temperature and their masses obtained with an analytical balance. Sample mass varied from 25–300 mg of dry weight algae. All samples were mixed with 10 mL 0.1 M acetic acid, sonicated for 15 minutes and centrifuged for 5 minutes. The resulting supernatant was removed, passed through a 0.45-micron nylon filter and analyzed by liquid chromatography-mass spectrometry. We also investigated the role of a strong acid as the extraction solvent as a potential variable that could affect the measured concentration of LWTs in field samples. Extractions and subsequent dilutions were repeated using 0.1 M HCl and 0.01 M HCl. The mass to volume ratio was kept constant at 10 mg of dry weight algae for every 1 mL of extraction solvent in the extraction procedure to produce extracts for subsequent sample dilution experiments.

2.4. Chromatography and Mass Spectrometry

Toxins were analyzed using a Waters (Milford, MA, USA) Acquity ultra performance liquid chromatograph (UPLC) coupled with a Xevo triple quadrupole (TQ) mass spectrometer equipped with an electrospray ionization (ESI) source in positive ion mode. High resolution analyte confirmation was performed on an Agilent (Santa Clara, CA, USA) 1290 Infinity II ultrahigh performance liquid chromatograph (UHPLC) system coupled to an Agilent 6545 quadrupole (Q)-time-of-flight (TOF) tandem mass spectrometer with electrospray ionization (ESI) in positive ion mode. High resolution Q-TOF data was processed using Agilent B.

08.00 software. Separations were performed on a BEH Amide (2.1×150 mm) 1.7 µm particle size column (Waters). The mobile phases were aqueous 5.6 mM formate buffered pH 3.5 (A) and 95:5 acetonitrile:water 5.6 mM formate buffer pH 3.5 (B). The gradient LC method used for both instruments (TQ and Q-TOF) was as follows: 80% B held for one minute, ramped to 60% B over the next 3 minutes and held for 2 minutes, at 7 minutes ramped back to the original conditions over one minute (80% B) and held for re-equilibration for 8 minutes (16 minutes total).

Saxitoxin was optimized manually by direct infusion into the source, using an optimized cone voltage of 0.5 kV and cone energy of 80 V. The source temperature was 150 °C. The desolvation temperature, extractor voltage, desolvation gas flow, cone gas flow, and collision gas flow are shown in Table S1. Limit of detection for saxitoxin on the UPLC-TQ was 0.1 ppb (Table S2). Due to the lack of commercial standards, optimization of source conditions on the UPLC-TQ mass spectrometer was done by optimizing chromatographic peak areas. A series of source methods was developed varying capillary and cone voltages to determine the optimal ionization parameters for LWT1, 4, 5, and 6 (Figure S2). A capillary voltage of 0.5 kV was optimal for all LWTs observed, consistent with the voltage for saxitoxin. LWT1 experienced in-source fragmentation at cone potentials significantly above 30 V, therefore this value was maintained at 30 V at the retention time window corresponding to LWT1 elution. The other LWTs did not experience this issue, and a cone energy of 80 V was optimal for LWT4, LWT5, and LWT6. The limit of detection was calculated for saxitoxin

Instrument parameters previously optimized for identifying small molecules by UHPLCQTOF were utilized for LWT confirmation (Huang et al., 2018). The mass spectrometer was operated at a fragmentation voltage of 110 V, capillary voltage of 4000 V, gas temperature of 300 °C, drying gas flow of 12 L min^{-1}, and nebulizer pressure of 35 psi, with a m/z scan range of 50 to 750. During initial analyte screening, the collision energy was ramped from 0, 20, to 40 eV every scan to obtain both MS and MS/MS spectra for each peak. Once LWTs of interest were identified in algae extracts, targeted analysis was performed with a collision energy of 30 eV to obtain high resolution MS/MS spectra.

3. Results

3.1. Toxin Identification

Previous published studies on the analysis of LWTs were the result of mass spectrometers with unit-mass resolution, along with NMR (nuclear magnetic resonance) spectroscopy (Dell'Aversano et al., 2005; Foss et al., 2012a; Foss et al., 2012b; Onodera et al., 1996). In our study, saxitoxin analogues were initially detected in Lyngbya wollei extracts by full scan analysis at unit mass resolution on the UPLC-TQ mass spectrometer (Figure 2). LWTs lose a proton during ionization, forming an $[M^{2+} – H^{+}]^{+}$ parent ion, which is consistent with previously published work on doubly charged, low molecular weight poly amines by ESIMS (Castro et al., 2001; Pizzutti et al., 2016; Wang et al., 2008). High resolution analysis by UHPLC-QTOF-MS was utilized for confirmation of the identity of saxitoxin and the suspected LWTs (Figure S3–S7). High resolution data provided exact masses of precursor and product ions, correlating to a specific molecular formula for each

peak, which allowed additional confidence in the chemical structures for these toxins (Table 1).

The structural similarities between the LWTs and saxitoxin means that similar product ion profiles were seen across multiple analytes of interest. For example, fragments with m/z 72.0556 and m/z 60.0556, corresponding to elemental formulae of $C_2H_6N_3$ (< 6 ppm mass error) and CH_6N_3 (< 2 ppm mass error), respectively, were observed for all LWTs (Table 1). Fragmentation of LWT1 resulted in ten fragment ions. The sulfur-containing functional group was lost from each fragment ion observed. Thirteen fragment ions were observed for LWT4 (Table 1). Similarly to LWT1, the most abundant fragment was from loss of the OH functional group, as well loss of nitrogenous fragments (such as CH_5N_3 and CH_4N_3). Six identical product ions were observed between LWT4 and LWT6.

Fragment ions obtained for LWT5 and saxitoxin were nearly identical (Table 1 and Table S3). Eleven fragment ions were observed for LWT5, of those eleven, eight were identical ions to saxitoxin. The three unique product ions were the result of losses from locations other than the carbamate ester (for saxitoxin) or the acetyl ester (for LWT5). Resulting mass differences in these product ions differed by 1 Da. For example, the loss of water from LWT5 resulted in the product ion m/z 281.1357, whereas the loss of water from saxitoxin resulted in m/z 282.1309. The agreement between fragments for saxitoxin and LWTs increases the confidence in the LWT identifications. Importantly, this agreement suggests parallels between the ionization chemistry of these two families of analytes, supporting the use of saxitoxin as a quantification standard for the LWTs, in the absence of commercially available standards for these toxins.

LWT2 and LWT3 are structural isomers (hereafter referred to as LWT2/3) with the same molecular weight. They were not detected using the UPLC-TQ mass spectrometer, but at least one isomer was detected with the QTOF mass spectrometer during the high resolution analysis of the algae extract (Figure S8, Table S4). LWT2/3 are structural isomers, and likely were not separable with the chromatographic approaches used in this study; thus, it is possible that both isomers were present, but coeluted. Similar to LWT1, LWT2/3 has a sulfur-containing functional group which was lost in four out of the six product ions observed. LWT2/3 were 2 orders of magnitude lower in peak intensity, relative to LWT1, 4, 5, and 6 (which had peak intensities on the order of 10^5) on the QTOF mass spectrometer, and LWT2/3 were undetectable at these concentrations on the UPLC-TQ mass spectrometer.

3.2. Matrix Effects

The initial extraction procedure used 0.1 M acetic acid, sonication for 15 min, and filtration before analysis by UPLC-MS. However, the method response (peak area) from this extraction procedure showed a non-linear relationship vs the mass of the algae extracted ($R^2 < 0.6838$) for LWT4, 5, and 6. Furthermore, peak area vs mass extracted showed a negative slope for LWT5 (Figure 3). This behavior is consistent with the presence of co-extracted materials in the sample acting to suppress the ionization of the LWTs in the mass spectrometer (Annesley, 2003).

A commercially available standard, saxitoxin, was added to the sample as a surrogate LWT to probe for the nature of matrix effects. Saxitoxin calibration curves were prepared from 0.1 M acetic acid and algae extracts for comparative purposes (Figure 4). The slope for saxitoxin in acetic acid was 7820 ppb^{-1} with an R^2 of 0.9923, whereas in the algae matrix, the slope was 926 ppb^{-1} saxitoxin with an R^2 of 0.2455. The concentration dependence was determined by diluting saxitoxin-spiked algae extracts in 0.1 M acetic acid (Figure 5) over a range of dilution factors (corresponding to a dilution factor of zero to 1000). Comparison of peak areas vs log dilution factor for the LWTs (Figure 5) showed a parabolic function for LWT 4, 5, and 6.

Examination of the dilution factor effect revealed that sample dilution of 50 or more reduced the interfering species to a level essentially below "detection" based on their ability to disproportionately affect the standard. The full calibration curve for saxitoxin was repeated at a dilution factor of 1:50 for extract:acetic acid. The corresponding curve (Figure 5 inset) was linear with a slope of 7975 ppb^{-1} and an R^2 of 0.9959. In order to test the linearity of our toxins at a DF of 50, the mass of dry algae was varied over the range of 25 – 300 mg, extracted, and the resulting extracts were diluted by a factor of 50. The peak area vs mass was linear ($R^2 > 0.9522$) for all toxins observed (Figure 6).

3.3. Extraction in Hydrochloric acid

As shown in the literature, the choice of extraction solvent is important, and the presence of strong acids can alter the apparent toxin profile. We investigated the role of such strong acids in relation to the matrix effects experienced by the LWTs. LWT5 and LWT6 were affected strongly by the addition of HCL as the extraction solvent. This change caused an increase in the required dilution by a factor of 2 to ensure dilution of the matrix beyond visible suppression effects (Figure S9). Therefore, our results indicate the addition of HCl in any
capacity during LWT analysis is inadvisable.

The high-resolution fragmentation analysis presented here provides an unprecedented range of fragment ion options that can be used to conclusively indicate the presence and retention time of LWTs 1 through 6 in a sample, even in the absence of commercial standards. These same transitions can be used for MRM-based analyses in quantification. The presence of ion suppression factors can vary within environmental matrices. Smaller, polar molecules are more susceptible to ion suppression, as well as amine analytes. Biological samples are more likely to contain nonvolatile and less volatile solutes, leading to a change in spray droplet solution properties, which can be a major source of ion suppression when using electrospray. Given that saxitoxin analogues are small, polar molecules, usually extracted from natural samples, matrix effects will most likely be present in any algae extract, therefore, the current results suggest analysis of saxitoxin and its analogues extracted from algae should be subjected to a dilution factor-based assay. A strategy to obtain linear saxitoxin calibration within the algae matrix as well as linear toxin vs. mass correlations is demonstrated. The current work suggests a safe dilution factor of at least 10 for the Lake Wateree based samples, however for our work we chose 50 to ensure adequate dilution of the matrix during lake turnover events.

Accurate risk assessments for Lyngbya wollei are extremely difficult due to reference standards for the mixture of toxins produced by this algae being commercially unavailable. Effect-based assays for the analysis of these toxins remain largely non-specific, fail to provide a molecular toxin profile, and often require secondary verification by mass spectrometry. The combination of a lack of standards for quantification and qualification make risk assessment and remediation a gamble each time this species is encountered, as historically the relative concentrations of LWTs are variable and unpredictable. Utilizing a dilution factor-based assay, as presented here, provides selective detection with minimal sampling processing to avoid interferences from ion-suppressing matrix effects.

Supplementary Material

Refer to Web version on PubMed Central for supplementary material.

Acknowledgments

The authors would to extend special thanks to WaterWatch, Randy Kelly ,and volunteers for their aid in access to Lake Wateree by boat. This work is a product of the Oceans and Human Health Center on Climate Change Interactions at the University of South Carolina and was supported by NIEHS Grant 1P01ES028942-01.

Abbreviations:

LWT	Lyngbya wollei toxin
UPLC-TQ	Ultra performance liquid chromatograph – triple quadrupole
UHPLC-QTOF	ultrahigh performance liquid chromatograph – quadrupole time-of-flight
ESI	electrospray ionization
MS/MS	tandem mass spectrometry

References

Al-Tebrineh J, Mihali TK, Pomati F, Neilan BA, 2010 Detection of Saxitoxin-Producing Cyanobacteria and Anabaena circinalis in Environmental Water Blooms by Quantitative PCR. Applied and Environmental Microbiology 76(23), 7836–7842. [PubMed: 20935128]

Annesley TM, 2003 Ion suppression in mass spectrometry. Clinical Chemistry 49(7), 1041–1044. [PubMed: 12816898]

Carmichael WW, 1994 Toxins of cyanobacteria. Sci.Am 270(1), 78–86. [PubMed: 8284661]

Carmichael WW, Evans WR, Yin QQ, Bell P, Moczydlowski E, 1997 Evidence for paralytic shellfish poisons in the freshwater cyanobacterium Lyngbya wollei (Farlow ex Gomont) comb. nov. Applied and Environmental Microbiology 63(8), 3104–3110. [PubMed: 9251196]

Castro R, Moyano E, Galceran MT, 2001 Ion-trap versus quadrupole for analysis of quaternary ammonium herbicides by LC-MS. Chromatographia 53(5–6), 273–278.

Chu FS, Huang X, Hall S, 1992 Production and characterization of antibodies against neosaxitoxin. Journal of Aoac International 75(2), 341–345.

Cowell BC, Botts PS, 1994 Factors influencing the distribution, abundance and growth of Lyngbya wollei in central Florida. Aquatic Botany 49(1), 1–17.

Cusick KD, Sayler GS, 2013 An Overview on the Marine Neurotoxin, Saxitoxin: Genetics, Moleuclar Targets, Methods of Detection and Ecological Functions. Marine Drugs 11, 991–1018. [PubMed: 23535394]

D'Agostino PM, Boundy MJ, Harwood TD, Carmichael WW, Neilan BA, Wood SA, 2019 Re-evaluation of paralytic shellfish toxin profiles in cyanobacteria using hydrophilic interaction liquid chromatography-tandem mass spectrometry. Toxicon 158, 1–7. [PubMed: 30471380]

Davio SR, Fontelo PA, 1984 A competitive displacement assay to detect saxitoxin and tetrodotoxin. Analytical Biochemistry 141(1), 199–204. [PubMed: 6496928]

Dell'Aversano C, 2011 Hydrophilic Interaction Liquid Chromatography-Mass Spectrometry (HILICMS) of Paralytic Shellfish Poisoning Toxins, Domoic Acid, and Assorted Cyanobacterial Toxins, In: Wang PG, He W (Eds.), Hydrophilic Interaction Liquid Chromatography. Crc Press-Taylor & Francis Group, Boca Raton, pp. 105–132.

Dell'Aversano C, Hess P, Quilliam MA, 2005 Hydrophilic interaction liquid chromatography-mass spectrometry for the analysis of paralytic shellfish poisoning (PSP) toxins. Journal of Chromatography A 1081(2), 190–201. [PubMed: 16038209]

Dell'Aversano C, Tattaglione L, Polito G, Dean K, Giacobbe M, Casabianca S, Capellacci S, Penna A, Turner AD, 2019 First detection of tetrodotoxin and high levels of paralytic shellfish poisoning toxins in shellfish from Sicily (Italy) by three different analytical methods. Chemosphere 215, 881–892. [PubMed: 30408884]

Doucette GJ, Logan MM, Ramsdell JS, VanDolah FM, 1997 Development and preliminary validation of a microtiter plate-based receptor binding assay for paralytic shellfish poisoning toxins. Toxicon 35(5), 625–636. [PubMed: 9203287]

Foss AJ, Phlips EJ, Aubel MT, Szabo NJ, 2012a Investigation of extraction and analysis techniques for Lyngbya wollei derived Paralytic Shellfish Toxins. Toxicon 60(6), 1148–1158. [PubMed: 22960450]

Foss AJ, Phlips EJ, Yilmaz M, Chapman A, 2012b Characterization of paralytic shellfish toxins from Lyngbya wollei dominated mats collected from two Florida springs. Harmful Algae 16, 98–107.

Gallacher S, Birkbeck TH, 1992 A tissue culture assay for direct detection of sodium-channel blocking toxins in bacterial culture supernates. Fems Microbiology Letters 92(1), 101–108.

Harada T, Oshima Y, Yasumoto T, 1982 Studies on paralytic shellfish poisoning in tropical waters .4. Structures of 2 paralytic shellfish toxins, gonyautoxin-V and gonyautoxin-VI isolated from a tropical dinoflagellate, pyrodinium bahamense var compressa. Agricultural and Biological Chemistry 46(7), 1861–1864.

Huang Y, Kong M, Westerman D, Xu EG, Coffin S, Cochran KH, Liu Y, Richardson SD, Schlenk D, Dionysiou DD, 2018 Effects of HCO3- on Degradation of Toxic Contaminants of Emerging Concern by UV/NO3. Environmental Science & Technology 52(21), 12697–12707. [PubMed: 30284820]

Humpage AR, Magalhaes VF, Froscio SM, 2010 Comparison of analytical tools and biological assays for detection of paralytic shellfish poisoning toxins. Analytical and Bioanalytical Chemistry
397(5), 1655–1671. [PubMed: 20101494]

Humpage AR, Rositano J, Bretag AH, Brown R, Baker PD, Nicholson BC, Steffensen DA, 1994 Paralytic shellfish poisons from australian cyanobacterial blooms. Australian Journal of Marine and Freshwater Research 45(5), 761–771.

Jackim E, Gentile J, 1968 Toxins of a blue green alga - similarity to saxitoxin. Science 162(3856), 915–&. [PubMed: 5684499]

Jellett JF, Marks LJ, Stewart JE, Dorey ML, Watsonwright W, Lawrence JF, 1992 Paralytic shellfish poison (saxitoxin family) bioassays - automated end-point determination and standardization of the invitro tissue-culture bioassay, and comparison with the standard mouse bioassay. Toxicon 30(10), 1143–1156. [PubMed: 1440621]

Jochimsen EM, Carmichael WW, An JS, Cardo DM, Cookson ST, Holmes CEM, Antunes MBD, de Melo DA, Lyra TM, Barreto VST, Azevedo S, Jarvis WR, 1998 Liver failure and death after exposure to microcystins at a hemodialysis center in Brazil. N. Engl. J. Med 338(13), 873–878. [PubMed: 9516222]

Kao CY, 1993 Paralytic shellfish poisoning. Algal toxins in seafood and drinking water., 75–86.

Kogure K, Tamplin ML, Simidu U, Colwell RR, 1988 A tissue culture assay for tetrodotoxin, saxitoxin and related toxins. Toxicon 26(2), 191–197. [PubMed: 3363566]

Lagos N, Onodera H, Zagatto PA, Andrinolo D, Azevedo S, Oshima Y, 1999 The first evidence of paralytic shellfish toxins in the freshwater cyanobacterium Cylindrospermopsis raciborskii, isolated from Brazil. Toxicon 37(10), 1359–1373. [PubMed: 10414862]

Lajeunesse A, Segura PA, Gelinas M, Hudon C, Thomas K, Quilliam MA, Gagnon C, 2012 Detection and confirmation of saxitoxin analogues in freshwater benthic Lyngbya wollei algae collected in the St. Lawrence River (Canada) by liquid chromatography-tandem mass spectrometry. Journal of Chromatography A 1219, 93–103. [PubMed: 22169195]

Landsberg JH, 2002 The effects of harmful algal blooms on aquatic organisms. Reviews in Fisheries Science 10(2), 113–390.

Mahmood NA, Carmichael WW, 1986 Paralytic shellfish poisons produced by the freshwater cyanobacterium Aphanizomenon-flos-aquae NH-5. Toxicon 24(2), 175–&. [PubMed: 3085292]

Manger RL, Leja LS, Lee SY, Hungerford JM, Wekell MM, 1993 Tetrazolium-based cell bioassay for neurotoxins active on voltage sensitive sodium channels - semiautomated assay for saxitoxins, brevetoxins, and ciguatoxins. Analytical Biochemistry 214(1), 190–194. [PubMed: 8250223]

Negri AP, Jones GJ, Hindmarsh M, 1995 Sheep mortality associated with paralytic shellfish poisons from the cyanobacterium anabaena circinalis. Toxicon 33(10), 1321–1329. [PubMed: 8599183]

Onodera H, Oshima Y, Watanabe MF, Watanabe M, Bolch CJ, Blackburn S, Yasumoto T, 1996 Screening of paralytic shellfish toxins in freshwater cyanobacteria and chemical confirmation of the toxins in cultured Anabaena circinalis from Australia, In: Yasumoto T, Oshima Y, Fukuyo Y (Eds.), Harmful and Toxic Algal Blooms. IOS UNESCO, Paris, pp. 563–566.

Onodera H, Satake M, Oshima Y, Yasumoto T, Carmichael WW, 1997 New saxitoxin analogues from the freshwater filamentous cyanobacterium Lyngbya wollei. Natural Toxins 5(4), 146–151. [PubMed: 9407557]

Oshima Y, Hasegawa M, Yasumoto T, Hallegraeff G, Blackburn S, 1987 Dinoflagellate Gymnodinium catenatum as the source of paralytic shellfish toxins in tasmanian shellfish. Toxicon 25(10), 1105– 1111. [PubMed: 3424391]

Pizzutti IR, Vela GME, de Kok A, Scholten JM, Dias JV, Cardoso CD, Concenco G, Vivian R, 2016
Determination of paraquat and diquat: LC-MS method optimization and validation. Food Chemistry 209, 248–255. [PubMed: 27173559]

Pomati F, Sacchi S, Rosetti C, Giovannardi S, Onodera H, Oshima Y, Neilan BA, 2003 The freshwater cyanobacterium Planktothrix Sp. FP1: Molecular identification and detection of paralytic shellfish poisoning toxins. Journal of Phycology 36(3), 553–562.

Sawyer PJ, Gentile JH, Sasner JJ, 1968 Demonstration of a toxin from Aphanizomenon flos aquae (L)
Ralfs. Canadian Journal of Microbiology 14(11), 1199–&. [PubMed: 5724889]

Schantz EJ, McFarren EF, Schafer ML, Lewis KH, 1958 Purified shellfish poison for bioassay standardization. Journal of the Association of Official Agricultural Chemists 41(1), 160–168.

Turner AD, Dhanji-Rapkova M, Algoet M, Suarez-Isla BA, Cordova M, Caceres C, Murphy CJ, Casey M, Lees DN, 2012 Investigations into matrix components affecting the performance of the official bioassay reference method for quantitation of paralytic shellfish poisoning toxins in oysters. Toxicon 59(2), 215–230. [PubMed: 22138287]

Usup G, Leaw CP, Cheah MY, Ahmad A, Ng BK, 2004 Analysis of paralytic shellfish poisoning toxin congeners by a sodium channel receptor binding assay. Toxicon 44(1), 37–43. [PubMed: 15225560]

Van Dolan FM, Fire SE, Leighfield TA, Mikulski CM, Doucette GJ, 2012 Determination of Paralytic
Shellfish Toxins in Shellfish by Receptor Binding Assay: Collaborative Study. Journal of Aoac International 95(3), 795–812. [PubMed: 22816272]

Wang KC, Chen SM, Hsu JF, Cheng SG, Lee CK, 2008 Simultaneous detection and quantitation of highly water-soluble herbicides in serum using ion-pair liquid chromatography-tandem mass spectrometry. J. Chromatogr. B 876(2), 211–218.

Wiese M, D'Agostino PM, Mihali TK, Moffitt MC, Neilan BA, 2010 Neurotoxic Alkaloids: Saxitoxin and Its Analogs. Marine Drugs 8(7), 2185–2211. [PubMed: 20714432]

Yin QQ, Carmichael WW, Evans WR, 1997 Factors influencing growth and toxin production by cultures of the freshwater cyanobacterium Lyngbya wollei Farlow ex Gomont. Journal of Applied Phycology 9(1), 55–63.

Highlights

- High resolution mass spectra and unique fragmentation ions obtained for the algal toxins observed
- Dilution of algal extracts resulted in linear biomass relationships
- Saxitoxin exhibited similar ion suppression to the extracted algal toxins
- Optimized sample extraction method developed to decrease ion suppression

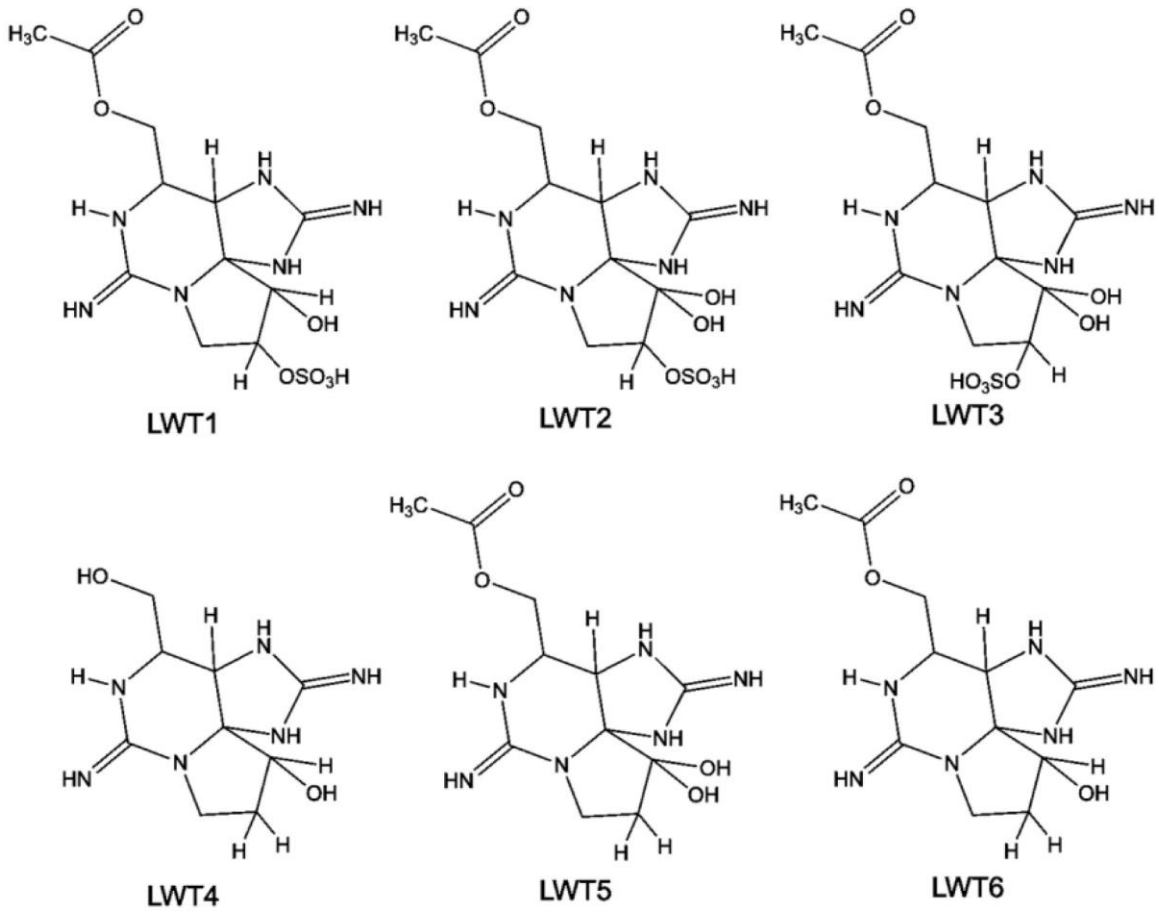

Figure 1.
Molecular structures of the Lyngbya wollei toxins (LWTs) 1–6 (free base).

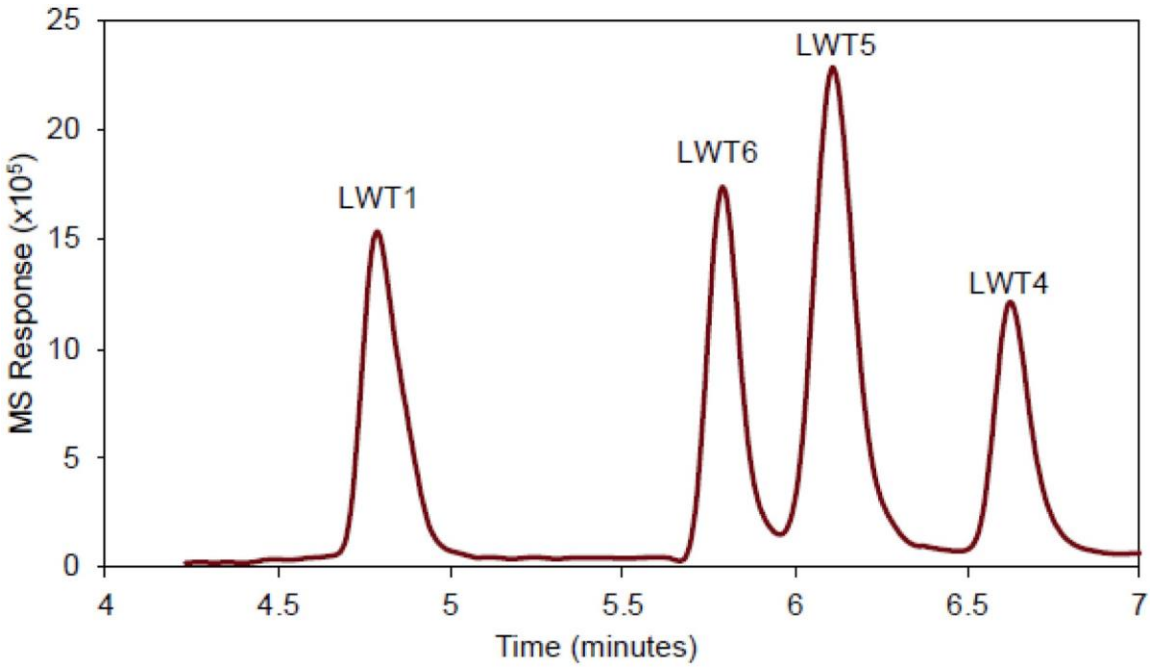

Figure 2.
LC-MS chromatogram for LWT1 (RT = 4.79 min), LWT4 (RT = 6.64 min), LWT5 (RT = 6.11 min), and LWT6 (RT =5.79 min).

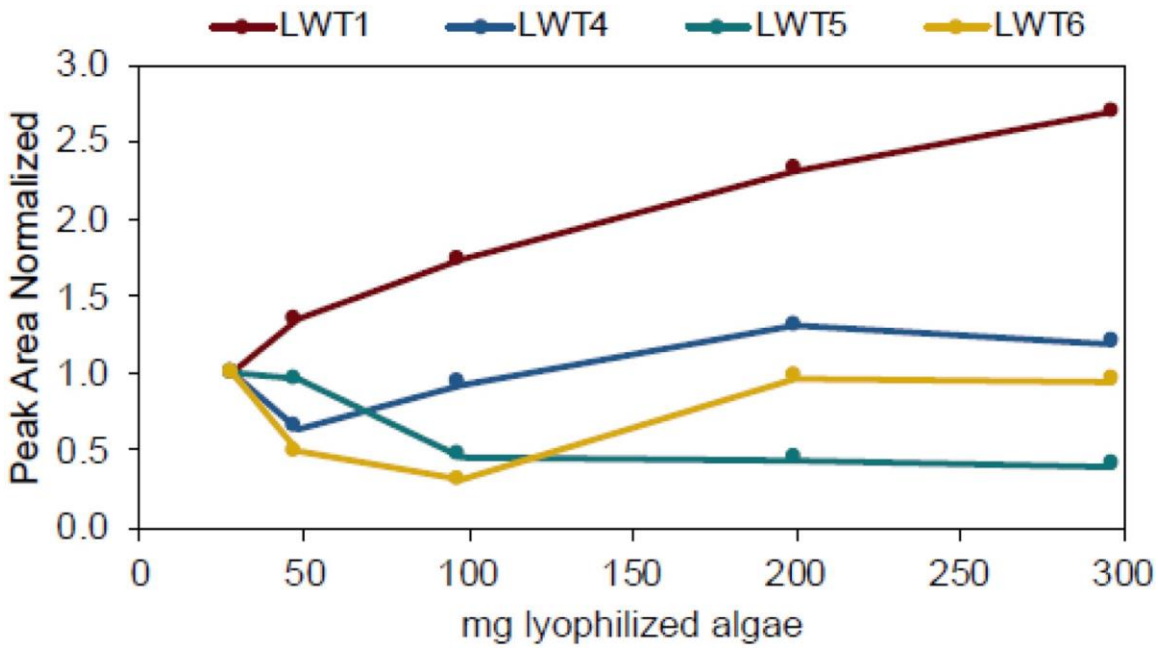

Figure 3.
Normalized MS peak area vs. mass of lyophilized L. wollei. The peak area of each toxin was normalized against the MS response from the lowest mass of algae.

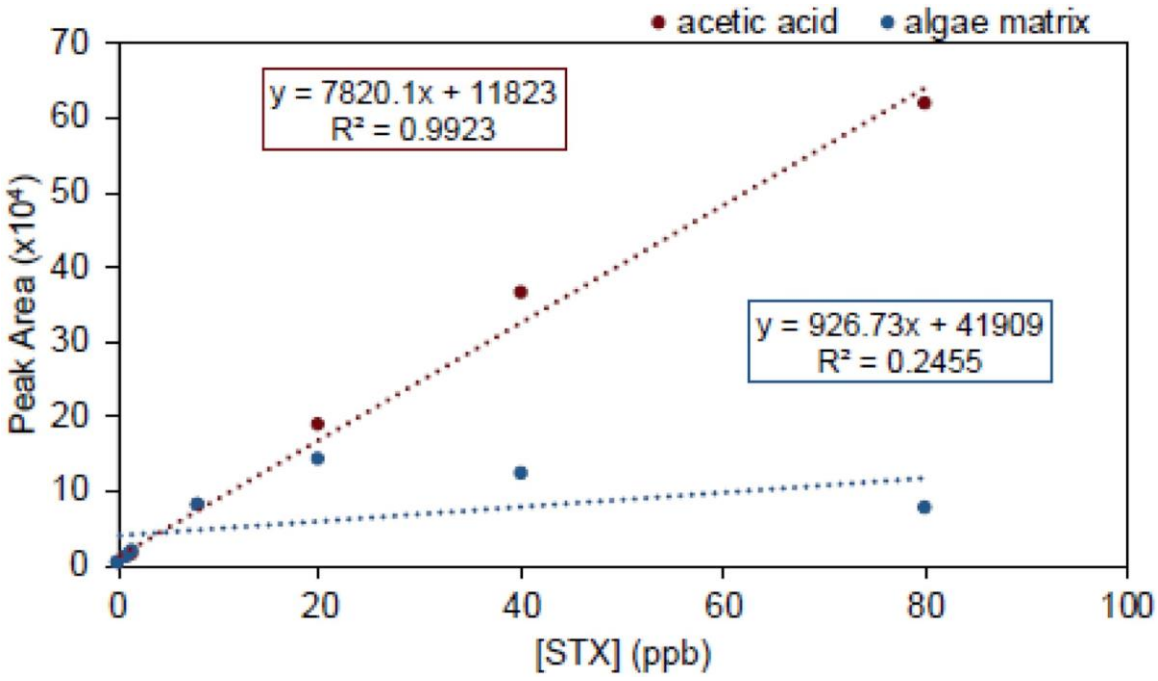

Figure 4.
Calibration curve for saxitoxin, a model LWT, in 0.1 M acetic acid (red) and in algal extract (blue).

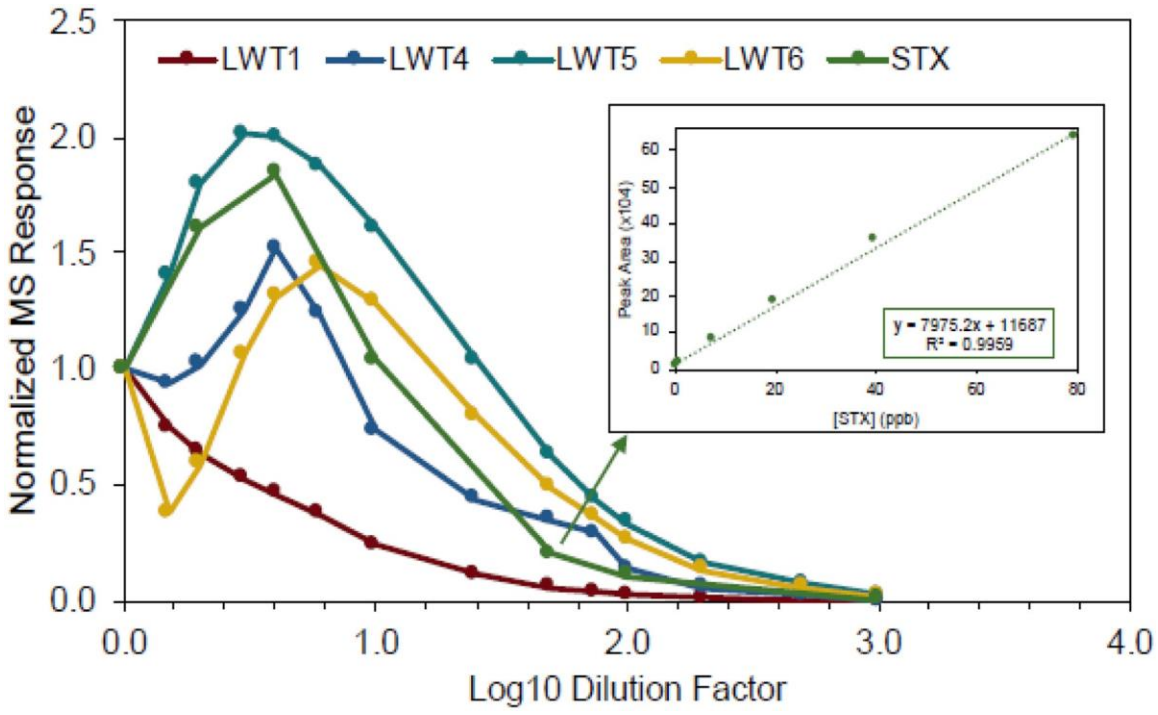

Figure 5.
Normalized MS peak area of LWTs and saxitoxin in the algal matrix as a function of (log10) dilution factor. Peak area is normalized against the area at a dilution factor of one. Inset:
Calibration curve of saxitoxin, a model LWT, in an extract of algae diluted by a factor of 50.

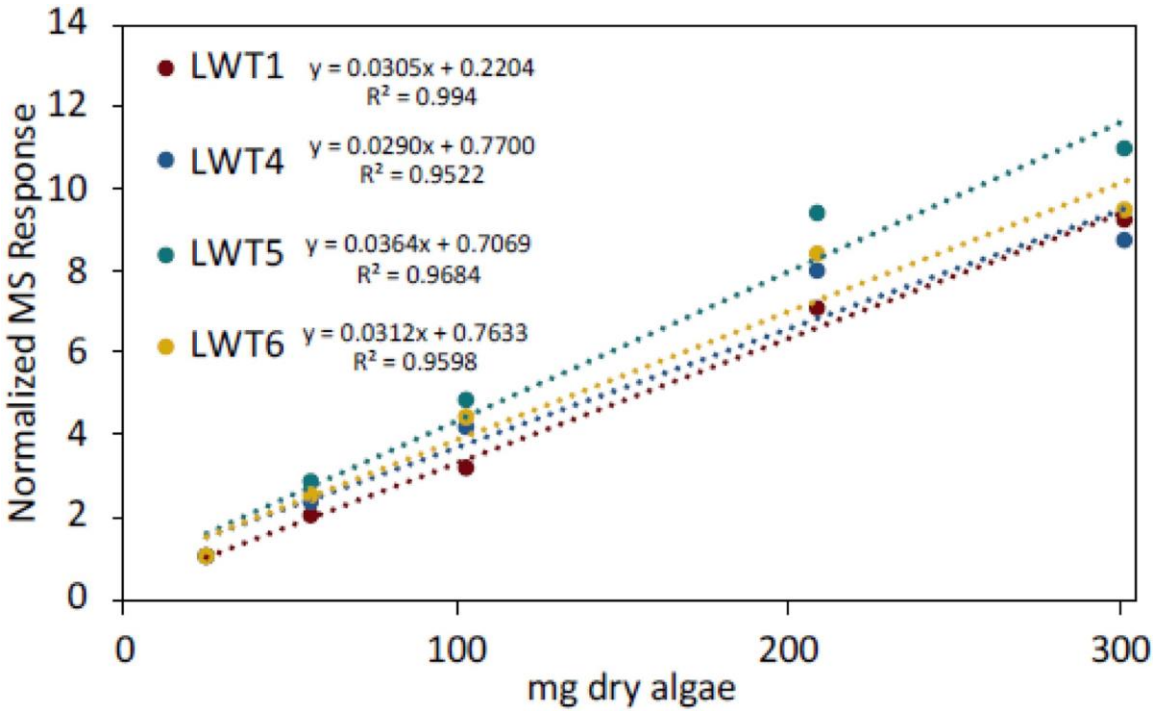

Figure 6.

Normalized MS peak area vs. mass of lyophilized Lyngbya wollei. The peak area of each toxin was normalized against the MS response from the lowest mass of algae (25 mg).

Response as a function of dry mass is linear for all 4 toxins (r_2 = 0.952 to 0.994).

Table 1.

High resolution fragmentation data for A: LWT1, B:LWT4, C: LWT5, and D: LWT6 (ESI+).

A: LWT1					
m/z	**Formula**	**Mass loss**	**Formula Loss**	**Theoretical Mass**	**ppm Mass Error**
379.1040	$C_{11}H_{19}N_6O_7S$			379.1030	2.53
299.1464	$C_{11}H_{19}N_6O_4$	79.9576	$-SO_3$	299.1462	0.67
281.1350	$C_{11}H_{17}N_6O_3$	97.9690	$-SO_3, -H2O$	281.1351	0.43
240.0981	$C_{10}H_{14}N_3O_4$	157.9895	$-SO_3, -H_2O, -C_2H_4O_2$	240.0979	0.92
221.1145	$C_9H_{13}N_6O$	175.0161	$-SO_3, -H_2O, -C_2H_4O_2, -NH_3$	221.1145	0.00
204.0880	$C_9H_{10}N_5O$	139.0059	$-SO_3, -CH5N_3$	204.0880	0.20
197.1034	$C_8H_{13}N_4O_2$	182.0006	$-SO_3, -CH4N_2, -C_2H_3O_2$	197.1033	0.51
180.0771	$C_8H_{10}N_3O_2$	199.0269	$-SO_3, -CH_5N_3, -C2H_4O_2$	180.0768	1.94
162.0663	$C_8H_8N_3O$	217.0377	$-SO_3, -CH_5N_3, -C2H4O_2, -H_2O$	162.0662	0.68
110.0712	$C_5H_8N_3$	269.0328	$-SO_3, -C_2H_4O_2, -C_4H_8N_3O_2$	110.0713	0.64
102.0661	$C_3H_8N_3O$	277.0379	$-C_2H_3O, -C_6H_8N_3O_5S$	102.0662	0.88
72.0556	$C_2H_6N_3$	307.0484	$-C_9H_{13}N_3O_7S$	72.0556	0.28
60.0557	CH_6N_3	319.0483	$-C_{10}H_{13}N_3O_7S$	60.0556	1.33
B: LWT4					
m/z	**Formula**	**Mass loss**	**Formula Loss**	**Theoretical Mass**	**ppm Mass Error**
241.1405	$C_9H_{17}N_6O_2$			241.1408	1.04
223.1295	$C_9H_{15}N_6O$	18.0110	$-H_2O$	223.1302	3.09
205.1192	$C_9H_{13}N_6$	36.0213	$-H_2O, -H_2O$	205.1196	2.05
177.0886	$C_7H_9N_6$	64.0519	$-H_2O, -H_2O, -C_2H_4$	177.0883	1.58
164.0821	$C_8H_{10}N_3O$	77.0584	$-H_2O, -CH_5N_3$	164.0818	1.58
152.0819	$C_7H_{10}N_3O$	89.0586	$-CH_4N_3, -CH_3O$	152.0818	0.39
136.0867	$C_7H_{10}N_3$	105.0538	$-CH_4N_3, -H_2O, -CH_2O$	136.0869	1.62
122.0711	$C_6H_8N_3$	119.0694	$-CH_4N_3, -CH_3O, -CH_2O$	122.0713	1.39

110.0712	$C_5H_8N_3$	131.0693	$-C_4H_8N_3O$, $-OH$	110.0713	0.64
94.0650	C_6H_8N	147.0755	$-C_3H_9N_5O_2$	94.0651	1.28
80.0492	C_5H_6N	161.0913	$-C_4H_{11}N_5O_2$	80.0495	3.44
72.0556	$C_2H_6N_3$	169.0849	$-C_4H_{11}N_5O_2$	72.0556	0.28
69.0447	$C_3H_5N_2$	172.0958	$-CH_3O$, $-C_5H_9N_4O$	69.0447	0.29
60.0555	CH_6N_3	181.0850	$-C_8H_{11}N_3O_2$	60.0556	2.00

C: LWT5

m/z	Formula	Mass loss	Formula Loss	Theoretical Mass	ppm Mass Error
299.1460	$C_{11}H_{19}N_6O_4$			299.1462	0.77
281.1353	$C_{11}H_{17}N_6O_3$	18.0107	$-H_2O$	281.1357	1.28
257.1240	$C_{10}H_{17}N_4O_4$	42.0220	$-CH_2N_2$	257.1244	1.67
239.1157	$C_{10}H_{15}N_4O_3$	60.0303	$-H_2O$, $-CH_2N_2$	239.1139	7.65
204.0880	$C_9H_{10}N_5O$	95.0580	$-H_2O$, $-H_2O$, $-NH_2$, $-C_2H_3O$	204.0880	0.05
197.1030	$C_8H_{13}N_4O_2$	102.0430	$-C_2H_4O_2$, $-CH_2N_2$	197.1033	1.52
179.0927	$C_8H_{11}N_4O$	120.0533	$-C_2H_4O_2$, $-CH_2N_2$, $-H_2O$	179.09274	0.22
150.0755	$C_{11}H_{20}N_6O_4$	—	—	150.0768	8.00
138.0673	$C_6H_8N_3O$	161.0787	$-C_2H_4O_2$, $-CH_2N_2$, $-H_2O$, $-C_2H_3N$	138.0662	8.04
96.0442	C_5H_6NO	203.1018	$-CH_2N_2$, $-CH_4N_3$, $-C_2H_4O_2$, $-C_2H_3O$	96.0444	1.98
83.0604	C_4H_7N2	216.0856	$-C_2H_3O_2$, $-C_5H_9N_4O_2$	83.0604	0.36
72.0552	$C_2H_6N_3$	227.0908	$-C_9H_{13}N_3O_4$	72.0556	5.83
60.0557	CH_6N_3	239.0903	$-C_{10}H_{13}N_3O_4$	60.0556	1.33

D: LWT6

m/z	Formula	Mass loss	Formula Loss	Theoretical Mass	ppm Mass Error
283.1513	$C_{11}H_{19}N_6O_3$			283.1513	0.04
241.1301	$C_{10}H_{17}N_4O_3$	42.0212	$-CH_2N_2$	241.12952	2.41
224.1032	$C_{10}H_{14}N_3O_3$	59.0481	$-CH_5N_3$	224.1030	1.03
205.1194	$C_9H_{13}N_6$	78.0319	$-H_2O$, $-C_2H_4O_2$	205.1196	1.07
190.0958	$C_8H_{10}N_6$	93.0555	$-H_2O$, $-C_2H_4O_2$, $-CH_3$	190.0962	1.84

181.1082	$C_8H_{13}N_4O$	102.0431	$-C_2H_4O_2$, $-CH_2N_2$	181.1084	1.05
177.0883	$C_7H_9N_6$	106.0630	$-C_2H_4O_2$, $-H_2O$, $-C_2H4$	177.0883	0.11
164.0825	$C_8H_{10}N_3O$	119.0688	$-C_2H_4O_2$, $-CH_5N_3$	164.0818	4.02
146.0713	$C_8H_8N_3$	137.0800	$-C_2H_4O_2$, $-CH_5N_3$, $-H_2O$	146.0713	0.21
136.08679	$C_7H_{10}N_3$	147.0645	$-C_2H_4O_2$, $-CH_3N_3$, $-CH_2O$	136.0869	0.96
122.0713	$C_6H_8N_3$	161.0800	$-C_2H_4O_2$, $-CH_3N_3$, $-C_2H_4O$	122.0713	0.25
110.0713	$C_5H_8N_3$	173.0800	$-C_2H_4O_2$, $-C_4H_8N_3O$	110.0713	0.27
102.0655	$C_5H_8N_3$	181.0858	$-C_2H_3O$, $-C_4H_8N_3O_3$	102.0662	6.76
94.0651	C_6H_8N	189.0862	$-C_5H_9N_5O_2$, $-H_2O$	94.0651	0.21
80.0495	C_5H_6N	203.1018	$-C_6H_{11}N_5O_2$, $-H_2O$	80.0495	0.31
72.0554	$C_2H_6N_3$	211.0959	$-C_9H_{13}N_3O_3$	72.0556	3.05
60.0556	CH_6N_3	223.0957	$-C_{10}H_{13}N_3O_3$	60.0556	0.33